# Protein Nuclear Transport and Polyglutamine Toxicity

## CHAN, Wing Man

A Thesis Submitted in Partial Fulfillment

of the Requirements for the Degree of

Doctor of Philosophy

in

Molecular Biotechnology

## March 2009

UMI Number: 3392272

# UMI®

Dissertation Publishing

# ProQuest®

## Thesis/Assessment Committee

Professor TSUI, Kwok-wing Stephen (Chairman)
Professor CHAN, Ho-yin Edwin (Thesis Supervisor)
Professor SHAW, Pang-chui (Thesis Supervisor)
Professor WAN, Chi-cheong David (Committee Member)
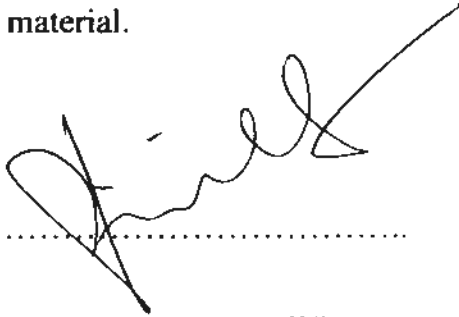Professor WONG, Ngok-shun Ricky (External Examiner)
Dr. O'KANE, Cahir (External Examiner)

# DECLARATION

I declare that this dissertation is entirely my own work except where otherwise stated,

either in the form of citation of published work, or acknowledgement of the source of any

unpublished material.

Signed ........................................................

CHAN Wing-man

# *Abstract*

Polyglutamine (polyQ) diseases are a group of progressive neurodegenerative disorders, which are caused by the expansion of an existing glutamine-coding CAG repeat in the coding region of disease genes. The cell nucleus is a major site of polyQ toxicity, and gene transcription is compromised in polyQ-induced neurodegeneration. Understanding the nuclear translocation of mutant polyQ proteins is therefore crucial to unfold the complex pathogenic mechanisms that underlie the neuronal toxicity of polyQ disease. The polyQ domain is the only common sequence found among different mutant disease proteins. Nuclear transport signals have been identified in some, but not all, polyQ disease proteins. The detection of those mutant polyQ proteins that carry no classical nuclear transport signal, but not their normal counterparts, in the cell nucleus suggests the existence of uncharacterized nuclear transport signals in mutant polyQ proteins. Thus, the objective of the present study is to elucidate the nuclear transport pathway(s) adopted by an expanded polyQ domain and determine its correlation with polyQ toxicity.

Through a series of genetic and biochemical studies in cell culture, mouse and transgenic *Drosophila* models, exportin-1 was found to modulate the nucleocytoplasmic localization of mutant polyQ protein and its toxicity. Further, mutant polyQ protein was also demonstrated to be a novel transport substrate of exportin-1. By promoting the nuclear

export of mutant polyQ protein, exportin-1 suppressed polyQ toxicity by reducing the interference of mutant polyQ protein on gene transcription. It was found that the protein level of exportin-1 diminished in the normal ageing process, which would result in an exaggeration of nuclear mutant polyQ toxicity. Thus, the age-dependent decline of exportin-1 level, at least in part, accounts for the progressive degeneration observed in polyQ patients. Results obtained from this project first demonstrated that expanded polyQ domain is a nuclear export signal, and further provided mechanistic explanation of how protein nuclear transport receptors modulate polyQ toxicity.

## *Abstract in Chinese* 摘要

多聚谷氨酰胺病 (polyglutamine diseases, polyQ diseases) 是由一段過度擴增的多聚谷氨酰胺序列所引致，屬於累進性神經退化疾病的一種。在過往的研究中，發現多聚谷氨酰胺毒性 (polyQ toxicity) 的根源地為細胞核 (cell nucleus)，而基因轉錄 (gene transcription) 亦受其影響。在已發現的九種多聚谷氨酰胺疾病蛋白中，多聚谷氨酰胺結構域 (polyQ domain) 是唯一共有的序列。由於所有多聚谷氨酰胺疾病都有著共同的病理特徵，包括細胞核內的蛋白聚集 (nuclear protein aggregation)，因此，找出多聚谷氨酰胺結構域如何控制蛋白核運輸 (protein nuclear transport) 將有助了解多聚谷氨酰胺的病原機制。此研究旨在解構多聚谷氨酰胺突變蛋白 (mutant polyQ protein) 所採用的核運輸途徑，從而說明核運輸在多聚谷氨酰胺毒性上的角色。利用細胞培養，小鼠和基因改造果蠅為研究模型，外輸蛋白一型 (exportin-1) 被發現對多聚谷氨酰胺突變蛋白亞細胞內的定位 (subcellular localization) 及其毒性扮演著重要的角色。多聚谷氨酰胺突變蛋白乃外輸蛋白一型新發現的運輸底物 (transport substrate)。研究發現，外輸蛋白一型能促進核外輸 (nuclear export)，從而減少細胞核內的多聚谷氨酰胺突變蛋白，並降低它對基因轉錄的影響。此外，研究亦發現外輸蛋白一型的蛋白質水平會隨著年齡增長而下降，細胞核內的多聚谷氨酰胺突變蛋白遂積聚起來，加強了細胞核內的毒性。總括而言，此項研究證實了多聚谷氨酰胺突變蛋白為外輸蛋白一型的運輸底物，並強調外輸蛋白一型所負責的核外輸對累進性多聚谷氨酰胺突變蛋白神經退化疾病的影響。

# *Acknowledgement*

I would like to express my sincere gratitude to my supervisor Dr. Edwin H. Y. Chan for his patient guidance, continuous enlightenment and encouragement throughout these years of graduate study. I am deeply indebted for his challenge through the dissertation process. I am also grateful to my co-supervisor Dr. P. C. Shaw for his valuable advice during the course of study.

Special thanks are given to Dr. Norbert Perrimon and Dr. S. Zhang at Harvard Medical School, Boston, MA, USA for the sharing of unpublished data and insightful discussion. I would also like to thank Dr. H. Y. Li and Dr. Eric C. H. Wong at Nanyang Technological University, Singapore for their collaboration on live-cell imaging. I am also grateful to Dr. K. F. Lau for his help in co-immunoprecipitation and preparation of mouse samples.

Gratitude is due to all current and past members of the Laboratory of *Drosophila* Research, CUHK, especially Mr Frankie H. Tsoi, Mr. T. C. Cheng, Mr. C. C. Wu and Mr. Alan S. L. Wong for their contributions to the project and inspiring suggestions. I also thank all members in MMW 509 for their persistent help and support.

Finally, I would like to express my heartfelt gratitude to all my friends and family members. Without their warmest care and concerns this dissertation would not have been possible. I thank them all.

# List of Abbreviations

| | |
|---|---|
| ANOVA | Analysis of Variance |
| AP-1 | Activator Protein-1 |
| AR | Androgen Receptor |
| BSA | Bovine Serum Albumin |
| *Cas* | *CSE1 segregation protein* |
| *cdm* | *cadmus* |
| cDNA | complementary Deoxyribonucleic Acid |
| co-IP | co-Immunoprecipitation |
| $CuSO_4$ | copper sulphate |
| DEPC | Diethyl Pyrocarbonate |
| dNTP | deoxyNucleoside Triphosphates |
| dpe | days post-eclosion |
| DRSC | *Drosophila* RNAi Screening Center |
| dsRNAs | double-stranded RNAs |
| DT | Double Transgenic |
| EGFP | Enhanced Green Fluorescent Protein |
| emb | embargoed |
| Fra | Fos related antigen |
| GDP | Guanosine Diphosphate |
| *gmr* | *glass multiple reporter* |
| GST | Glutathione-S-Transferase |
| GTP | Guanosine Triphosphate |
| HD | Huntington's Disease |
| HEK | Human Embryonic Kidney |
| hpi | hours post-induction |
| HPRT | Hypoxanthine Phosphoribosyltransferase |
| hpt | hours post-transfection |
| *hsp* | *heat shock protein* |
| Htt | Huntingtin |
| IB | Immunoblotting |
| IP | Immunoprecipitation |
| Jab1 | Jun activation domain-binding protein 1 |
| JNK | c-Jun $NH_2$ terminal Kinase |
| Jra | Jun related antigen |
| *kap-α1* | *karyopherin-α1* |
| *kap-α3* | *karyopherin-α3* |

| | |
|---|---|
| *kary-β3* | *karyopherin-β3* |
| kDa | kiloDalton |
| LMB | Leptomycin B |
| MJD | Machado-Joseph Disease |
| *MT* | *Metallothionein* |
| NA | Numerical Aperture |
| NES | Nuclear Export Signal |
| NLS | Nuclear Localization Signal |
| NPC | Nuclear Pore Complex |
| PBS | Phosphate Buffered Saline |
| PD | Parkinson's Disease |
| PNK | Polynucleotide Kinase |
| polyQ | Polyglutamine |
| RanBP3 | Ran-binding Protein 3 |
| RanGAP | Ran GTPase-Activating Protein |
| RanGEF | Ran Guanine Nucleotide Exchange Factor |
| RNAi | RNA interference |
| RT-PCR | Reverse Transcription-Polymerase Chain Reaction |
| S.D. | Standard Deviation |
| S.E.M. | Standard Error of the Mean |
| SBMA | Spinal Bulbar Muscular Atrophy |
| SCA | Spinocerebellar Ataxia |
| SDS | Sodium Dodecyl Sulfate |
| SV40 | Simian Virus 40 |
| TBE | Tris-Borate-EDTA |
| TBS | Tris-Buffered Saline |
| TBS-T | Tris-Buffered Saline-Tween 20 |
| TEMED | N,N,N,N-Di-(dimethylamino)ethane |
| UAS | Upstream Activator Sequence |
| Xpo1 | Exportin-1 |
| Xpo-t | Exportin-t |

# List of Figures

# List of Tables

# *Table of Contents*

## Chapter 1. Introduction

## Chapter 6. Exportin-1-mediated Modification of Polyglutamine Toxicity

# Chapter 7. Concluding Remarks

## *Chapter 1. Introduction*

**1.1 Receptor-mediated Protein Nucleocytoplasmic Transport**

**1.1.1 Introduction to Nucleocytoplasmic Transport**

The cell nucleus is spatially separated from other organelles by a bi-layer membrane or the nuclear envelope. Small molecules, such as ions, enter and leave the nucleus by passive diffusion, whereas the translocation of large proteins (>60 kDa) and RNAs across the nuclear envelope requires specific active transport machineries (Pemberton and Paschal, 2005; Terry et al., 2007). The specificity of such energy-dependent bidirectional trafficking depends on the transport signals present on the cargoes. These signals are recognized by transport receptors, which are collectively termed as karyopherins (Mosammaparast and Pemberton, 2004). Cargo proteins are transported in or out of the nucleus by forming complexes with karyopherins. The karyopherin-cargo complex translocates through the nuclear pore complexes (NPCs), macromolecular structures that serve as transport channels spanning the nuclear envelope, via interactions with protein components of NPCs (Fig. 1.1) (Tran and Wente, 2006).
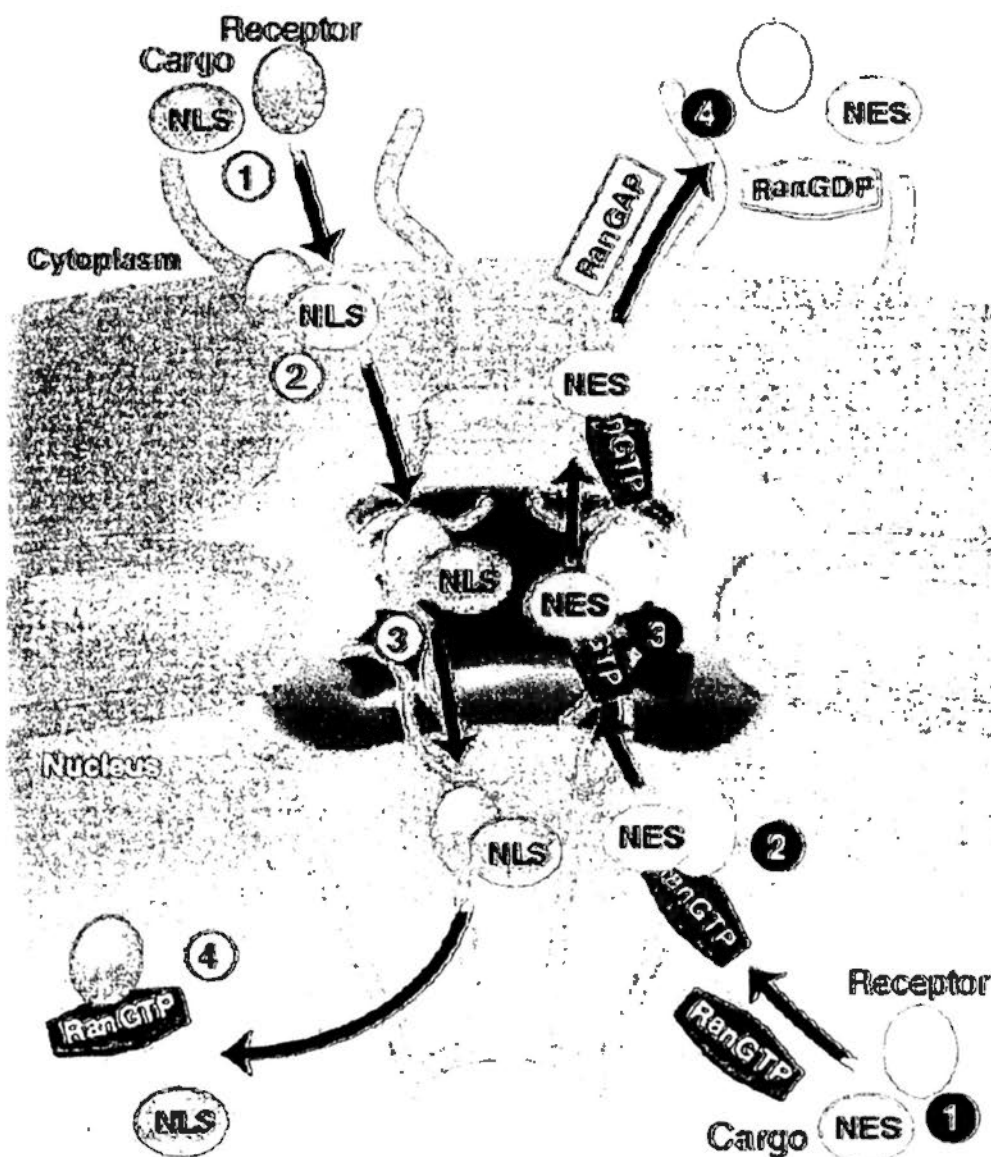
**Figure 1.1. The Ran-dependent nuclear transport pathway.**
Both protein nuclear import (white circles) and export (black circles)
involve sequential steps of protein-protein interactions. Nuclear
Import: (1) An import receptor first recognizes an NLS-containing
cargo and forms a receptor-cargo complex, (2) which docks on the
cytoplasmic side of the NPC and (3) translocate through the NPCs
by interacting with its protein components. (4) The binding of
RanGTP to the import receptor results in the release of transport
cargo in the nucleus. Nuclear Export: (1) The export receptor
recognizes an NES-containing cargo and forms a ternary complex
together with RanGTP, (2) which docks on the nuclear side of the
NPC and (3) translocate though the NPCs by interacting with its
protein components. (4) The hydrolysis of RanGTP to RanGDP by
RanGAP in the cytoplasm results in complex disassembly. (adapted
from Terry et al., 2007)

A small GTPase which belongs to the Ras superfamily, Ran, plays an indispensible role in the classical nuclear transport pathway. The nucleotide-bound states of Ran are tightly controlled by the cytoplasmic Ran GTPase-activating protein (RanGAP) and nuclear Ran guanine nucleotide exchange factor (RanGEF), and the shuttling of Ran between the GTP- and GDP-bound forms exquisitely dictates binding between cargoes and their transport receptors (Pemberton and Paschal, 2005; Terry et al., 2007). Owing to the compartmentalization of RanGAP and RanGEF, GDP-bound Ran (Ran-GDP) is enriched in the cytoplasm while GTP-bound Ran (Ran-GTP) is concentrated in the nucleus (Fig. 1.1). Such asymmetric distribution of Ran-GDP and Ran-GTP regulates the directionality of karyopherin-mediated transport (Izaurralde et al., 1997) (detailed in Sections 1.1.2 and 1.1.3). On the other hand, non-classical Ran-independent nuclear transport has also been reported for several cellular proteins (Huber et al., 2002; Rudt and Pieler, 2001); however the precise mechanisms of this are not well understood.

**1.1.2 Nuclear Localization Signals and Protein Nuclear Import**

Transport signals that direct nuclear entry of proteins are referred as nuclear localization signals (NLSs). They usually comprise one (monopartite) or two (bipartite) short stretches of basic amino acid residues (Lange et al., 2007). The simian virus 40 (SV40) large T antigen NLS (Kalderon et al., 1984) and the nucleoplasmin NLS (Robbins

et al., 1991) are representative monopartite and bipartite NLSs, respectively.

Karyopherins that participate in nuclear import are referred as importins. In the Ran-dependent pathway (Fig. 1.1), importin first recognizes the NLS-containing cargo and forms a complex with the cargo protein in the cytoplasm. Through a series of protein-protein interactions with components of the NPCs, the importin-cargo complex translocates into the nucleus. The interaction of importin with Ran-GTP causes the dissociation of the importin-cargo complex, leading to the release of the cargo inside the nucleus (Lange et al., 2007; Pemberton and Paschal, 2005; Terry et al., 2007).

There are 2 major types of importins: importin-α and importin-β (Lange et al., 2007). Importin-α serves as an adaptor that links NLS-containing cargoes to importin-β, while importin-β itself is responsible for interaction with the protein components of the NPCs during transport (Lange et al., 2007). In certain situations, importin-β is also capable of accomplishing protein nuclear import through direct interaction with cargoes in the absence of importin-α (Lange et al., 2007).

## 1.1.3 Nuclear Export Signals and Protein Nuclear Export

Similar to nuclear import, protein export from the nucleus is directed by transport

signals known as nuclear export signals (NESs) (Kutay and Guttinger, 2005). The most common type of NES contains a stretch of leucine residues, and an example of which is the human immunodeficiency virus type 1 Rev protein NES (Fischer et al., 1995). In the Ran-dependent export pathway (Fig. 1.1), exportins which correspond to karyopherins that participate in nuclear export binds the NES-containing cargo inside the nucleus co-operatively with Ran-GTP (Pemberton and Paschal, 2005; Terry et al., 2007). The exportin-cargo-Ran-GTP complex then translocates through the NPC to the cytoplasm, where the ternary complex dissociates upon the hydrolysis of Ran-GTP to Ran-GDP (Pemberton and Paschal, 2005; Terry et al., 2007).

The best characterized exportin is exportin-1 (Fornerod et al., 1997). Ran-binding protein 3 (RanBP3) serves as a co-factor for exportin-1 by enhancing its binding affinity toward Ran-GTP, which cooperatively promotes cargo binding (Englmeier et al., 2001; Lindsay et al., 2001). Thus, an efficient protein export is accomplished through the formation of a 4-component complex comprising exportin-1, RanBP3, Ran-GTP and the NES cargo (Englmeier et al., 2001; Lindsay et al., 2001). Exportin-1-mediated protein export is sensitive to leptomycin B (LMB) treatment (Kudo et al., 1999). Leptomycin B covalently binds to cysteine residue 529 of exportin-1, which is involved in NES recognition, and such modification results in steric hindrance for NES cargo access and

hence specific inhibition on exportin-1-mediated protein nuclear export (Kudo et al., 1999;

Petosa et al., 2004).

**1.1.4 Regulation of Nucleocytoplasmic Transport and Human Diseases**

The regulation of nucleocytoplasmic transport encompasses multiple levels of control

(Terry et al., 2007). In addition to the primary sequences of the NLSs/NESs,

post-translational modifications, such as phosphorylation, methylation and ubiquitination

have also been implicated in regulating the localization of transport cargoes (Terry et al.,

2007). For example, the NES on cyclin B1 undergoes phosphorylation at the onset of

mitosis and thus prevents nuclear export of cyclin B1 by exportin-1 (Yang et al., 2001). In

addition to post-translational modifications, the expression level of karyopherins also plays

a regulatory role (Terry et al., 2007). For instance, the expression levels of different

importin-$\alpha$ vary during neural differentiation of embryonic stem cells (Yasuhara et al.,

2007). This results in selective nuclear import of transcription factors which are important

for neural identity determination (Yasuhara et al., 2007).

Deregulation of nuclear transport pathways has been reported in different human

diseases, including various types of carcinomas (Kau et al., 2004) and viral infections

(Frieman et al., 2007; Reid et al., 2006). For example, over-expression of importin-$\beta$

and/or importin-α is detected in colon, breast, and lung cancers, leading to the redistribution of cellular proteins that are pivotal for tumor progression (Kau et al., 2004). In the present study, the influence of nucleocytoplasmic transport on a particular type of neurodegenerative disorder, polyglutamine (polyQ) disease, is extensively studied.

## 1.2 Introduction to Polyglutamine Diseases

### 1.2.1 Etiology of Polyglutamine Diseases

Polyglutaminopathy refers to a group of progressive neurodegenerative disorders characterized by abnormal expansion of existing CAG trinucleotide repeats in the coding region of disease genes, which are translated into elongated polyQ domains in the disease proteins (Orr and Zoghbi, 2007). Proteins harboring the expanded polyQ domains are defined as mutant proteins. The CAG codon is the most abundant codon repeat in the human genome (Alba and Guigo, 2004). Increase in its repeat number is attributed to meiotic instability during paternal transmission (Galvao et al., 2001; Heidenfelder and Topal, 2003). Polyglutamine diseases are inherited in an autosomal dominant fashion; the presence of only one mutated gene is sufficient to cause the disease (Orr and Zoghbi, 2007). Beyond a threshold of 35-40 repeats, the expanded polyQ domain confers toxicity.

### 1.2.2 Common Features of Different Types of Polyglutamine Diseases

There are nine polyQ diseases identified at present, and each of them is characterized by selective neuronal loss in specific regions of the brain (Table 1.1) (Orr and Zoghbi, 2007; Zoghbi and Orr, 2000). Despite their diverse regional vulnerabilities, several salient pathologic features are shared among different polyQ disorders. Polyglutamine diseases are all characterized by progressive neurodegeneration, typically striking in midlife, causing

neuronal dysfunction and eventual neuronal loss 10-20 years after the onset of symptoms (Zoghbi and Orr, 2000). Other common cellular pathologic hallmarks include the formation of insoluble intracellular protein aggregates, the impairment of ubiquitin-proteasome system and transcriptional dysregulation of essential genes in affected neurons (Orr and Zoghbi, 2007). The CAG repeat length shows a positive correlation with the aggregation potential of the disease proteins, and is inversely correlated to the age of disease onset. The longer the CAG repeats, the higher the chance of aggregate formation, and the earlier the onset of neuronal degeneration.

Table 1.1. Molecular characterization of polyQ diseases.

| Name of disease | Gene locus | Gene product | Size (kDa) | Normal CAG (n) | Expanded CAG (n) | Brain regions most affected |
|---|---|---|---|---|---|---|
| Dentatorubral Pallidoluysian Atrophy (DRPLA) | 12q | Atrophin-1 | 125 | 6 - 36 | 49 - 84 | Cerebellum. Cerebral cortex, Basal ganglia, Luys body |
| Huntington's Disease (HD) | 4p16.3 | Huntingtin | 350 | 6 - 34 | 36 - 121 | Striatum. Cerebral cortex |
| Spinobulbar Muscular Atrophy (SBMA) | Xq11-12 | Androgen Receptor | 100 | 9 - 36 | 38 - 62 | Anterior horn and bulbar neurons, Dorsal root ganglia |
| Spinocerebellar Ataxia (SCA) | | | | | | |
| Type 1 (SCA1) | 6p22-23 | Ataxin-1 | 90 | 6 - 44 | 39 - 82 | Cerebellar Purkinje cells, Dentate nucleus, Brain stem |
| Type 2 (SCA2) | 12q23-24 | Ataxin-2 | 140 | 15 - 31 | 36 - 63 | Cerebellar Purkinje cells, Brain stem. Fronto-temporal lobes |
| Type 3 (SCA3) | 14q24.3-31 | Ataxin-3 | 42 | 12 - 41 | 62 - 84 | Cerebellar dentate neurons, Basal ganglia, Brain stem, Spinal cord |
| Type 6 (SCA6) | 19p13 | P/Q-type $Ca^{2+}$ channel alpha1A (CACNA1A) | 270 | 4 - 18 | 21 - 33 | Cerebellar Purkinje cells, Dentate nucleus. Inferior olive |
| Type 7 (SCA7) | 3p12-q21.1 | Ataxin-7 | 95 | 4 - 35 | 37 - 306 | Cerebellum. Brain stem, Macula, Visual cortex |
| Type 17 (SCA17) | 6p27 | TATA-Binding Protein (TBP) | 38 | 25 - 42 | 45 - 63 | Cerebellum. Brain stem. Spinal cord |

modified from (Everett and Wood. 2004) and (Zoghbi and Orr. 2000)

### 1.3 Mutant Polyglutamine Protein Pathogenic Mechanisms

### 1.3.1 Loss-of-function

Extensive studies have been conducted to elucidate the endogenous functions of the normal unexpanded polyQ proteins. It has been suggested that the abnormal expansion of glutamine repeat in disease proteins causes a loss of normal polyQ protein function (Atwal et al., 2007; Busch et al., 2003; Friedman et al., 2007; Gidalevitz et al., 2006; Helmlinger et al., 2006a; Lieberman et al., 2002; Matsuyama et al., 2004; McMahon et al., 2005). For example, mutant androgen receptor (AR), the disease protein for spinalbulbar muscular atrophy (SBMA), fails to regulate the expression of certain androgen-responsive genes in an *in vitro* cell model (Lieberman et al., 2002). Apart from loss-of-function; mutant polyQ proteins also provoke a toxic gain-of-function property due to the aberrant conformation imposed by polyQ domain expansion (Gatchel and Zoghbi, 2005).

### 1.3.2 Gain-of-function

Misfolded mutant polyQ proteins adopt abnormal conformations (Fig. 1.2A), leading to the tendency of aggregation. This results in sequestration of cellular proteins, including transcription factors, molecular chaperones, ubiquitin and proteasome subunits, to the aggregates (Suhr et al., 2001). Recruitment of these cellular factors to polyQ aggregates perturbs their normal functions, and results in transcriptional dysregulation (Duenas et al.,

11

2006; Helmlinger et al., 2006b), imbalance of proper protein folding (Brignull et al., 2007;

Herbst and Wanker, 2006; Weydt and La Spada, 2006) and/or impairment of

ubiquitin-proteasome protein degradation machineries (Davies et al., 2007; Ortega et al.,

2007). Even if the mutant polyQ proteins do not form aggregates, the expanded polyQ

domain can confer abnormal interactions with cellular proteins, as a result the normal

functions of which are compromised (Schaffar et al., 2004; Shimohata et al., 2000). The

mechanisms of which mutant polyQ protein mediate pathogenesis are summarized in Fig.

1.2B.

A.

Wild-type polyglutamine protein

Mutant polyglutamine protein

Interactors

B.

Cytoskeletal abnormalities
Axonal transport defects

Mitochondrial
dysfunction

$Ca^{2+}$

Altered $Ca^{2+}$ influx/
homeostasis

Altered RNA metabolism

Transcriptional dysregulation

Activator

Repressor

DNA TATA

Chromatin

Protein accumulation

Ub

Ub

Quality-control mechanisms:
Ubiquitin-proteasome system
Chaperones
Autophagy

**Figure 1.2. Mechanisms of pathogenesis of polyQ diseases. (A)**
A mutant polyQ protein adopts an abnormal conformation, leading to
aberrant biomolecular interactions, which can be inappropriately
enhanced (light green circles), whereas others might be lost (red
circles). **(B)** Mutant polyQ proteins affect many cellular processes,
including calcium homeostasis, mitochondrial functions, axonal
transport, RNA metabolism, transcription and protein quality-control
machineries (adapted from Gatchel & Zoghbi, 2005)

## 1.4 Subcellular Localization of Polyglutamine Disease Proteins

### 1.4.1 Normal Unexpanded Protein

Subcellular localization of proteins is linked tightly to their cellular functions (Poukka et al., 2000; Riley et al., 2005; Saporita et al., 2003). For example, the AR protein regulates hormone-responsive gene transcription by shuttling between the cytoplasm and nucleus (Poukka et al., 2000; Saporita et al., 2003). The nucleocytoplasmic shuttling of AR is mediated by transport signals on the protein; its NLS is only active in the presence of ligand, while the activity of its NES is concomitantly repressed (Jenster et al., 1993; Poukka et al., 2000; Saporita et al., 2003). Indeed, classical NLSs and NESs are found in most polyQ disease proteins (Table 1.2). This highlights the involvement of Ran-dependent nuclear transport pathways (Fig. 1.1) in regulating subcellular localization and hence the cellular function of the unexpanded polyQ disease proteins.

### 1.4.2 Expanded Mutant Protein

Upon polyQ domain expansion, the functions of classical nuclear transport signals are compromised. It was reported that the nuclear export activities of NES on huntingtin (Htt; (Cornett et al., 2005)) and ataxin-7 (Taylor et al., 2006), the disease proteins for HD and SCA7 respectively, are weakened in the respective expanded polyQ disease proteins. One of the possible explanations is that the expanded polyQ domain impairs the

interactions between mutant polyQ proteins and protein components of NPCs (Cornett et al., 2005). The interaction between mutant Htt and the nuclear pore protein, translocated promoter region, is abolished upon polyQ expansion, which impairs its nuclear export and thus results in nuclear accumulation of mutant Htt (Cornett et al., 2005).

In addition to the nuclear transport signals on their primary protein sequences (Table 1.2), several other factors, including protein size (Hackam et al., 1998; Martindale et al., 1998) and interacting protein partners (Diamond et al., 2000), also play roles in modulating the subcellular localization of mutant polyQ proteins.

**Table 1.2. Classical nuclear transport signals on polyQ disease proteins.**

| PolyQ disease | Disease protein (GenBank Accession No.) | Subcellular localization | Nuclear transport signals identified (amino acid co-ordinates) |
|---|---|---|---|
| DRPLA | Atrophin-1 (NP_001931) | Cytoplasm | NLS (16-32): RKKEAPGPREELRSRGR (Nucifora et al., 2003) NES (1033-1041): LARLQMLNV (Nucifora et al., 2003) |
| HD | Huntingtin (NP_002102) | Cytoplasm | NLS (1184-1190): RRKGKEK (Bessert et al., 1995) NES (2364-2414): IIISLARLPL (Xia et al., 2003) |
| SBMA | Androgen Receptor (NP_000035) | Cytoplasm & Nucleus | NLS (618-634): RKCYEAGMTLGARKLKK (Jenster et al., 1993) NES (743-817): LMVFAMGWRSFTNVNSRMLYFAPDLVFNEYRMHKSRM (Saporita et al., 2003) |
| SCA1 | Ataxin-1 (NP_000323) | Nucleus | NLS (770-773): RKRR (Klement et al., 1998) |
| SCA2 | Ataxin-2 (NP_002964) | Cytoplasm | Not Studied |
| SCA3 | Ataxin-3 (NP_004984) | Cytoplasm | NLS (predicted) (282-285): RKRR (Albrecht et al., 2004) NES (predicted) (174-183): ADQLLQMIRV (Albrecht et al., 2004) |
| SCA6 | CACNA1A (BAA94766) | Cell Membrane & Nucleus | NLSs (2136-2142) PKARRLD (Kordasiewicz et al., 2006) (2208-2214): PKDRKHR (Kordasiewicz et al., 2006) (2285-2291): PRRGRRQ (Kordasiewicz et al., 2006) |
| SCA7 | Ataxin-7 (NP_000324) | Nucleus | NLSs (378-381): RRKR (Kaytor et al., 1999) (705-708): KKRK (Chen et al., 2004) (835-838) KKRK (Chen et al., 2004) NES (341-352): FDPDIHCGVIDL (Taylor et al., 2006) |
| SCA17 | TBP (NP_003185) | Nucleus | Not Studied |

## 1.5 Correlation between Nucleocytoplasmic Localization of Mutant Polyglutamine Proteins and Toxicity

### 1.5.1 Toxicity caused by Cytoplasmic Mutant Proteins

The nucleocytoplasmic localization of mutant polyQ proteins plays pivotal roles in the degenerative process of polyQ diseases. Toxicity has been reported for mutant polyQ proteins that localize in the cytoplasm. For example, mutant Htt carrying an expanded polyQ domain has been shown to confer toxicity when localized in the cytoplasm in both cultured cells (Hackam et al., 1999; Wang et al., 2008) and transgenic mice (Benn et al., 2005; Hackam et al., 1999). In addition, when mutant ataxin-3/MJD, the disease protein for SCA3, is targeted to the cytoplasm by an exogenous NES, a degenerative eye phenotype is observed in transgenic *Drosophila* model, indicating the toxic effect of cytoplasmic mutant polyQ protein (Gunawardena et al., 2003).

### 1.5.2 Toxicity caused by Nuclear Mutant Proteins

Nevertheless, nuclear localization of various mutant disease proteins is also important for toxicity (Benn et al., 2005; Bichelmeier et al., 2007; Jackson et al., 2003; Klement et al., 1998; Kordasiewicz et al., 2006; Nucifora et al., 2003; Peters et al., 1999; Saudou et al., 1998; Schilling et al., 2004; Schilling et al., 1999). For example, when the endogenous NLS of ataxin-1, the disease protein for SCA1, is mutated to abolish its nuclear

localization, expansion of its polyQ domain does not cause any symptoms in transgenic mice (Klement et al., 1998). In addition, nuclear targeting of mutant Htt by an exogenous NLS increases toxicity *in vitro* (Peters et al., 1999), and results in neurological abnormalities as well as premature cell death *in vivo* (Schilling et al., 2004). In an independent study focused on SCA3, nuclear localization of MJD has been demonstrated to be critical for pathogenesis. Targeting a mutant MJD protein to the nucleus using an exogenous NLS significantly aggravates the neurological phenotypes in those SCA3 transgenic mice, as indicated by an intensification of behavioral defects (Bichelmeier et al., 2007).

Nuclear toxicity of mutant polyQ proteins can be attributed to their interference on gene transcription (Huen et al., 2007; Truant et al., 2007) and/or association with the nuclear matrix which leads to alteration of nuclear structure (Perez et al., 1999; Skinner et al., 1997; Tait et al., 1998). Also, nuclear mutant polyQ proteins are less susceptible to autophagic degradation (Iwata et al., 2005) compared to cytoplasmic protein, their accumulation in the nucleus thus intensifies the severity of the diseases (Rubinsztein, 2006; Williams et al., 2006).

## 1.6 The Importance of Polyglutamine Domain

The polyQ track is a unique protein domain shared among different polyQ disease proteins; its influences on aggregation, nuclear localization and toxicity have been extensively studied (Kazantsev et al., 1999; Marsh et al., 2000; Moulder et al., 1999; Ordway et al., 1997; Takahashi et al., 2007).

### 1.6.1 Aggregate Formation

Polyglutamine aggregates found in patients of different polyQ diseases are reported to contain fragments of disease proteins carrying the expanded polyQ domain (Adachi et al., 2005; Goti et al., 2004; Hoffner et al., 2005). This underscores the importance of the polyQ domain in aggregate formation. Naked polyQ domain has been shown to be capable of initiating aggregate formation both *in vitro* (Kazantsev et al., 1999; Moulder et al., 1999; Takahashi et al., 2007) and *in vivo* (Marsh et al., 2000; Ordway et al., 1997). When a naked polyQ domain is expressed as fusion protein with enhanced green fluorescence protein (EGFP) in cultured cells, an unexpanded polyQ-EGFP protein only shows a diffuse pattern of fluorescence whereas aggregates are observed in cells expressing mutant polyQ-EGFP protein in a Q-length dependent manner (Fig. 1.3) (Kazantsev et al., 1999; Moulder et al., 1999; Takahashi et al., 2007). The aggregation potential of expanded polyQ domain is further corroborated in transgenic *Drosophila* and mouse models (Marsh et al., 2000;

Ordway et al., 1997).

Polyglutamine domains also play roles in the recruitment of cellular factors into aggregates. Cellular proteins that naturally carrying a short glutamine repeat domain, such as CREB-binding protein, are recruited to aggregates (Burke et al., 1996; Kazantsev et al., 1999; Nucifora et al., 2001; Perez et al., 1998). In particular, the normal unexpanded disease proteins, such as ataxin-2 and MJD, have also been shown to co-aggregate with mutant polyQ proteins in both cultured cell and *Drosophila* models (Al-Ramahi et al., 2007; Haacke et al., 2006; Perez et al., 1998). Therefore, the polyQ domains of both normal and mutant disease proteins are crucial to aggregation.

## 1.6.2 Nuclear Localization and Toxicity

Similar to aggregate formation, the toxic nature of a naked polyQ domain has been well documented. For example, expression of the EGFP-polyQ fusion proteins causes toxicity in primary rat cerebellar granule neurons (Moulder et al., 1999). When an expanded polyQ domain (Q146) is carried by an unrelated cytoplasmic protein, hypoxanthine phosphoribosyltransferase (HPRT), nuclear aggregates are detected and a progressive neurological phenotype develops in this HPRT$^{Q146}$ transgenic mouse model (Ordway et al., 1997). Eventually, the transgenic mice die prematurely (Fig. 1.4). This

experiment shows that the addition of an expanded polyQ domain causes re-localization of

HPRT from the cytoplasm to the nucleus, implying certain uncharacterized nuclear

targeting signal(s) are encoded within the polyQ track.
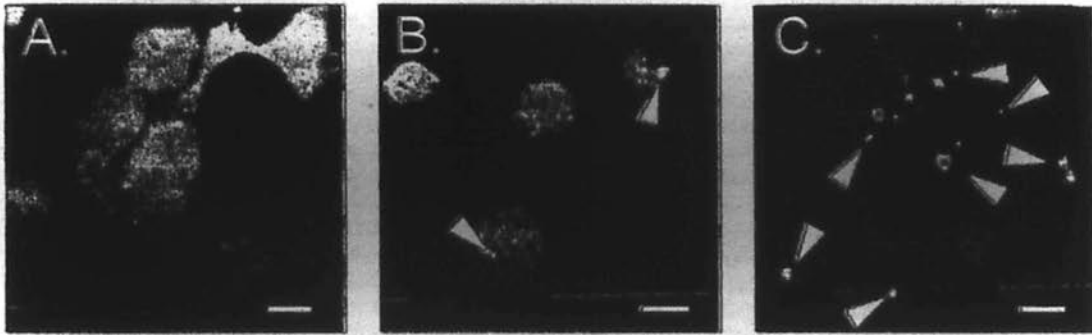
**Figure 1.3. Formation of protein aggregates triggered by polyQ domain expansion.** Confocal images of COS-7 cells expressing EGFP-polyQ fusion proteins. Transfected cells expressing EGFP-Q19 **(A)** show diffuse GFP signals, yet aggregates (arrowheads) are evident in both EGFP-Q45 **(B)** and -Q81 **(C)** expressing cells. More aggregates are observed in EGFP-Q81 expressing cells when compared to that of EGFP-Q45. Scale bars represent 10 μm. (adapted from Takahashi et al., 2007)
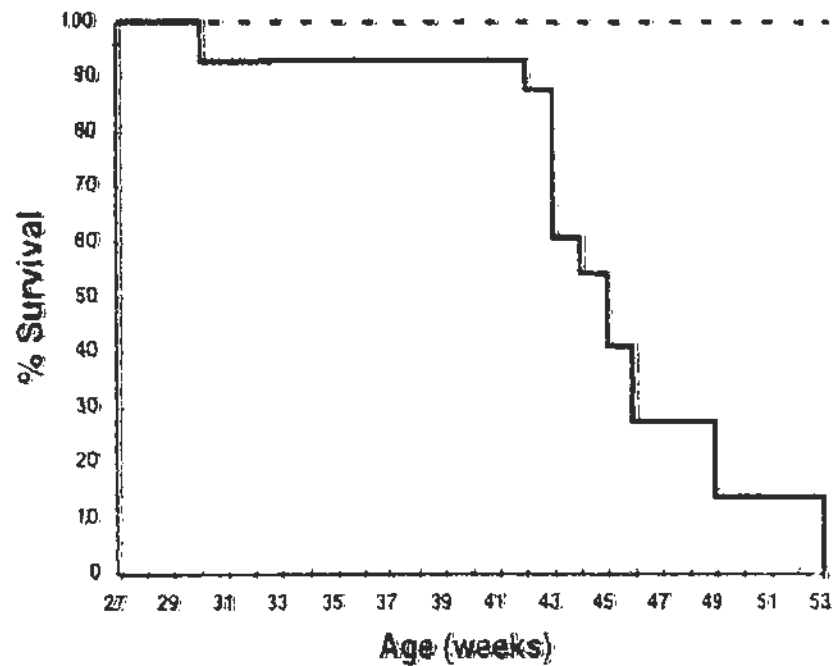
**Figure 1.4. Lifespan of HPRT$^{Q146}$ transgenic mice.** Percentage of HPRT$^{Q146}$ (solid line, n = 15) and wild-type non-transgenic (dash line, n = 17) mice surviving at various ages is shown The addition of an expanded polyQ domain (Q146) to HPRT results in premature death. (adapted from Ordway et al., 1997).

## 1.7 Research Plan of the Present Project

### 1.7.1 Project Objective

Although most of the classical nuclear transport signals carried by the nine known polyQ disease proteins are well characterized (Table 1.2), the nucleocytoplasmic transport properties of the expanded polyQ domain *per se* remain largely undefined. This project aims at 1) studying the effects of karyopherins on the subcellular localization of mutant polyQ proteins; 2) characterizing the roles of karyopherins on nuclear transport of mutant polyQ proteins; 3) investigating the modulatory effects of select karyopherins on polyQ toxicity; and 4) elucidating the mechanisms of which the karyopherins adopt to modulate polyQ toxicity.

### 1.7.2 Experimental Models

#### 1.7.2.1 *In vitro* Cell Culture Model

Both *Drosophila* and mammalian cultured cells have been employed in the present study. Owing to its neuronal characteristics (Ui et al., 1994), *Drosophila* BG2 cells, which have also been employed previously for polyQ studies (Kanuka et al., 2003; Nelson et al., 2005), were used to determine the effects of karyopherins on subcellular localization of mutant polyQ aggregates by means of RNA interference (RNAi).

Human embryonic kidney (HEK) 293 cells were used in live-cell imaging and biochemical analyses. HEK 293 cells were chosen because of its neuronal characteristics (Shaw et al., 2002) and its established use in nucleocytoplasmic transport studies of cellular proteins (Iosef et al., 2008; Julien et al., 2003; Kim et al., 2003). It is also widely used in different polyQ studies (Cornett et al., 2005; Klement et al., 1998; Perez et al., 1999). Human neuroblastoma cell line SH-SY5Y was also employed in the present study because of its neuronal properties (Encinas et al., 2000).

### 1.7.2.2 *In vivo Drosophila* Model

Being one of the best-studied and genetically-amenable organisms, *Drosophila* is instrumental to the dissection of conserved genetic pathways from flies to humans (Carpenter and Sabatini, 2004). For example, the regulatory roles of nucleoporins Nup88 and Nup214, proteins components of NPCs, on nuclear transport are first described in *Drosophila* (Roth et al., 2003) and later verified in mammalian systems (Bernad et al., 2004; Hutten and Kehlenbach, 2006). This demonstrates the evolutionary convergence of protein nuclear transport regulation between the two species (Bernad et al., 2004; Hutten and Kehlenbach, 2006; Roth et al., 2003). Furthermore, approximately 75% of human genes known to be associated with diseases have *Drosophila* orthologs (Reiter et al., 2001). Genetic conservation, together with its relatively short life-cycle (about 10 days at 25°C,

25

Introduction

Fig. 1.5) and ability to produce large number of progenies, makes *Drosophila* an excellent *in vivo* model for the study of human diseases (Bier, 2005). In particular, the recapitulation of many developmental and mechanistic processes of the mammalian nervous system in *Drosophila* (Nichols, 2006) highlights its usefulness for the study of neurodegenerative disorders (Bilen and Bonini, 2005; Marsh and Thompson, 2006).

The first *Drosophila* model of polyQ disease was described in 1998 for SCA3 (Warrick et al., 1998). Hereafter, numerous transgenic fly models have been developed for various polyQ disorders to study aspects such as the suppressive effects of molecular chaperones, disruption of axonal transport and impairment of protein clearance machinery (Marsh and Thompson, 2006). *Drosophila* was employed in the present study to elucidate the effects of karyopherins on polyQ toxicity.

## 1.7.3 Significance of the Present Study

This study brings insights into the mechanisms underlying the nucleocytoplasmic localization of mutant polyQ disease proteins governed by expanded polyQ domain, thus providing leads to a better understanding on how nuclear transport of mutant polyQ protein is involved in the progressive degeneration of polyglutaminopathies.
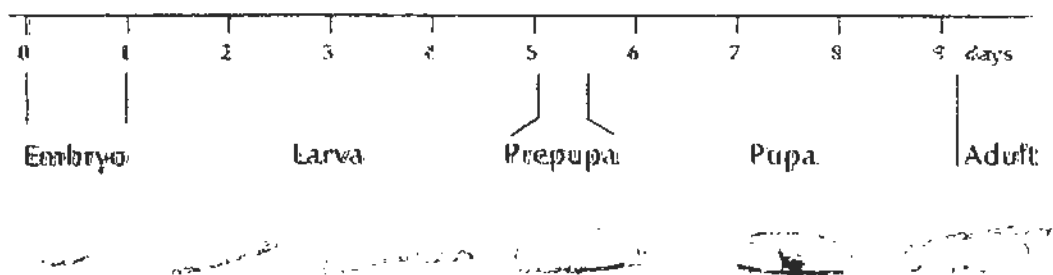
**Figure 1.5. The life-cycle of *Drosophila*.** Developmental stages of *Drosophila* include embryonic, larval, prepupal, pupal and adult. The entire cycle takes about 10 days to finish at 25°C. (adapted from thummel.genetics.utah.edu/text/research.html)

## *2. Materials and Methods*

### 2.1 Molecular Cloning

### 2.1.1 DNA Primers

Oligonucleotides used in this study are listed in Table 2.1 and they were either synthesized by Invitrogen Life Technologies (Carlsbad, CA, USA) or Tech Dragon Ltd. (HKSAR, China). The lyophilized primers were reconstituted in autoclaved double distilled water to a stock concentration of 100 $\mu$M. A working solution of 10 $\mu$M was diluted from the stock solution by autoclaved double distilled water. Both the stock and working solutions were kept at -20°C.

**Table 2.1. Primers used in plasmid construction.**

| Plasmid | Primer | Sequence | Product Size (bp) |
|---|---|---|---|
| *pMTv5-* | *Kpnl-EGFP-F* | 5'GGGTACCATGGCTCATAGGAGTAAAGGAG 3' | Q27: 890 |
| *EGFP-Q27-Q75-FLAG* | *Notl-FLAG-PolyQ-R* | 5'TGCGGCCGCTCATCACTTATC 3' | Q75: 1,034 |
| *pcDNA3.1-EGFP* | *Kpnl-EGFP-F* | 5'GGGTACCATGGCTCATAGGAGTAAAGGAG 3' | 741 |
| | *EcoRI-EGFP-R* | 5'TTAGAATTCCATATGTTGTATAGTTC 3' | |
| *pcDNA3.1-EGFP2* | *EcoRI-EGFP-F* | 5'TTAGAATTCATGGCTCATAGGAGTAAA 3' | 743 |
| | *Notl-EGFP-R* | 5'GATGCGGCCGCCATATGTTTGTATAGTTC 3' | |
| *pcDNA3.1-EGFP3* | *Notl-EGFP-F* | 5'TTAGCGGCCGCTATGGCTCATAGGAGTAAA 3' | 746 |
| | *Xbal-STOP-EGFP-R* | 5'TAATCTAGATTACATATGTTTGTATAGTTC 3' | |
| *pcDNA3.1-EGFP2GST* | *Notl-GST-F* | 5'CTAGCGGCCGCCTATGTCCCCTATACTAGGTTAT 3' | 741 |
| | *Xbal-FLAG-GST-R* | 5'TAATCTAGATTACTTATCGTCATCGTCCTTGTAATCCGCTGCAGATGTCGAGCTCGGA 3' | |
| *pcDNA3.1-Q26-Q75-EGFP2GST* | *Kpnl-PolyQ-F* | 5'GCGGTACCATGTTTGAAAAACAGCAG 3' | Q26: 120 |
| | *Kpnl-PolyQ-R* | 5'TGCGGTACCTCCTGATAGGTCCCG 3' | Q75: 267 |
| *pcDNA3.1-NLS-EGFP2GST* | *Kpnl-NLS-F* | 5'CATGCCACCAAGAAGAAGAGCGTAAGGTAGGTAC 3' | 33 |
| | *Kpnl-NLS-R* | 5'CTACCTTACGCTCTTCTTGGTGGCATGGTAC 3' | |
| *pcDNA3.1-trMJDQ-6-FLAG* | *EcoRI-FLAG-trMJD-F* | 5'TTGAATTCATGGATTACAAGGACGATGACGATAAGGATGAAGCCTACTTTGAAAAA 3' | 423 |
| | *Xbal-STOP-trMJD-R* | 5'AGTCTAGATTATGTCAGATAAAGTGTGAA 3' | |

Restriction sites used in cloning are bolded and underlined.

## 2.1.2 Polymerase Chain Reaction (PCR)

<u>1) Phusion High Fidelity DNA Polymerase</u>

The DNA fragments used in plasmid construction were amplified by Phusion high fidelity DNA polymerase (New England Biolabs, Ipswich, MA, USA) on an i-Cycler thermocycler (Bio-Rad Laboratories, Hercules, CA, USA). Templates used are specified in Section 2.1.12. The PCR amplification began with an initial denaturation of 2 minutes at 98°C, followed by 30 amplification cycles consisting of a 20-second denaturation step at 98°C, a 15-second annealing step at 55°C and an extension step at 72°C. Depending on the PCR product size, the extension time in the final step of the amplification cycle was adjusted accordingly based on the processing rate of the enzyme at 2 kbp/minute. The reactions were set up according to Table 2.2.

**Table 2.2. Reaction components for PCR with Phusion DNA polymerase.**

|  | Volume (µl) |
|---|---|
| 5X Buffer HF | 10 |
| 20 mM dNTPs | 0.5 |
| 10 µM primer F | 2.5 |
| 10 µM primer R | 2.5 |
| Template | 0.1 |
| Autoclaved $H_2O$ | 34.1 |
| Phusion DNA polymerase (2 U/µl) | 0.3 |
| Total: | 50 |

## 2) Low Fidelity *Taq* DNA Polymerase

The transformed bacterial colonies were first checked by PCR using the low fidelity *Taq* DNA polymerase (GeneSys Ltd., UK). Bacterial cells, served as PCR templates, were streaked from the agar plates to PCR tubes by toothpicks. The reaction mixture was initially denatured for 5 minutes at 95°C, followed by 25 amplification cycles consisting of a 30-second denaturation step at 95°C, a 30-second annealing step at 50°C and an extension step at 72°C. Depending on the PCR product size, the extension time in the final step of the amplification cycle was adjusted accordingly based on the processing rate of the enzyme at 1 kbp/minute. The reactions were set up according to Table 2.3.

**Table 2.3. Reaction components for PCR with *Taq* DNA polymerase.**

|  | Volume (µl) |
|---|---|
| 10X reaction buffer | 2.5 |
| 25 mM MgCl$_2$ | 1.5 |
| 20 mM dNTPs | 0.25 |
| 10 µM primer F | 0.5 |
| 10 µM primer R | 0.5 |
| Autoclaved H$_2$O | 19.55 |
| *Taq* DNA Polymerase (5 U/µl) | 0.2 |
| Total: | 25 |

**2.1.3 Preparation of Adult Fly Extracts**

**2.1.3.1 Reagents**

<u>1) Proteinase K Stock Solution</u>

Storage buffer for proteinase K was prepared by dissolving 0.12 g of Tris base (10 mM), 0.28 g of $CaCl_2$ (25 mM) and 50 ml of glycerol (50%, v/v) in double distilled water to a total volume of 100 ml with pH value adjusted to 7.5. For every 10 ml of storage buffer, 0.1 g of proteinase K powder (Sigma, St. Louis, MO, USA) was added to make up a stock solution of 10 mg/ml. The proteinase K stock solution was stored as aliquots at -20°C.

<u>2) Squishing Buffer</u>

Squishing buffer was prepared by dissolving 0.06 g of Tris base (10 mM), 0.07 g of NaCl (25 mM) and 0.1 ml of 0.5 M EDTA (1 mM) in double distilled water to a total volume of 50 ml with pH value adjusted to 8.2. The stock solution was stored at 4°C. Squishing buffer (50 µl) was freshly supplemented with 1 µl of proteinase K stock solution (200 µg/ml) immediately before use.

**2.1.3.2 Procedures**

One adult fly was mashed for 10 seconds with a pipette tip in a micro-centrifuge tube. Fifty microliters of squishing buffer was added and the homogenate was incubated at 37°C

for 30 minutes. Proteinase K was then inactivated at 85°C for 2 minutes. The extract was

used directly as PCR template or stored at 4°C for future use.

## 2.1.4 Agarose Gel Electrophoresis

### 2.1.4.1 Reagents

1) 6X DNA Gel Loading Solution

DNA gel loading solution (6X) was prepared by dissolving 0.125 g of bromophenol blue

(0.25%, w/v), 0.125 g of xylene cyanol FF (0.25%, w/v) and 20 ml of glycerol (40%, v/v)

in double distilled water to a total volume of 50 ml. Aliquots were stored at 4°C.

2) Tris-borate-EDTA (TBE) Buffer

Stock TBE buffer (5X) was prepared by dissolving 54 g of Tris base (0.45 M), 27.5 g of

boric acid (0.45 M) and 20 ml of 0.5 M EDTA, pH 8.0 (0.01 M) in double distilled water to

a total volume of 1 L. Working solution (1X) was prepared by diluting the stock solution

5-fold in double distilled water. Both stock and working solutions were kept at room

temperature.

3) Ethidium Bromide Solution

Stock solution (10 mg/ml) of ethidium bromide (Amresco, Ohio, USA) was kept in dark at

room temperature.

4) DNA Markers

The GeneRuler™ DNA markers were purchased from Fermentus (Hanover, MD, USA). The working solution was prepared by mixing 1 volume of stock DNA markers and 1 volume of 6X gel loading solution with 4 volumes of autoclaved double distilled water. The stock solution was kept at -20°C while the working solution was stored at 4°C.

## 2.1.4.2 Procedures

DNA fragments were mixed with 6X gel loading solution and separated on 1% (w/v) agarose gel (Bio-Rad Laboratories, Hercules, CA, USA) in 1X TBE buffer. For every 20 ml of agarose gel solution, 1 µl of stock ethidium bromide solution was added. Working DNA markers (1.5 µl) was loaded alongside with DNA fragments for size estimation.

## 2.1.5 Restriction Digestion

Restriction enzymes were purchased from New England Biolabs (Ipswich, MA, USA). The buffers used in double digestion were according to the Double Digest Finder available online (http://www.neb.com/nebecomm/DoubleDigestCalculator.asp). Digestion was carried out at 37°C for either 3 hours or overnight.

**2.1.6 Removal of 5' Phosphate Groups on Linearized Plasmids**

In case of non-directional cloning, the linearized vectors were dephosphorylated by calf intestinal alkaline phosphatase (Promega Corporation, Madison, WI, USA). The digested vector DNA was incubated at 37°C for 30 minutes with the addition of 1 μl of enzyme (1 U). The enzyme was then heat-inactivated by incubating at 65°C for 15 minutes. The dephosphorylated linearized plasmids were purified by commercial DNA purification kit (Viogene, Sunnyvale, CA, USA) and either used immediately in subsequent cloning or stored at 4°C until use.

**2.1.7 Annealing of Linker Oligonucleotides**

Equal volume (5 μl each) of the 2 complementary oligonucleotides (100 μM) were mixed in a micro-centrifuge tube. To allow annealing of the 2 oligonucleotides, the mixture was put in a heat block pre-heated to 99°C, which was then turned off at the time of linker mixture was put in and allowed to cool down to room temperature. After annealing, the double-stranded oligonucleotides were phosphorylated according to Section 2.1.8.

**2.1.8 Addition of 5' Phosphate Group to Linker Oligonucleotides**

Phosphorylation was carried out using polynucleotide kinase (PNK) purchased from New England Biolabs (Ipswich, MA, USA) and reactions were set up according to Table

2.4 and performed at 37°C for 30 minutes. The enzyme was subsequently heat-inactivated at 65°C for 15 minutes. The phosphorylated linkers were either used immediately or stored at 4°C for future use.

**Table 2.4. Reaction components for DNA 5' phosphorylation reaction.**

|  | Volume ($\mu$l) |
|---|---|
| 10X PNK Buffer | 2 |
| Annealed Linker | 10 |
| 20 mM ATP solution | 1 |
| PNK (5 U/$\mu$l) | 0.5 |
| Autoclaved $H_2O$ | 6.5 |
| Total: | 20 |

## 2.1.9 Ligation Reaction

Ligation reaction was carried out using T4 DNA ligase purchased from New England Biolabs (Ipswich, MA, USA). Reaction was carried out at either room temperature for more than 1 hour or 16°C overnight.

## 2.1.10 BacterialTransformation

### 2.1.10.1 Reagent

1) Ampicillin Stock Solution

Stock ampicillin solution was prepared at a concentration of 5 mg/ml in autoclaved double distilled water. After sterilization through a 0.22 $\mu$m filter unit (Millipore, Billerica, MA,

USA), it was kept as aliquots at -20°C.

## 2.1.10.2 Procedures

Competent *E. coli* bacterial cells (DH5α) stored at -70°C were thawed on ice. After the addition of ligation product (10 µl) prepared from Section 2.1.9, the ligation product/competent cells mixture were put on ice for 15 minutes, followed by a 2-minute heat shock treatment at 42°C and a 2-minute recovery time on ice. Autoclaved Luria-Bertani (LB) broth (800 µl) was then added and the transformed competent cells were cultured at 37°C for 30 minutes. The bacterial cells were then pelleted at 13,000 x $g$ for 30 seconds at room temperature. The recovered cell pellet was resuspended in 100 µl of LB broth and spread over LB agar plates with 50 µg/ml amplicillin.

## 2.1.11 Bacterial Glycerol Stock for Long-term Storage

After confirming the identity and accuracy of the cloned DNA by DNA sequencing, overnight bacterial culture in LB broth containing ampicillin (50 µg/ml) and 15% glycerol was prepared for long-term storage at -70°C.

**2.1.12 Procedures for Generating Recombinant DNA Constructs**

1) *pMT/v5-EGFP-Q27-FLAG* and *pMT/v5-EGFP-Q75-FLAG*

The *EGFP-polyQ* fragments were PCR-amplified from *pUAST-EGFP-Q27* (Echo Chan and Edwin Chan, unpublished material) and *pUAST-EGFP-Q76* (Wong et al., 2008) plasmids by the primers *Kpn*I-*EGFP*-F and *Not*I-*FLAG-PolyQ*-R (Table 2.1). The PCR-amplified DNA fragments were restriction digested and cloned into *pMT/v5-A* vector at *Kpn*I and *Not*I sites (Invitrogen, Carlsbad, CA, USA). DNA sequencing was performed to determine the accuracy of the *EGFP* and *FLAG* sequences and the number of *CAG* repeats.

2) *pcDNA3.1-Q26-EGFP2GST* and *pcDNA3.1-Q75-EGFP2GST*

The *EGFP2GST* insert was cloned via 3 consecutive rounds of PCR cloning. The first *EGFP* fragment was amplified from *pMT/v5-EGFP-Q27-FLAG* by primers *Kpn*I-*EGFP*-F and *EcoR*I-*EGFP*-R (Table 2.1). The PCR fragment was digested by restriction enzymes and cloned into *pcDNA3.1/neo(+)* at *Kpn*I and *EcoR*I sites (Invitrogen, Carlsbad, CA, USA). Sequence accuracy was confirmed by DNA sequencing. The second *EGFP* fragment was amplified using primers *EcoR*I-*EGFP*-F and *Not*I-*EGFP*-R (Table 2.1) and cloned into *pcDNA3.1-EGFP* generated in the previous step at *EcoR*I and *Not*I sites. DNA sequencing was performed to determine sequence accuracy. The *glutathione-S-transferase*

(*GST*) fragment was amplified from the *pGEX-6P* vector (GE Healthcare, Uppsala, Sweden) by primers *Not*I-*GST*-F and *Xba*I-*FLAG-GST*-R (Table 2.1) with DNA sequence encoding a FLAG tag at the 5' end of the reverse primer. The *GST* fragment was then cloned into *pcDNA3.1-EGFP2* generated previously at *Not*I and *Xba*I sites. Sequence accuracy was confirmed by DNA sequencing. The *polyQ* sequences (Q26 and Q75) were amplified by primers *Kpn*I-*PolyQ*-F and *Kpn*I-*PolyQ*-R (Table 2.1) from *pMT/v5-EGFP-Q27/Q75-FLAG* constructs generated in Section 2.1.12.1 and non-directionally cloned into *pcDNA3.1-EGFP2GST* at the *Kpn*I site. The *CAG* repeat lengths were determined by DNA sequencing.

### 3) *pcDNA3.1-NLS-EGFP2GST*

Annealed oligonucleotides encoding the NLS sequence from SV40 large T antigen (PKKKRKVG, (Kalderon et al., 1984)) was cloned into the *pcDNA3.1-EGFP2GST* plasmid generated in Section 2.1.12.2. The *Kpn*I-digested *pcDNA3.1-EGP2GST* plasmid was dephosphorylated as described in Section 2.1.6, and the linker oligonucleotides (*Kpn*I-*NLS*-F and *Kpn*I-*NLS*-R; Table 2.1) were annealed and phosphorylated according to Sections 2.1.7 and 2.1.8 respectively. Ligation was carried out between the dephosphorylated *Kpn*I-digested *pcDNA3.1-EGFP2GST* plasmid and the phosphorylated *NLS* linker.

## 4) *pcDNA3.1-EGFP3*

An *EGFP* fragment was amplified using the primers *Not*I-*EGFP*-F and *Xba*I-*STOP-EGFP*-R (Table 2.1) and cloned into *pcDNA3.1-EGFP2* generated in Section 2.1.11.2 at *Not*I and *Xba*I sites. DNA sequencing was performed to determine sequence accuracy.

## 5) *pcDNA3.1-trMJDQ76*

The truncated *MJDQ76* fragment was amplified from an adult fly carrying the *MJDtrQ78* transgene (Warrick et al., 1998) using primers *EcoRI-FLAG-trMJD*-F and *Xba*I-*STOP-trMJD*-R (Table 2.1). After restriction digestion, the inserts were cloned into *pcDNA3.1/neo(+)* at *EcoR*I and *Xba*I sites. Sequence accuracy and *CAG* repeat number were determined by DNA sequencing.

**2.1.13 Other Constructs**

The following plasmids were generous gifts from other laboratories. The *pcDNA3.1-EGFP-Q19-myc*, *pcDNA3.1-EGFP-Q81-myc*, *pcDNA3.1-EGFP-Q75P2-myc*, and *pcDNA3.1-EGFP-Q73P7-myc* constructs were obtained from Dr. Y. Nagai of Hokkaido University, Japan (Takahashi et al., 2007). The *pCMV-Htt$_{1-550}$Q83-FLAG* construct was an unpublished material from Dr. K.F. Lau from The Chinese University of Hong Kong, Hong Kong.

## 2.2 Double-stranded RNAs Synthesis

### 2.2.1 DNA Primers

Primers used in the synthesis of double-stranded RNAs (dsRNAs) are shown in Table 2.5. To allow transcription, *T7* promoter sequence (5' TAATACGACTCACTATAGGGAGA 3') is present at the 5' end of each oligonucleotide. These primers were handled the same way as DNA primers used for molecular cloning as described in Section 2.1.1.

**Table 2.5. Primers used for dsRNAs synthesis.**

| Primer | Sequence | Product Size (bp) |
|---|---|---|
| *T7 promoter* | 5' TAATACGACTCACTATAGGGAGA 3' | *LacZ*: 500 |
| *T7-dsEGFP*-F | 5' TAATACGACTCACTATAGGGAGAGATGGAGTTGTCCCAATTCTTGT 3' | 545 |
| *T7-dsEGFP*-R | 5' TAATACGACTCACTATAGGGAGAGCTTCCATCTTCAATGTTGTG 3' | |
| *T7-emb*-F | 5' TAATACGACTCACTATAGGGAGAAAGGAGCACGGCAAACTG 3' | 550 |
| *T7-emb*-R | 5' TAATACGACTCACTATAGGGAGACCAATGGCCCAGCACAAC 3' | |
| *T7-fra*-F | 5' TAATACGACTCACTATAGGGAGACGCGAATACCTCAAATACG 3' | 550 |
| *T7-fra*-R | 5' TAATACGACTCACTATAGGGAGAGAGCCGCCGGCTTGAGATCCA 3' | |
| *T7-jra*-F | 5' TAATACGACTCACTATAGGGAGATCGCACCACTGGTCATCAACT 3' | 556 |
| *T7-jra*-R | 5' TAATACGACTCACTATAGGGAGATTAAGTACCTTCACGCGATCC 3' | |
| *T7-kapα3*-F | 5' TAATACGACTCACTATAGGGAGACGCCCTCCTTTCGGATCTT 3' | 502 |
| *T7-kapα3*-R | 5' TAATACGACTCACTATAGGGAGAGGCCCTGGGCAACATCA 3' | |

## 2.2.2 Production of DNA Templates for Double-stranded RNAs Synthesis

The template used in dsRNA synthesis was generated by PCR using *Taq* DNA polymerase (Table 2.3). One microliter of cDNA prepared from *Drosophila* BG2 cells (Section 2.5) was used to replace 1 µl of autoclaved water as templates. For *LacZ*, DNA template was provided by Dr. Norbert Perrimon (Harvard Medical School, Boston, MA, USA) and its template for dsRNA synthesis was amplified by standard T7 promoter primer (Table 2.5). Owing to the presence of the 23-bp *T7* promoter sequence at the 5' end of both the forward and reverse primers, the templates were amplified by a 2-step PCR protocol. The first step was performed at a lower annealing temperature (50°C) for 5 cycles, which allows the generation of *T7* promoter-containing template. The second step was then performed at the predicted $T_m$ of the primers (65°C) for 30 cycles, which allows specific amplification of targets. The denaturation and extension steps are described in Section 2.1.2. After checking the product size by agarose gel electrophoresis (1% (w/v); Section 2.1.4), the PCR products were used directly in dsRNA synthesis without purification or stored at -20°C for future use.

## 2.2.3 Synthesis, Purification and Quantification of Double-stranded RNAs

The dsRNAs were synthesized by the MEGAscript T7 Kit (Ambion, Austin, TX, USA) according to manufacturer's instructions. The reaction mixture was prepared at room

44

temperature and components were added in the sequence presented in Table 2.6. The tubes

were then mixed by gentle flicking, followed by a brief centrifugation step to collect all the

reaction mixture to the bottom of the tube. Reaction was allowed to take place at 37°C

overnight. On the following day, the DNA template was digested by TURBO DNase (1

µl/reaction) provided by the kit at 37°C for 15 minutes. The dsRNAs were then purified by

the NucAway Spin Column (Ambion, Austin, TX, USA) according to manufacturer's

instructions. The quality of the synthesized dsRNAs was determined by agarose gel

electrophoresis (1% (w/v); Section 2.1.4), and dsRNA concentration was measured using a

BioPhotometer (Eppendorf, hamburg, Germany). The purified dsRNAs were stored at

-20°C.

**Table 2.6. Reaction components for dsRNAs synthesis.**

|  | Volume (µl) |
| --- | --- |
| 4 ribonucleotides solution (75 mM) | 2 @ |
| PCR product | 8 |
| 10X reaction buffer | 2 |
| enzyme mix | 2 |
| Total: | 20 |

## 2.3 Cell Culture

### 2.3.1 Reagents

<u>1) Serum Free M3 Medium</u>

The Shield and Sang M3 medium was prepared by dissolving one pack of powder (Sigma, St. Louis, MO, USA) in 1 L of double distilled water supplemented with 0.5 g of potassium hydrogencarbonate, and the pH value was adjusted to 6.6. After pH adjustment, 2.5 g of bactopeptone and 1 g of yeast extract were added. The medium was first filtered sterilized through a 0.45 $\mu$m bench-top filter unit followed by a 0.22 $\mu$m filter unit (Millipore, Billerica, MA, USA) inside a cell culture hood. The filtered medium was stored at 4°C.

<u>2) Complete M3 Medium</u>

Complete M3 medium composed of 10% heat-inactivated fetal bovine serum (FBS, Invitrogen, Carlsbad, CA, USA), 1% penicillin-streptomycin antibiotic mixture (P/S, Invitrogen, Carlsbad, CA, USA) and 10 $\mu$g/ml insulin (Sigma, St. Louis, MO, USA).

<u>3) Complete DMEM</u>

The high glucose DMEM was prepared by dissolving one pack of powder (Invitrogen, Carlsbad, CA, USA) in 1 L of double distilled water supplemented with 3.7 g of sodium bicarbonate. The medium was adjusted to pH 7.2 - 7.4 and sterilized by filtration through a

0.22 μm filter (Millipore, Billerica, MA, USA) in a cell culture hood. Complete DMEM contained 10% FBS (JRH Biosciences, Victoria, Australia) and 1% P/S (Invitrogen, Carlsbad, CA, USA).

## 4) Complete MEM

Liquid MEM was purchased from Hyclone (Logan, UT, USA). Complete MEM composed of 20% FBS (JRH Biosciences, Victoria, Australia) and 1% P/S (Invitrogen, Carlsbad, CA, USA).

## 5) Phosphate Buffered Saline (PBS)

Stock PBS solution (10X) was prepared by dissolving 80 g of NaCl (1.37 M), 2 g of KCl (27 mM), 14.4 g of $Na_2HPO_4$ (100 mM) and 2.4 g of $KH_2PO_4$ (20 mM) in 1 L of double distilled water. Working PBS solution (1X) was prepared by 10-fold dilution of the stock solution.

## 6) Stock Copper Sulphate ($CuSO_4$) Solution

Stock $CuSO_4$ solution (0.1 M) was prepared by dissolving 1.25 g of $CuSO_4$ powder in 50 ml of double distilled water, followed by filtration through a 0.22 μm filter unit (Millipore, Billerica, MA, USA) in a cell culture hood and stored at 4°C.

## 7) Stock G418 Solution

Stock G418 solution (Calbiochem, Gibbstown, NJ, USA) was prepared at a concentration of 50 mg/ml in 1X PBS. The stock solution was sterilized by filtration through a 0.22 µm filter unit (Millipore, Billerica, MA, USA) and stored in dark at 4°C.

## 8) Stock Poly-D-lysine Solution

Stock poly-D-lysine solution (Sigma, St. Louis, MO, USA) was prepared at a concentration of 30 mg/ml in 1X PBS and kept at -20°C.

## 9) Stock Retinoic Acid Solution

Stock *all-trans* retinoic acid (Sigma, St. Louis, MO, USA) was prepared at a concentration of 20 mM in DMSO and stored in aliquots at -70°C.

### 2.3.2 *Drosophila* Cultured Cells

The *Drosophila* neuronal DmBG2-c6 (BG2) cells were purchased from *Drosophila* Genomics Resource Center (Bloomington, IN, USA) and maintained in complete M3 medium. To sub-culture BG2 cells, cell scraper was first used to detach the cells from culture flasks after cells had been grown for 4-5 days and, the detached cells were transferred to new culture flasks at a dilution of 1:10. Since the growth of BG2 cells was density-dependent, the sub-culture dilution should not be over 1:10.

### 2.3.2.1 Effects of Copper Sulphate on Growth of BG2 Cells

The growth rate of BG2 cells treated with different concentrations of $CuSO_4$ was measured. BG2 cells seeded at a density of $2 \times 10^5$ cells/well were allowed to settle on 24-well plates overnight at 25°C. After being synchronized in serum free M3 medium for 48 hours at 25°C, BG2 cells were cultured in complete M3 medium containing different concentrations of $CuSO_4$ (0, 0.5, 0.8, 1 and 2 mM). At 48, 96 and 144 hours post treatment, BG2 cells were scraped off from wells and cell number was counted by a haemocytometer (Sigma, St. Louis, MO, USA). Data from four wells were collected to calculate the mean values and standard deviation (S.D.) of cell number. Mean differences of cell number between time points and $CuSO_4$ concentrations were compared by two-tailed, unpaired Student's t-test, and statistical significance was demonstrated by a $p$-value of less than

49

0.05.

## 2.3.2.2 Establishment of Stable BG2 Cells

Transfection of BG2 cells with *pMT/v5-EGFP-polyQ-FLAG* constructs was performed using Cellfectin reagent (Invitrogen, Carlsbad, CA, USA). One day prior to transfection, $2 \times 10^6$ cells were seeded on 6-well plates. In each well, 2 μg of *pMT/v5-EGFP-polyQ* construct and 0.1 μg of the *pHSneo* selection vector, which carries the G418 resistance gene, were mixed with 6 μl of Cellfectin in 200 μl of serum free M3 medium. After a 30-minute incubation period, 800 μl of serum free M3 medium was added. BG2 cells were incubated with the diluted Cellfectin-DNA complex at 25°C overnight. Fresh complete M3 medium was then used to replace the transfection mix at 24 hours post-transfection. On the following day, cells were scraped off and split at a dilution of 1:5 to new wells. Starting from 72 hours post-transfection, G418-containing complete M3 medium was used to culture and select for transfected cells in the culture wells. The initial concentration of G418 used was 1 mg/ml, and was further increased to 1.5 mg/ml 5 days later. After another 5 days of incubation, the G418 concentration was further increased to 2 mg/ml and selection continued at this concentration for ~1 month. After checking the expression of EGFP-polyQ proteins by fluorescence microscopy (Section 2.6.4) and Western blotting (Section 2.10), the stably transfected cells were used for further

experiments. Frozen stocks were prepared using complete M3 medium supplemented with

10% DMSO (Sigma, St. Louis, MO, USA) and the cells were stored in liquid nitrogen.

### 2.3.2.3 RNA Interference Experiments in BG2 Cells

RNA interference experiments were performed on stably transfected BG2 cells

generated in Section 2.3.2.2. On the day of dsRNA treatment, $2 \times 10^5$ cells were seeded on

wells of 24-well plates containing 500 µl of serum free M3 medium. Double stranded

RNAs were added to cells at a concentration of 3 µg/well (in 10 µl DEPC-treated $H_2O$)

followed by manual vigorous shaking for 15 seconds. After a 30-minute incubation period

at room temperature, 500 µl of 20% FBS-containing M3 medium was added to the wells.

The cells were then incubated at 25°C for 3 days. At the end of the 3-day incubation period,

copper sulphate was added to a final concentration of 1 mM to induce *EGFP-polyQ*

transgene expression. At 72 hours post-induction, cells were scraped off and re-plated on

new wells to minimize cell clumping at the time of imaging. At 96 hours post-induction,

cells were either subjected to RNA extraction (Section 2.5) or fixed with 3.7%

formaldehyde (Sigma, St. Louis, MO, USA) for fluorescence microscopy (Section 2.6).

The nuclear to cytoplasmic ratio of EGFP-Q75 aggregates was determined according

to (Sabri et al., 2007). In brief, the ratio was calculated as the number of cells with nuclear

aggregates / the number of cells with cytoplasmic aggregates. The subcellular localization of EGFP-Q75 aggregates of at least 100 individual cells was analyzed in each single experiment. Data collected from three independent sets of dsRNA-treated cells were used to calculate the mean values and S.D.. Mean differences between the water-treated control and dsRNA-treated experimental groups were compared by two-tailed, unpaired Student's t-test, and statistical significance was demonstrated by a $p$-value of less than 0.05.

### 2.3.3 Mammalian Cultured Cells

### 2.3.3.1 Human Embryonic Kidney 293 Cells

The human embryonic kidney 293 (HEK 293) cells (Invitrogen, Carlsbad, CA, USA) were generous gift from Dr. Faye S.Y. Tsang from The Chinese University of Hong Kong, Hong Kong. The HEK 293 cells were maintained in complete DMEM in a 37°C humidified incubator supplemented with 5% $CO_2$. To sub-culture HEK 293 cells, trypsin-EDTA (0.05%) solution (Invitrogen, Carlsbad, CA, USA) was applied to detach cells from culture flasks.

Cells were seeded on either 6- or 24-well plates one day prior to transfection. Transfection experiments were performed with Lipofectamine 2000 (Invitrogen, Carlsbad, CA, USA) in Opti-MEM (Invitrogen, Carlsbad, CA, USA). The DNA to transfection reagent ratio was fixed at 1 μg : 2.5 μl, and the DNA-transfection mix was prepared according to Table 2.7 followed by a room temperature incubation period for 20 minutes. Subsequently, additional Opti-MEM was added to the DNA-transfection mix. At the same time, the complete DMEM was removed from the culture plates and cells were overlaid with the diluted DNA-transfection mix. After an incubation period of 4-6 hours at 37°C, the DNA-transfection mix was replaced by complete DMEM and cells were harvested at specific time points.

**Table 2.7. Transfection mix for HEK 293 cells.**

|  | 6-well plate | 24-well plate |
| --- | --- | --- |
| Cell Density | $1 \times 10^6$ | $2 \times 10^5$ |
| Plasmid DNA ($\mu$g) | 2 | 0.4 |
| Lipofectamine 2000 ($\mu$l) | 5 | 1 |
| Opti-MEM during 20-minute incubation ($\mu$l) | 200 | 40 |
| Opti-MEM added for incubation with cells ($\mu$l) | 800 | 260 |
| Complete DMEM added for cell recovery ($\mu$l) | 1,500 | 500 |
| Experiments | immunoprecipitation | fluorescence microscopy, total protein and nucleocytoplasmic protein extraction |

For fluorescence microscopy, transfected HEK 293 cells were passed at a dilution of

1:3 at 24 hours post-transfection and seeded on new 24-well plates containing

poly-D-lysine-coated cover-slips (Paul Marienfeld GmbH & Co., Lauda-Koenigshofen,

Germany). To coat cover-slips, they were first sterilized with 70% ethanol inside a cell

culture hood and then incubated in solution containing 5 $\mu$g/ml poly-D-lysine in 1X PBS

overnight. Cells seeded on cover-slips were fixed with 3.7% formaldehyde (Sigma, St.

Louis, MO, USA) and then subjected to fluorescence microscopy (Section 2.6) at 48 hours

post-transfection.

### 2.3.3.2 Human Neuronal SH-SY5Y Cells

The human SH-SY5Y neuroblastoma cells (American Type Culture Collection, Manassas, VA, USA) were a generous gift of Prof. K.N. Leung from The Chinese University of Hong Kong, Hong Kong. The cells were maintained in complete MEM in a 37°C humidified incubator supplemented with 5% $CO_2$. The SH-SY5Y cells were sub-cultured at no more than 80% confluency. To subculture fells, 0.05% trypsin-EDTA solution (Invitrogen, Carlsbad, CA, USA) was applied to detach cells from culture flasks.

Transfection of SH-SY5Y cells was essentially the same as that for HEK 293 cells (Table 2.7). In brief, $2 \times 10^5$ cells were seeded on 24-well plates one day prior to transfection. The plasmid DNA to Lipofectamine 2000 ratio was set at 2 μg : 2 μl. The differentiation of transfected SH-SY5Y cells was performed as previously described (Encinas et al., 2000). One day after transfection, complete MEM was removed from wells and transfected cells were washed once with 1X PBS, followed by trypsinization at 37°C for 5 minutes. The cells were then passed at a dilution of 1:4 to new 24-well plates with uncoated cover-slip placed inside. Transfected cells were maintained in MEM containing 10% FBS and 10 μM *all-trans* retinoic acid. After a 5-day incubation period, cells were fixed with 3.7% formaldehyde (Sigma, St. Louis, MO, USA) and subjected to fluorescence microscopy (Section 2.6).

## 2.4 *Drosophila* Culture

## 2.4.1 Reagent

### 1) Cornmeal-yeast-glucose-agar medium

The fly culture medium was prepared by dissolving 12.5 g of agar (1.25%, w/v), 105 g of dextrose (10.5%, w/v), 105 g of cornmeal (10.5%, w/v) and 21 g of yeast (2.1%, w/v) in 900 ml of double distilled water. The mixture was boiled for about 20 minutes, followed by an addition of 80 ml of 1% nipagen (methyl p-hydroxybenzoate; dissolved in ethanol, Sigma, St. Louis, MO, USA) as mold inhibitor, and the mixture was made up to 1 L by double distilled water. A volume of 15 ml medium was dispensed into each plastic culture vial.

## 2.4.2 *Drosophila* Stocks and Crosses Maintenance

Fly stocks and genetic crosses were raised in cotton-plugged plastic vials containing cornmeal-yeast-glucose-agar medium and maintained in temperature-controlled incubators (LMS, UK). Depending on experiments, genetic crosses were maintained at 22°C, 25°C or 29°C. For each cross, around 3 male and 4 virgin female flies were put together in a fly vial supplemented with dry yeast. For collection of virgin females, adult flies were initially removed from vials, and virgin females were collected within 8 hours at 25°C or 16 hours at 18°C. Information of *Drosophila* stocks used in this study is summarized in Table 2.8.

**Table 2.8. Summary of *Drosophila* strains used in this study.**

| Transgenic Line | Stock Number | Genotype | Chromosomal Location | Description | Reference |
|---|---|---|---|---|---|
| *gmr-gal4* | LDR 8 | *w; gmr-gal4* | 2 | *glass multiple reporter (gmr)-gal4* is a promoter-gal4 line direct transgene expression in all eye cells posterior to the morphological furrow | Ellis et al., 1993 |
| *gmr-gal4 UAS-myc-MJDQ27* | MJDQ27 | *w; gmr-gal4, UAS-myc-MJDQ27/CyO* | 2 | For ectopic expression of myc-tagged full length human MJD protein of 27 glutamines under *gmr*-gal4 regulation | Warrick et al., 2005 |
| *gmr-gal4 UAS-myc-MJDQ84* | MJDQ84 | *w; gmr-gal4/CyO; UAS-myc-MJDQ27/MKRS* | 2; 3 | For ectopic expression of myc-tagged full length human MJD protein of 84 glutamines under *gmr*-gal4 regulation | Warrick et al., 2005 |
| *gmr-gal4 UAS-HA-MJDtrQ78 (w)* | LDR2 | *w; gmr-gal4/CyO; UAS-HA-MJDtrQ78/Tb* | 2; 3 | For ectopic expression of hemagglutinin (HA)-tagged truncated human MJD protein of 78 glutamines under *gmr*- gal4 regulation | Warrick et al., 1998 |
| *gmr-gal4 UAS-HA-MJDtrQ78 (s)* | LDR1 | *w; gmr-gal4, UAS-HA-MJDtrQ78/CyO* | 2 | For ectopic expression of hemagglutinin (HA)-tagged truncated human MJD protein of 78 glutamines under *gmr*- gal4 regulation | Warrick et al., 1998 |
| *gmr-gal4 UAS-HA-ARtrQ112* | ARtrQ112 | *w; gmr-gal4/CyO; UAS-HA-ARtrQ112/MKRS* | 2; 3 | For ectopic expression of hemagglutinin (HA)-tagged truncated human AR protein of 112 glutamines under *gmr*- gal4 regulation | Chan et al. 2002 |
| *gmr-gal4 UAS-Httexon1Q93* | Httex1Q93 | *w UAS-Httex1Q93; gmr-gal4/CyO* | X: 2 | For ectopic expression of exon1 of human huntingtin protein of 93 glutamines under *gmr*- gal4 regulation | Steffan et al. 2001 |

| Transgenic Line | Stock Number | Genotype | Chromosomal Location | Description | Reference |
|---|---|---|---|---|---|
| *gmr-gal4 UAS-EGFPQ76-FLAG* | EGFPQ76 | *w; gmr-gal4/CyO; UAS-EGFPQ76-FLAG/MKRS* | 2; 3 | For ectopic expression of FLAG-tagged EGFP protein with 76 glutamines fused to its N-terminus under *gmr-gal4* regulation | Wong et al., 2008 |
| *UAS-Hsp70* | LDR6 | *w; P{UAS-Hsap\HSPA1 L.W}53.1/CyO* | 2 | For ectopic expression of human molecular chaperone Hsp70 protein | Warrick et al., 1999 |
| *UAS-emb dsRNA* | CG13387-4(II) | *w; UAS-emb dsRNA* | 2 | For ectopic expression of dsRNA against *emb* | National Institute of Genetics, Japan |
| *EP-emb* | E128-1A | *w; emb^EP-E128-1A/CyO* | 2 | For over-expression of the endogenous *emb* gene | Bilen & Bonini, 2007 |
| *gmr-gal4 UAS-α-synucleinWT* | 8146 | *w; gmr-gal4/CyO; UAS-α-synucleinWT/ MKRS* | 2; 3 | For ectopic expression of human α-synuclein (wild-type) protein under *gmr- gal4* regulation | Auluck et al. 2002 |
| *EP-emb UAS-kap-α3 dsRNA* | 3.1 | *w; emb^EP-E128-1A UAS-kap-α3 dsRNA CyO* | 2 | For concomitant over-expression of *emb* and knockdown of *Kap-α3* expression | This study |

58

**2.4.3 Phenotypic Examination of Adult Flies External Eyes**

Adult fly eyes of appropriate genotypes and age were examined under a stereomicroscope (Olympus SZX-12, Japan). External eye images were captured by a SPOT Insight CCD camera controlled by the SPOT Advanced software (version 4.1; Diagnostic instruments Inc., Sterling Heights, MI, USA). Image processing was performed using the Adobe Photoshop CS software (Adobe, San Jose, CA, USA).

**2.4.4 Deep Pseudopupil Assay**

Adult fly heads of appropriate genotypes and age were decapitated, put in the space between 2 glass cover-slips on a glass slide, and immersed in a drop of immersion oil (Olympus, Japan). The fly heads were arranged in an orientation that the antennae were faced upward while ocelli were faced forward. A third glass cover-slip was then carefully placed on top of the other 2 glass cover-slips and to cover the fly heads. Ommatidia were examined under a light microscope (Olympus CX31, Japan) using a 60X oil objective with a numerical aperture (NA) of 1.25. Ommatidial images were captured by a SPOT Insight CCD camera controlled by the SPOT Advanced software (version 4.1; Diagnostic instruments Inc., Sterling Heights, MI, USA). Images processing was performed using the Adobe Photoshop CS software (Adobe, San Jose, CA, USA).

The ommatidia integrity was revealed by the number of rhabdomeres per ommatidium. In each experiment, at least 100 ommatidia were counted at random from 5 – 10 fly eyes, and the average number of rhabdomeres per ommatidium was determined. Each experiment was repeated independently at least for three times. Sample mean values and S.D. were calculated to determine the variation among independent experiments. The Mann-Whitney rank sum test was performed to determine mean differences of average number of rhabdomeres per ommatidium between the control group and each of the experimental groups (Figs. 3.9, 3.11 and 3.14). When the double transgenics and their single knockdown or over-expression lines were compared (Fig. 3.14), the Kruskal-Wallis one way analysis of variance (ANOVA) on ranks was performed followed by Dunn post-test. A significance of difference was determined at $p$-value of less than 0.05.

## 2.4.5 Heat Shock Treatment

Adult flies of appropriate genotypes and age were heat shocked at 37°C in an air bath for 30 minutes, followed by a 30-minute recovery period. After three rounds of heat shock treatment, fly heads were homogenized immediately in TRIZOL reagent for RNA extraction (Section 2.5).

## 2.5 Semi-quantitative Reverse Transcription-Polymerase Chain Reaction (RT-PCR)

### 2.5.1 Reagent

1) Diethyl pyrocarbonate (DEPC)-treated Water

Diethyl pyrocarbonate was added to double distilled water at a volume ratio of 1:1,000 in a chemical hood, and stirred overnight. The treated-water was then autoclaved to inactivate the DEPC. Autoclaved DEPC-treated water was kept at room temperature.

### 2.5.2 RNA Extraction from Cultured *Drosophila* Cells

RNA was extracted from BG2 cells using TRIZOL reagent (Invitrogen, Carlsbad, CA, USA) at 96 hours post-induction to check the gene knockdown efficiency of dsRNAs. Cells from each well of 24-well plates were lysed in 500 μl of TRIZOL reagent (Invitrogen, Carlsbad, CA, USA). After incubating at room temperature for 5 minutes, 100 μl of chloroform (Sigma, St. Louis, MO, USA) was added. The homogenates were vortexed vigorously for 15 seconds, followed by a 5-minute incubation period at room temperature. The homogenates were then centrifuged at 12,000 x $g$ for 15 minutes at 4°C. The upper aqueous layer was collected, and the RNA was precipitated with 500 μl of isopropanol (Sigma, St. Louis, MO, USA) at -20°C overnight. The RNA pellet was collected by centrifugation at 12,000 x $g$ for 10 minutes at 4°C, and the supernatant was discarded. The resultant RNA pellet was washed with 1 ml of 70% ethanol, and centrifuged at 12,000 x $g$

for 5 minutes at 4°C. Ethanol was then removed by aspiration. The RNA pellet was then

air-dried and dissolved in 20 µl of DEPC-treated water.

## 2.5.3 RNA Extraction from Adult *Drosophila* Heads

Ten fly heads were homogenized in 100 µl of TRIZOL reagent (Invitrogen, Carlsbad,

CA, USA) with a motorized plastic pestle (Kontes, Vineland, NJ, USA). After complete

homogenization as indicated by the disappearance of intact fly heads, an additional 700 µl

of TRIZOL reagent and 160 µl of chloroform (Sigma, St. Louis, MO, USA) were added to

the samples. The subsequent steps were essentially the same as detailed in Section 2.5.2.

## 2.5.4 Reverse Transcription (RT)

Reverse transcription was performed using oligo(dT) primer (5'

TTTTTTTTTTTTTTT 3') and ImProm-II Reverse Transcriptase (Promega Corporation,

Madison, WI, USA). The reaction mixture was prepared according to Table 2.9. For RNA

extracted from BG2 cells, 2 µg of RNA was used in each reaction. For RNA extracted from

adult fly heads, 5 µl of RNA was employed. The RNase inhibitor was purchased from

Invitrogen Life Technologies (Carlsbad, CA, USA). The RNA was first mixed with

oligo(dT) and incubated at 70°C for 5 minutes to completely denature the RNA, and then

chilled at 4°C for 2 minutes. The remaining components were subsequently added as a

master mix to the reaction mixture. The RT reaction was performed on an i-Cycler thermocycler (Bio-Rad Laboratories, Hercules, CA, USA) at 42°C for 60 minutes, followed by a heat denaturation step at 70°C for 15 minutes to inactivate the enzyme. The synthesized complementary DNA (cDNA) was diluted 2-fold by adding 20 μl of autoclaved double-distilled water and used for subsequent PCR reactions. The unused samples were stored at -20°C for future use.

**Table 2.9. Reaction components for reverse transcription.**

|  | Volume (μl) |
| --- | --- |
| RNA in DEPC-treated water | 10.6 |
| 50 μM oligo(dT) | 1 |
| 5X reaction buffer | 4 |
| 25 mM MgCl$_2$ | 2.4 |
| 20 mM dNTPs | 0.5 |
| RNase inhibitor | 0.5 |
| Reverse Transcriptase | 1 |
| Total: | 20 |

### 2.5.5 Polymerase Chain Reaction (PCR)

The primers used in PCR are shown in Tables 2.5 and 2.10. They were handled in the same way as primers used for molecular cloning as described in Section 2.1.1. The mRNA expression levels of genes of interest were examined using low fidelity *Taq* DNA polymerase (GeneSys Ltd., UK), and *β-actin* was used as loading control. Primers used are listed in Table 2.10. Reactions were set up according to Table 2.3, with the exception that

2.6 μl of 25 mM MgCl$_2$ was used for the PCR of *β-actin*. To normalize the cDNA of the samples, an initial volume of 2 μl of cDNA was added which was then adjusted according to the relative band intensities of *β-actin* amplicon between the control and experimental groups. The PCR protocols used were essentially the same as in Section 2.1.2. The exact cycle numbers for individual amplicons were adjusted empirically to ensure that the band intensity of PCR products did not reach saturation on the gel.

Band intensity of amplicons was measured by the ImageJ software (version 1.32; Research Services Branch, National Institute of Mental Health, Bethesda, MD, USA). Sample mean values and S.D. were calculated from three independent experiments. Differences in sample means were compared using Kruskal-Wallis one way ANOVA on ranks followed by Dunn post-test (Fig. 3.24). A *p* value of less than 0.05 was considered statistically significant.

**Table 2.10. Primers used for RT-PCR reactions.**

| Primer | Sequence | Product Size (bp) |
|---|---|---|
| *β-actin*-F | 5' ATGTGCAAGGCCGGTTTCGC 3' | 241 |
| *β-actin*-R | 5' CGACACGCAGCTCATTGTAG 3' | |
| *hsp22-F* | 5' GGAGTGTGGCGCTACCGA 3' | 377 |
| *hsp22-R* | 5' CCGGCTCGCCAGTCTGCT 3' | |
| *hsp40-F* | 5' CGAGCATGATCTGTTCGTGTCG 3' | 317 |
| *hsp40-F* | 5' CTGACCAGTGCCTCGCACAAG 3' | |
| *hsp70-F* | 5' AATCCTGAACGTCAGCGCCAAG 3' | 299 |
| *hsp70-R* | 5' GTGTTGCTGTCCAGCCACCG 3' | |
| *MJD-F* | 5' CGGAAGAGACGAGAAGC 3' | 237 |
| *MJD-R* | 5' GTGAAGGTAGCGAACATG 3' | |

## 2.6 Microscopy

### 2.6.1 Reagents

<u>1) Stock Solution of Hoechst 33342</u>

Stock solution of Hoechst 33342 (Molecular Probes, Invitrogen Life Technologies, Carlsbad, CA, USA) was prepared at a concentration of 5 $\mu M$ in 1X PBS and aliquots were kept at 4°C.

<u>2) Stock Propidium Iodide Solution</u>

Stock solution of propidium iodide (Sigma, St. Louis, MO, USA) was prepared at a concentration of 3 mg/ml in 1X PBS and aliquots were kept at -20°C.

<u>3) Blocking Buffer</u>

Blocking buffer containing 5% goat serum (v/v) and 0.3% Triton-X 100 (v/v) in 1X PBS was prepared freshly before use.

### 2.6.2 Staining of the Cell Nucleus

Cells seeded on cover-slips were fixed in 3.7% formaldehyde (Sigma, St. Louis, MO, USA) for 10 minutes at room temperature. After three rounds of washes by 1X PBS, each for 5 minutes, cell nuclei were labeled with either Hoechst 33342 (5 $\mu M$) or propidium

iodide (10 µg/ml) in 1X PBS at room temperature for 15 minutes. Cells were washed four times with 1X PBS, and cover-slips were mounted on glass slides using mounting medium (DAKO, Carpinteria, CA, USA). In general, 4 µl of mounting medium was used to mount one cover-slip.

### 2.6.3 Visualization of Cellular Protein by Immunostaining

The fixed cells were permeabilized in 100% ice-cold methanol for 10 minutes at -20°C. After being washed once by 1X PBS at room temperature for 5 minutes, cells were blocked in blocking buffer for 1 hour at room temperature. Primary antibody against human Lamin A/C (1:100, Cell signaling Technology, Danvers, MA, USA) was prepared in blocking buffer and cells were incubated with the primary antibody solution at 4°C overnight. On the following day, cells were washed four times at room temperature with blocking buffer, each for 5 minutes. After the final wash, cells were incubated with secondary antibody, goat anti-rabbit Cy3 (1:250, Zymed Laboratories, San Francisco, CA, USA) diluted in blocking buffer, for 2 hours in dark at room temperature. Cells were again washed four times with blocking buffer, each for 5 minutes. The cell nuclei were then labeled and samples were mounted as detailed in Section 2.6.2.

## 2.6.4 Fluorescence Microscopy

Samples were examined under a fluorescence microscope (Olympus BX51, Japan) equipped with a 40X/ NA 0.95 objective. Images were captured by a SPOT Insight CCD camera using SPOT Advanced software (version 4.1; Diagnostic Instruments Inc. Sterling Heights, MI, USA). Image processing was performed using the Adobe Photoshop CS software (Adobe, San Jose, CA, USA).

## 2.6.5 Confocal Microscopy

Confocal microscopy was performed on the TCS SP5 confocal system attached to a Leica DMI 6000 inverted microscope (Leica, Mannheim, Germany) using a 40X oil objective with NA of 1.25. Cellular images were captured by photomultiplier tubes controlled by the Leica Application Suite Advanced Fluorescence software (Leica, Mannheim, Germnay). Image processing was performed using the Adobe Photoshop CS software (Adobe, San Jose, CA, USA).

## 2.7 Protein Sample Preparation and Concentration Measurement

### 2.7.1 Reagents

1) Total Lysis Buffer

For every 50 ml of total lysis buffer, 0.12 g of Tris base (20 mM) and 1 g of SDS (2%, w/v) was dissolved in double distilled water with pH value adjusted to 8.0 using hydrochloric acid. The stock solution was stored at 4°C and warmed in a 37°C water bath before use. It was freshly supplemented with 50 mM dithiothreitol (DTT). Stock DTT solution (0.5 M) was prepared by dissolving 3.86 g of DTT powder in 50 ml of double distilled water, and aliquots were stored at -20°C.

2) Fractionation Buffer

For every 250 ml of fractionation buffer, 0.3 g of Tris base (10 mM), 0.14 g of NaCl (10 mM), 0.15 g of $MgCl_2.6H_2O$ (3 mM) and 1.25 ml of NP-40 (0.5%, v/v) was dissolved in double distilled water with pH value adjusted to 7.4 using hydrochloric acid. The stock solution was stored at 4°C and freshly supplemented with protease inhibitor cocktail (Sigma, St. Louis, MO, USA) with a 100-fold dilution.

3) Resuspension Buffer

Resuspension buffer was composed of 1 M Tris-HCl, pH 8.0 and 6X SDS sample buffer

(Section 2.10.1) at a volume ratio of 2:1. The stock Tris-HCl solution (1M) was prepared

by dissolving 6 g of Tris base in 50 ml of double distilled water with pH value adjusted to

8.0 using hydrochloric acid. It was kept at 4°C.

### 4) Bovine Serum Albumin (BSA) Standard

Stock BSA solution (Sigma, St. Louis, MO, USA) was prepared at a concentration of 1

mg/ml in double distilled water and aliquots of 500 μl were stored at −20°C.

### 2.7.2 Total Lysates Preparation

### 2.7.2.1 Cultured Cells

Cells from each well of 24-well plates were lysed in 50 μl of total lysis buffer and

samples were stored at -20°C.

### 2.7.2.2 Adult Fly Heads

Ten fly heads were homogenized in 50 μl (5 μl/head) of total lysis buffer and samples

were stored at -20°C.

### 2.7.2.3 Whole Brain Lysates from Wild-type Mice

Wild-type mice of appropriate age were scarified by cervical dislocation. The whole

brain was homogenized in total lysis buffer (w/v: 1/10). After complete homogenization, the homogenates were mixed with 6X SDS sample buffer and boiled at 99°C for 10 min. Samples were stored at -20°C for future use.

### 2.7.3 Nucleocytoplasmic Fractionation

### 2.7.3.1 Cultured Cells

Fractionation was performed as described (Cornett et al., 2005) with minor modifications. For 24-well plates, 80 µl of fractionation buffer was applied to each well after a 1X PBS wash. The cell lysates were then vortexed for 30 seconds. After a 10-minute incubation period on ice, lysates were centrifuged at 500 x *g* for 10 minutes at 4°C. The supernatant was then subjected to centrifugation at 13,000 x *g* for 5 minutes at 4°C, and stored at -20°C as the cytoplasmic fractions. The pellet was washed 3 times in 50 µl of fractionation buffer. For the first two washes, lysates were vortexed for 30 seconds, followed by centrifugation at 500 x *g* for 5 minutes at 4°C. After the final wash, lysates were centrifuged at 8,000 x *g* for 5 minutes at 4°C, and the nuclear pellet was resuspended in 50 µl of total lysis buffer and stored at -20°C.

### 2.7.3.2 Adult Fly Heads

Twelve fly heads were homogenized in 60 µl of fractionation buffer for 30 seconds.

After a 10-minute incubation period on ice, lysates were centrifuged at 500 x *g* for 10 minutes at 4°C. The supernatant was then subjected to centrifugation at 13,000 x *g* for 5 minutes at 4°C, and stored at -20°C as the cytoplasmic fractions. The pellet was washed 3 times in 50 μl of fractionation buffer with homogenization. For the first two washes, lysates were centrifuged at 500 x *g* for 5 minutes at 4°C after homogenization. Lysates in the final wash were centrifuged at 8,000 x *g* for 5 minutes at 4°C, and the nuclear pellet was resuspended in 60 μl of total lysis buffer and stored at -20°C.

## 2.7.4 Protein Assay

Protein concentration of cell lysates was determined by the DC protein assay kit (Bio-Rad Laboratories, Hercules, CA, USA), and BSA was used as standard (Sigma, St. Louis, MO, USA). Different concentrations of BSA solution (0.2, 0.4, 0.6, 0.8 and 1 mg/ml) were prepared from the 1 mg/ml stock solution by serial dilution in either total lysis or fractionation buffer. The reaction mixtures were allowed to stand at room temperature in dark for 15 minutes before absorbance at 750 nm was measured by a BioPhotometer (Eppendorf, Hamburg, Germany). The dye reagent was used as blank.

## 2.7.5 Formic Acid Treatment

For cell lysates, 5 μg of total, cytoplasmic or nuclear proteins were incubated with

100 µl of 100% formic acid at 37°C for 30 minutes. Subsequently, the formic acid was removed by SpeedVac at low speed for 1 hour. For adult fly head samples, 20 µl (corresponded to 4 heads) of cytoplasmic or nuclear fractions was incubated with 200 µl of 100% formic acid at 37°C for 30 minutes. The formic acid was subsequently removed by SpeedVac at low speed for 2 hours. The pellets after formic acid removal were resuspended in 15 µl of resuspension buffer and boiled at 99°C for 5 minutes, followed by SDS-PAGE and immunoblotting (Section 2.10).

## 2.8 Co-Immunoprecipitation

### 2.8.1 Reagent

<u>1) Exportin-1 Binding Buffer</u>

For every 500 ml of binding buffer, 2.38 g of HEPES (20 mM), 4.38 g of NaCl, 0.3 g of

$MgCl_2.6H_2O$ (3 mM) and 0.5 ml of NP-40 (0.1%, v/v) was dissolved in double distilled

water (Hakata et al., 2002). The buffer was stored at 4°C.

### 2.8.2 Procedures

Cells were first washed once with 1X PBS. For 6-well plates, 200 μl of binding buffer

was applied to each well and cell lysates were sonicated for 5 seconds at power 3 on ice for

2 times (Sonifier 150, Branson, Danbury, CT, USA). The lysates were then clarified at

16,000 x $g$ for 10 minutes at 4°C. The supernatant was collected and 20 μl was saved as

"inputs" of the reaction. For each sample, 90 μl of supernatant was incubated with (1 μl) or

without antibody at 4°C overnight with shaking. For experiments concerning

*pcDNA3.1-EGFP-Q19-myc*, *pcDNA3.1-EGFP-Q81-myc*, *pcDNA3.1-EGFP-Q75P2-myc*

and *pcDNA3.1-EGFP-Q73P7-myc* constructs (Figs. 3.18, 3.20 and 3.21), anti-myc

antibody (9B11, Cell Signaling Technology, Danvers, MA, USA) was used. For

experiments concerning *pcDNA3.1-trMJDQ76-FLAG* or *pCMV-Htt$_{1-550}$Q83-FLAG*

plasmids (Fig. 3.19), anti-FLAG antibody (M2, Sigma, St Louis, MO, USA) was used. For

the immunoprecipitation of endogenous exportin-1 protein (Fig. 3.18), anti-human exportin-1 antibody (Calbiochem, Gibbstown, NJ, USA) was used. On the following day, 20 μl of protein A-agarose fast flow beads (Sigma, St Louis, MO, USA) was washed 2 times with 1X PBS. After 1X PBS removal, lysates from the overnight incubation were applied and incubated at 4°C for ~2 hours with shaking. The protein A-agarose was then washed three times with 1 ml of binding buffer. After the final wash, the protein A-agarose was resuspended in 30 μl of 6X SDS sample buffer (Section 2.10.1), boiled for 10 minutes and followed by SDS-PAGE and immunoblotting (Section 2.10).

## 2.9 Gel Filtration Chromatography

Human embryonic kidney 293 cells were transfected with either *pcDNA3.1-EGFP-Q19-myc* or *pcDNA3.1-EGFP-Q81-myc* construct in 100 mm culture dishes and harvested at 48 hours post-transfection using 1 ml of binding buffer as described in Section 2.8.1. Reagents used in HEK 293 cells transfection in 100 mm dishes were 5 times of that of the 6-well plates (Table 2.7). At 48 hours post-transfection, cells were lysed in 1 ml of binding buffer (Section 2.8.1) and handled in the same way as described in Section 2.8. The supernatant collected after centrifugation was filtered through a 0.22 μm filter unit (Millipore, Billerica, MA, USA) to clear cell debris. A HiPrep 26/60 Sephacryl S-300 column (GE Healthcare, Uppsala, Sweden) was equilibrated with binding buffer (Section 2.8.1) pre-filtered through a 0.22 μm filter unit (Millipore, Billerica, MA, USA); and then the filtered lysates were loaded onto the column at a flow rate of 2.3 ml/minute. The flow rate was controlled by the AKTAprime Plus System (GE Healthcare, Uppsala, Sweden). Fractions were collected at a volume of 3 ml/fraction starting from 82 ml after protein injection. The elution profile of exportin-1 was analyzed by SDS-PAGE and immunoblotting (Section 2.10). For each fraction, 25 μl of samples were mixed with 5 μl of 6X SDS sample buffer and boiled at 99°C for 5 minutes.

## 2.10 Sodium Dodecyl Sulfate-Polyacrylamide Gel Electrophoresis (SDS-PAGE) and Immunoblotting

### 2.10.1 Reagents

<u>1) 6X SDS Sample Buffer</u>

Protein loading buffer (50 ml) was prepared by adding 5ml of 1M Tris-HCl, pH 6.8 (0.1 M), 10 ml of 10% SDS solution (2%, w/v), 10 ml of glycerol (20%, v/v), 2.5 ml of β-mercaptoethanol (5%, v/v) and 0.01 g of bromophenol blue (0.02%, w/v) to double distilled water. The buffer was stored at -20°C as aliquots.

<u>2) SDS Electrophoresis Buffer</u>

Stock SDS electrophoresis buffer (10X) was prepared by dissolving 30.28 g of Tris base (0.25 M), 144.13 g of glycine (1.92 M) and 10 g of SDS (1%, w/v) in 1 L of double distilled water. Working buffer (1X) was prepared by diluting the stock buffer 10-fold with double distilled water. Both stock and working solutions were kept at room temperature.

3) Running Gel and Stacking Gel Solutions

For each 1.5 mm mini gel, running gel and stacking gel solutions were freshly prepared according to Tables 2.11 and 2.12.

**Table 2.11. Components of running gel solution.**

|  | Volume ($\mu$l) | Final Concentration |
|---|---|---|
| 30% acrylamide / Bis solution, 37.5:1 | 3,500 | 12% (v/v) |
| 1 M Tris-HCl, pH 8.8 | 3,255 | 0.4 M |
| Double distilled water | 1,900 | - |
| 10% SDS solution (w/v) | 87.5 | 1% (w/v) |
| 10% Ammonium persulfate (w/v) | 40 | 0.04% |
| N,N,N,N-Di-(dimethylamino)ethane (TEMED) | 4 | 0.04% |

**Table 2.12. Components of stacking gel solution.**

|  | Volume ($\mu$l) | Final Concentration |
|---|---|---|
| 30% acrylamide / Bis solution, 37.5:1 | 490 | 4% (v/v) |
| 0.1 M Tris-HCl, pH 6.8 | 966 | 0.03 M |
| Double distilled water | 1,960 | - |
| 10% SDS solution (w/v) | 35 | 1% (w/v) |
| 10% Ammonium persulfate (w/v) | 20 | 0.04% |
| N,N,N,N-Di-(dimethylamino)ethane (TEMED) | 2 | 0.04% |

## 4) Transfer Buffer

Stock transfer buffer (10X) was prepared by dissolving 30.28 g of Tris base (0.25 M) and 144.13 g of glycine (1.92 M) in 1 L of double distilled water and kept at room temperature. Working transfer buffer (1X) for every two 1.5 mm mini gels was freshly prepared by mixing 70 ml of 10X stock buffer and 70 ml of methanol with 560 ml of double distilled water.

## 5) Tris-buffered Saline (TBS)

Stock TBS buffer (10X) was prepared by dissolving 24.22 g of Tris base (0.2 M) and 80.06 g of NaCl (1.37 M) in 1 L of double distilled water with pH value adjusted to 7.6 using hydrochloric acid. Working buffer (1X) was prepared by dilution the stock solution 10-fold with double distilled water. Both stock and working solutions were kept at room temperature.

## 6) Tris-buffered saline-Tween-20 (TBS-T)

Working TBS-T solution was prepared by adding 1 ml of Tween-20 (0.1%, v/v) to 1 L of 1X TBS. The TBS-T solution was kept at room temperature.

## 7) Blocking buffer

Blocking buffer was prepared by dissolving 5 g of non-fat dry milk powder (5%, w/v) in 100 ml of TBS-T. It can be kept at 4°C for a week.

## 8) Chemiluminescent Solution

Chemiluminescent solution was prepared by dissolving 0.22 g of luminal (1.25 mM), 0.03 g of p-coumaric acid (0.2 mM) and 12.11 g of Tris base (100 mM) in 1 L of double distilled water with pH value adjusted to 8.5 using hydrochloric acid. It was kept at 4°C. Each milliliter of chemiluminescent solution was freshly supplemented with 0.4 μl of hydrogen peroxide ($H_2O_2$) solution.

## 2.10.2 SDS-polyacrylamide Gel Electrophoresis

SDS polyacrylamide gel electrophoresis was carried out using the Mini-PROTEAN III electrophoresis cell (Bio-Rad Laboratories, Hercules, CA, USA). Protein samples mixed with 6X SDS sample buffer were denatured at 99°C for 5 minutes. Five microliters of Seeblue Plus pre-stained protein standard (Invitrogen Life Technologies, Carlsbad, CA, USA) was loaded as molecular weight marker. Electrophoresis was performed at a constant voltage of 100 V initially, which was then adjusted to 180 V after the dye front reached the running gel. The gel was run and stopped at appropriate positions, depending on the size of the target proteins being analyzed.

## 2.10.3 Immunoblotting

After electrophoresis, the acrylamide gels were rinsed briefly with distilled water to remove SDS that could hinder subsequent protein transfer. Polyvinylidene fluoride (PVDF) membrane (PALL, NY, USA) was first activated by analytical grade methanol and then equilibrated in 1X transfer buffer. After activation and equilibration, the PVDF membrane, together with two pieces of 3 MM filter paper (Whatmann, Kent, UK) and two pieces of sponge (Bio-Rad Laboratories, Hercules, CA, USA) pre-wetted with 1X transfer buffer, were assembled in the Mini Trans-Blot electrophoretic transfer cell (Bio-Rad Laboratories, Hercules, CA, USA). The assembled sandwich was rolled over by a glass tube to expel any

air bubbles trapped. Proteins on the gel were electroblotted onto the PVDF membrane at 120 V for 1 hour.

After the transfer, the PVDF membranes were activated again by methanol and then rinsed briefly in TBS-T. The membranes were incubated in blocking buffer with continuous shaking for 1 hour at room temperature. Membranes were then incubated with primary antibodies diluted in blocking buffer (Table 2.13) at 4°C overnight with continuous rolling. After primary antibody incubation, membranes were washed with continuous shaking for four times in TBS-T at room temperature, each for 5 minutes, and followed by secondary antibody (Table 2.13) incubation in blocking buffer for 1 hour at room temperature with continuous rolling. Secondary antibodies used were affinity purified goat anti-rabbit or anti-mouse immunoglobulin G horseradish peroxidase-conjugate (Cell Signaling Technology, Danvers, MA, USA). Membranes were again washed four times with TBS-T, each for 5 minutes. After the final wash, membranes were subjected to chemiluminescent detection. The $H_2O_2$-activated chemiluminescent solution was applied onto the membranes and incubated for 1 minute at room temperature. Membranes were then wrapped in plastic wrap, with protein side down, and exposed to X-ray film (FUJI super RX, Greenwood, SC, USA) at desired time intervals. For re-probing, membranes were incubated in Western blot stripping buffer (Pierce, Rockford,

IL, USA) for 10 minutes at room temperature with continuous shaking. After being rinsed with TBS-T for two times, the membranes were blocked again in blocking buffer for 30 minutes at room temperature, and incubated with another set of primary and secondary antibodies (Table 2.13).

**Table 2.13. Summary of antibodies used in immunoblotting.**

| Primary Antibody | Dilution (Company, catalog no.) | Host Species | Secondary Antibody Dilution |
|---|---|---|---|
| Exportin-1 | 1:1,000 (Calbiochem, ST1100) | Rabbit | 1:2,000 |
| Exportin-t | 1:500 (Abcam, ab49933) | Mouse | 1:2,000 |
| FLAG M2 | 1:4,000 (Sigma, F3165) | Mouse | 1:5,000 |
| Fibrillarin 38F3 | 1:500 (Fibrillarin, ab4566) | Mouse | 1:2,000 |
| GFP JL-8 | 1:5,000 (Clontech, 632381) | Mouse | 1:5,000 |
| Histone H3 (acetyl) | 1:2,500 (Abcam, ab47915) | Rabbit | 1:2,000 |
| Histone H3 (total) | 1:10,000 (Abcam, ab1791) | Rabbit | 1:10,000 |
| Myc 9B11 | 1:1,000 (CST, 2276) | Mouse | 1:2,000 |
| Myc 71D10 | 1:1,000 (CST, 2278) | Rabbit | 1:2,000 |
| β-tubulin E7 | 1:10,000 (Developmental Studies Hybridoma Bank, E7) | Mouse | 1:10,000 |

### 2.10.4 Quantification of Protein Band Intensity

Protein band intensity was measured using the ImageJ software (version 1.32; Research Services Branch, National Institute of Mental Health, Bethesda, MD, USA). For the determination of nucleocytoplasmic ratio of polyQ proteins, the band intensity of the nuclear polyQ protein was normalized to that of histone H3, which was then divided by the band intensity of the cytoplasmic polyQ protein normalized to that of β-tubulin (Figs. 3.12 and 3.14). Sample mean values and S.D. were calculated from three independent sets of experiments. Differences in sample means were compared by the Mann-Whitney rank sum test. A *p*-value of less than 0.05 was considered statistically significant.

For immunoprecipitation of the QPQ proteins (Fig. 3.21), protein band intensity of exportin-1 was normalized to that of the SDS-soluble QPQ protein. For temporal analysis of exportin-1 protein level in whole brain lysates isolated from wild-type mice (Fig. 3.28), protein band intensity of exportin-1 was normalized to that of β-tubulin. Sample mean values and S.D. were calculated from three independent sets of experiments. The Kruskal-Wallis one way ANOVA on ranks followed by Dunn post-test was performed to determine difference between experimental groups, and a *p*-value of less than 0.05 was considered statistically significant.

## 2.11 Filter Retardation Assay

A cellulose acetate membrane with pore size of 0.22 μm (Sartorius, Goettingen, Germany) was inserted into the Slot Blot Manifold blot apparatus (PR 648, GE Healthcare, Uppsala, Sweden) connected to a vacuum pump. Double distilled water, 0.01% SDS solution (w/v), and 2% SDS solution (w/v) were sequentially applied onto each slot to wet and equilibrate the membrane. After heating the protein samples at 99°C for 5 minutes, 10 μg of cell lysates were loaded onto the slots. Each slot was then washed for three times with 2% SDS solution (w/v). The membrane was then removed from the blot apparatus, and immunodetection was carried out as described in Section 2.10.3.

Unless otherwise stated, chemicals were purchased from USB cooperation via GE Healthcare (Uppsala, Sweden).

# Chapter 3. Identification of Genetic Modifiers of Mutant Polyglutamine

## Protein Subcellular Localization

Being a unique protein domain shared among different polyQ disease proteins, the cellular mechanisms mediated by the expanded polyQ domain on regulating the subcellular localization of mutant protein was the primary focus of this project. An inducible *Drosophila* cell model was established for identifying genetic factors that are involved in mutant polyQ-mediated nuclear translocation

## 3.1 Characterization of a Stable EGFP-polyglutamine BG2 Cell Model

*Drosophila* BG2 cells were chosen as the cell model in this study. Being derived from the larval central nervous system (Ui et al., 1994), BG2 cells are commonly used to dissect neuronal functions at the cellular level (Lee et al., 2008; Takagi et al., 2000). Stably transfected BG2 cell lines carrying *EGFP-Q27* or *EGFP-Q75* transgenes were established according to Section 2.3.2.2. The general transport mechanism initiated by naked polyQ domain was studied by taking advantage of such artificial *EGFP-polyQ* constructs. The EGFP was used as a fusion tag due to the absence of any intrinsic nuclear transport signal in its primary sequence. Also, the native fluorescence property of EGFP allows direct visualization of polyQ protein without the need of immunolabelling. Featured in other EGFP-polyQ models (e.g. (Kazantsev et al., 1999; Takahashi et al., 2007)), the detection of SDS-insoluble protein species and formation of microscopically visible aggregates were two criteria used to verify the current BG2 polyQ cell model.

### 3.1.1 Optimization of the Induction of EGFP-polyglutamine Protein Expression

Expression of EGFP-polyQ protein in BG2 cells was driven by a copper ion-inducible *metallothionein* (*MT*) promoter (Otto et al., 1987). The optimal $CuSO_4$ concentration for EGFP-polyQ protein induction was determined empirically. Prior to the optimization, the effect of $CuSO_4$ on the growth of BG2 cells was first studied in untransfected cells. The

addition of as low as 0.5 mM $CuSO_4$ to the culture medium already elicited an inhibitory

effect on cell growth when compared to cells maintained in $CuSO_4$-free normal complete

medium (Fig. 3.1A). Nonetheless, a further increase in $CuSO_4$ concentration did not

exacerbate such growth inhibition; and the cell number remained roughly the same from 0

to 96 hours post induction (hpi) with $CuSO_4$ concentration raised up to 1 mM (Fig. 3.1A).

However, the cell number at 96 hpi dropped significantly when $CuSO_4$ concentration was

further increased to 2 mM (Fig. 3.1A). Since the expression level of recombinant protein

was positively correlated with $CuSO_4$ concentration used for induction (Fig. 3.1B), 1 mM

$CuSO_4$ was chosen to induce EGFP-polyQ protein in BG2 cells in order to minimize cell

death. In fact, the same induction condition was previously employed in another study

using cultured *Drosophila* cells (Tota et al., 1995).

**A.**
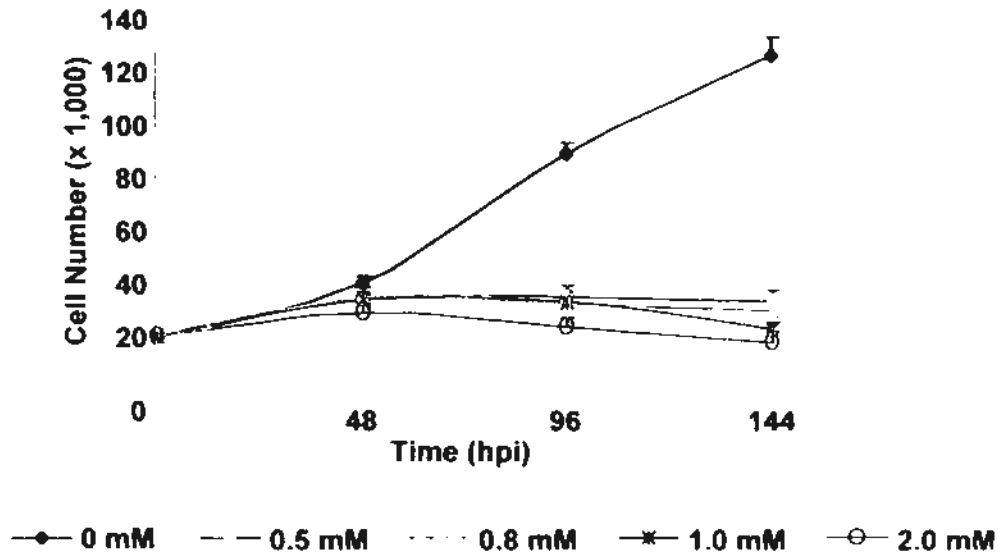


**B.**
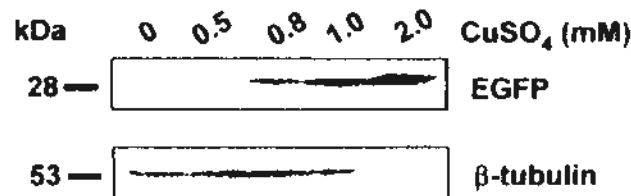


**Figure 3.1. Optimization of $CuSO_4$ concentration for inducing recombinant protein expression in BG2 cells. (A)** Growth curves of untransfected BG2 cells maintained in 10% FBS-containing medium supplemented with different concentrations of $CuSO_4$. The addition of 0.5 – 1.0 mM $CuSO_4$ showed similar extent of inhibition on BG2 cell growth. A further increase of $CuSO_4$ to 2 mM resulted in a significant reduction in cell number at 96 hours post-induction, hpi ($p$ < 0.05, compared to 0.5 mM $CuSO_4$, by Student's t-test). Error bars represent S.D. of four separate wells in a single experiment and data shown is representative of two independent experiments. **(B)** Immunoblot detection of EGFP protein induced by different concentrations of $CuSO_4$ at 96 hpi by anti-GFP antibody (JL-8). The expression level of EGFP protein increased as higher dosages of $CuSO_4$ were used for induction. $\beta$-tubulin was used as loading control.

### 3.1.2 Detection of SDS-soluble EGFP-polyglutamine Protein in BG2 Cells

Upon $CuSO_4$ induction, SDS-soluble EGFP-Q27 protein was initially detected at 24 hpi by immunoblotting with its expression increased afterwards (Fig. 3.2A). The EGFP-Q75 protein was initially detected at 24 hpi. Unlike EGFP-Q27, the level of SDS-soluble EGFP-Q75 remained steady with time. The expression level of EGFP-Q75 was lower than that of EGFP-Q27. Clonal variations of recombinant protein expression among the stable cell lines might explain such difference. In addition, the conversion of SDS-soluble EGFP-Q75 protein to SDS-insoluble species was another possible explanation.

### 3.1.3 Detection of SDS-insoluble Protein Species in EGFP-Q75-expressing Cells

Filter retardation assay was developed for the detection of SDS-insoluble protein species formed by mutant polyQ protein (Wanker et al., 1999). A time-dependent accumulation of such polyQ species was detected in EGFP-Q75 cell lysates, but not in that of EGFP-Q27 (Fig. 3.2B). Although no signal was detected in the stacking gel of SDS-PAGE (Fig. 3.2A), where SDS-insoluble species retained, filter retardation assay is an alternative to show the presence of SDS-insoluble polyQ protein (Fig. 3.2B). Thus, it was possible that the lower level of SDS-soluble EGFP-Q75 (Fig. 3.2A) was attributed to its conversion to SDS-insoluble conformers.
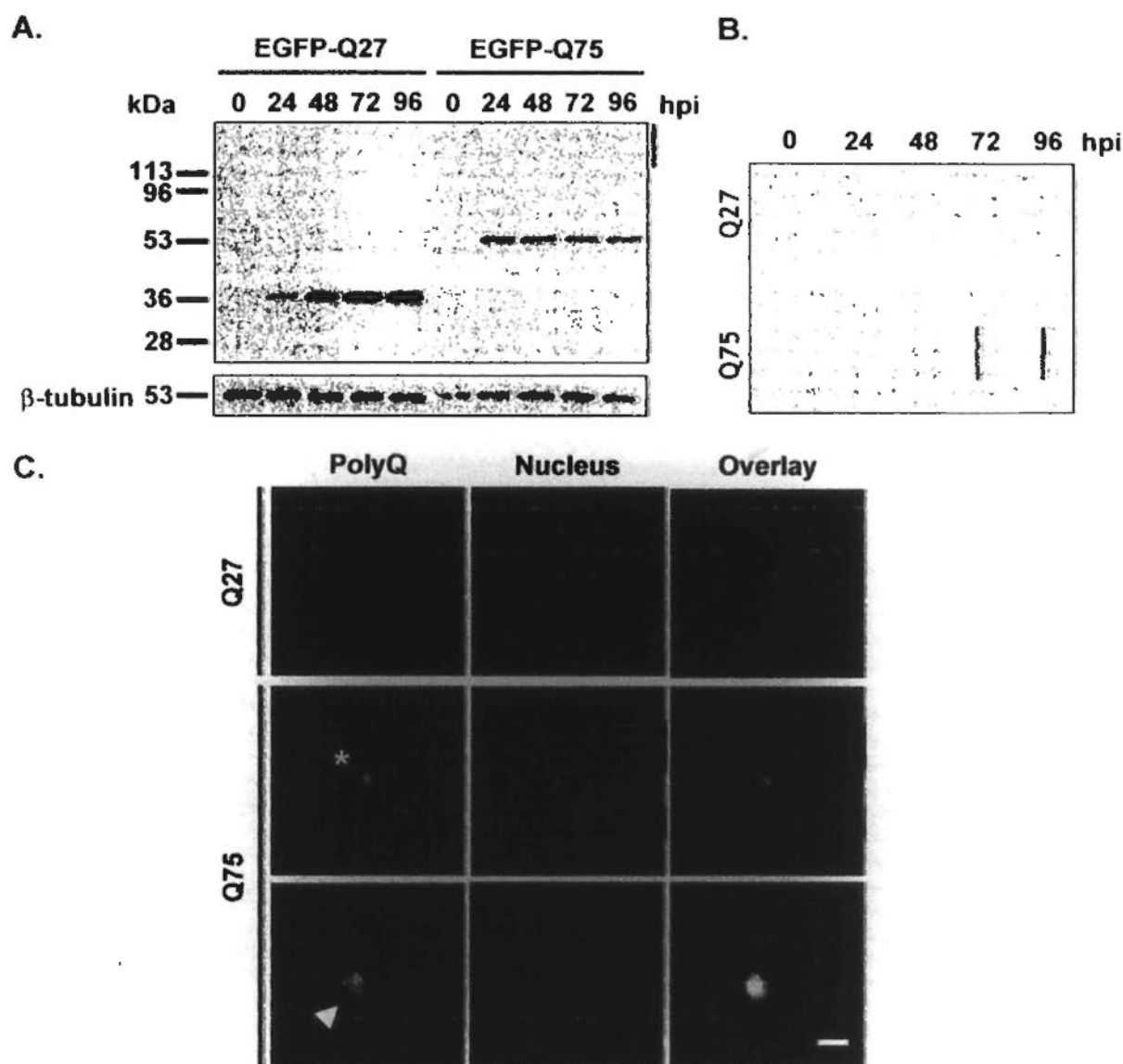
**Figure 3.2. Characterization of BG2 cells stably expressing EGFP-Q27 and -Q75 proteins. (A)** Immunoblot detection of EGFP-Q27 and -Q75 proteins from total cell lysates (5 μg) harvested at indicated hours post-induction (hpi) by $CuSO_4$ with anti-GFP antibody (JL-8). More SDS-soluble EGFP-Q27 was detected than -Q75. β-tubulin was used as loading control. No SDS-insoluble protein was detected in the stacking gel (vertical bar). **(B)** Filter retardation assay on EGFP-Q27 and -Q75 total cell lysates (10 μg) by anti-GFP antibody (JL-8). No SDS-insoluble protein was detected in EGFP-Q27 lysates, while the level of SDS-insoluble EGFP-Q75 increased in a time-dependent manner. **(C)** Fluorescence microscopy of EGFP-Q27 and -Q75 expressing cells at 96 hpi. Cells were fixed and stained with Hoechst (in blue) to label the cell nuclei. The EGFP-Q27 protein was diffusely localized in BG2 cells while the EGFP-Q75 protein formed aggregates in both cytoplasm (asterisk) and nucleus (arrowhead) of BG2 cell. Scale bar represents 5 μm.

### 3.1.4 Formation of Microscopically Visible Aggregates in both Cytoplasm and Nuclei of EGFP-Q75-expressing Cells

In line with the filter retardation assay result (Fig. 3.2B), polyQ aggregates, which are defined as microscopically visible punctuate fluorescence foci in this study, were also detected by fluorescence microscopy (Fig. 3.2C). The EGFP-Q27 protein localized homogeneously in both cytoplasm and nuclei of BG2 cells. On the contrary, although diffuse GFP signals could still be detected in EGFP-Q75-expressing cells, these cells also displayed both cytoplasmic and nuclear aggregates (Fig. 3.2C).

The BG2 polyQ cell model described above recapitulated the characteristic features of polyQ disease, including the detection of SDS-insoluble protein species (Fig. 3.2B) and formation of microscopically visible aggregates (Fig. 3.2C). Thus, it was employed for the elucidation of genetic pathway governing the nucleocytoplasmic localization of mutant polyQ protein.

## 3.2 An Attempt to Identify Genetic Factors Involved in Mutant Polyglutamine Protein Nuclear Translocation by a Genome-wide RNA Interference Approach

RNA interference (RNAi) was employed to dissect the genetic pathways governing the nuclear translocation mediated by an expanded polyQ domain. In *Drosophila*, long double-stranded RNAs (dsRNAs) of 300 - 800 bp are routinely used instead of small interfering RNAs (siRNAs) employed in mammalian systems to elicit gene silencing effect (Kavi et al., 2008). A full genome set of *Drosophila* dsRNAs (~91% coverage of the whole *Drosophila* genome) is available at the *Drosophila* RNAi Screening Center (DRSC, Boston, MA, USA). By taking advantage of high-throughput facilities at the DRSC, including Evotec Opera (Perkin Elmer, Waltham, MA, USA), a confocal fluorescence screening system with automated plate-loading robotic arm, genes that are involved in the nuclear translocation of EGFP-Q75 protein could be determined in a genome-wide manner.

### 3.2.1 Optimization of RNA Interference Gene Knockdown Conditions in 384-well Plates

As an initial step to perform the genome-wide RNAi screen in a high-throughput manner, the dsRNA-mediated gene knockdown efficiency had to be first optimized in 384-well plate format. A dsRNA specific to EGFP was synthesized and used to determine the knockdown efficiency in BG2 cells stably transfected with *EGFP-Q75* construct. After

a few rounds of trials, the amount of dsRNA to cell number ratio (0.25 µg dsRNA to 0.8 x

$10^4$ cells/well) in 384-well plate was successfully optimized, as indicated by a significant

loss of GFP signals compared to the $H_2O$-treated cells (Fig. 3.3). Cells treated with dsRNA

against *LacZ*, a gene absent in the *Drosophila* genome, was the negative control to

demonstrate the specificity of the knockdown effect conferred by dsRNA against *EGFP*

(Fig. 3.3).
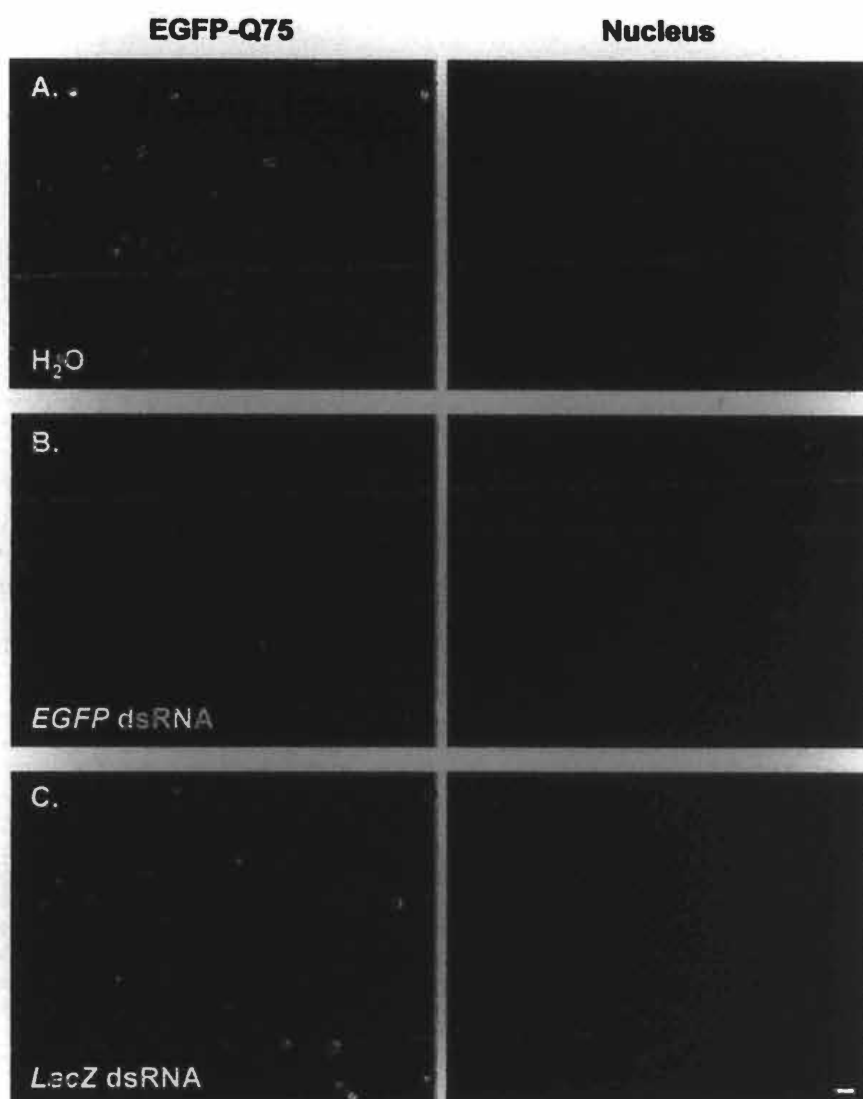
**Figure 3.3. Optimization of dsRNA knockdown efficiency in BG2 cells in 384-well plates.** BG2 cells stably transfected with *EGFP-Q75* construct were treated with **(A)** $H_2O$, **(B)** *EGFP* dsRNA or **(C)** *LacZ* dsRNA. Expression of EGFP-Q75 was induced by 1 mM $CuSO_4$ and cells were imaged by a fluorescence microscope at 96 hours post-induction. Cell nuclei were labeled with Hoechst (in blue). Compared to the **(A)** $H_2O$-treated control, treatment of BG2 cells with **(B)** dsRNA against *EGFP* significantly reduced the expression of EGFP-Q75, while BG2 cells treated with **(C)** dsRNA against *LacZ* showed no alteration on expression or aggregation of EGFP-Q75 protein. Scale bar represents 20 μm.

### 3.2.2 Optimization of Automated Imaging with Evotec Opera

Since the whole DRSC dsRNA library is deposited in sixty-two 384-well plates, the development of a reliable and automated analysis is a pre-requisite for a feasible screen. BG2 cells expressing the EGFP-Q75 protein were imaged with Evotec Opera, and both cytoplasmic and nuclear aggregates were readily detected (Fig. 3.4A-C). The subcellular distribution of EGFP-Q75 aggregates was chosen as readout to measure if the knockdown of genes by dsRNAs would affect the nucleocytoplasmic localization of EGFP-Q75 protein. Unfortunately, the clumping properties of BG2 cells (Fig. 3.4D and E) limited the use of automatic cell counting in the analysis. After several rounds of attempts, the analysis software of Evotec Opera, Evotec Acapella, was still unable to accurately differentiate individual cells from cell clumps, and thus resulted in inaccurate determination of EGFP-Q75 aggregate subcellular localization.
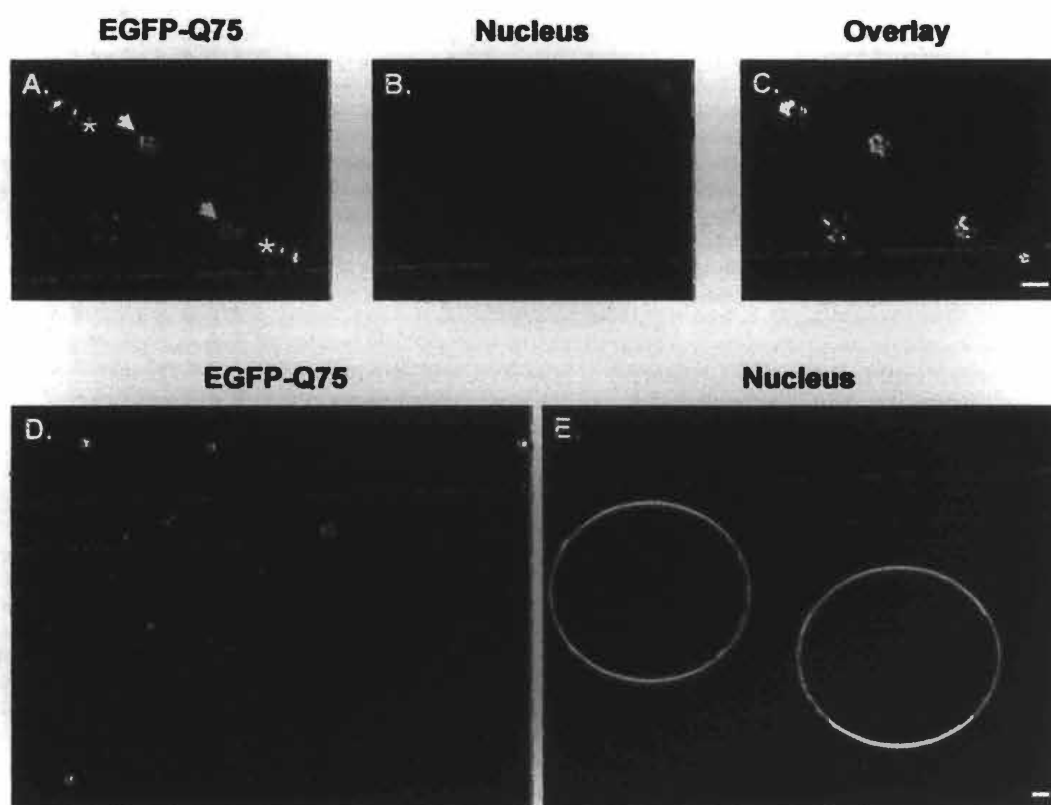
**Figure 3.4. BG2 cells expressing EGFP-Q75 imaged by the confocal system, Evotec Opera.** Expression of EGFP-Q75 was induced by 1 mM $CuSO_4$. At 96 hours post-induction, cells were fixed and nuclei were stained by Hoechst (in blue). **(A-C)** Detection of EGFP-Q75 aggregates in BG2 cells. Both cytoplasmic (asterisks) and nuclear (arrowheads) aggregates were detected. Scale bar represents 5 μm. **(D and E)** Intrinsic clumping property of BG2 cells. BG2 cells have an intrinsic tendency to clump together (circled areas). This caused the software, Evotec Acapella, unable to identify individual cell nucleus and accurately determine the subcellular localization of EGFP-Q75 aggregates. Scale bar represents 20 μm.

Despite the successful optimization of dsRNA-mediated gene knockdown (Fig. 3.3) and the detection of both cytoplasmic and nuclear EGFP-Q75 aggregates (Fig. 3.4A-C) in 384-well plates, the intrinsic cell clumping property of BG2 cells (Fig. 3.4D and E) hindered the use of high-throughput automated imaging platform to perform the genome-wide dsRNA screen. When BG2 cells were monitored manually, cells that did not clump together could be preferentially imaged and hence its clumping problem could be avoided. In view of this, small-scale candidate gene approach was employed to identify genetic factors involved in expanded polyQ domain-mediated nuclear translocation.

### 3.3 RNA Interference Experiments in BG2 Cells by a Candidate Gene Approach

### 3.3.1 Components of the c-Jun NH$_2$ Terminal Kinase Pathway

From a genome-wide RNAi screen performed by Dr. Sheng Zhang (Norbert Perrimon Lab, Harvard Medical School, Boston, MA, USA), several genes in the c-jun NH$_2$ terminal kinase (JNK) pathway were identified as modifiers of mutant huntingtin (Htt) protein aggregation (Sheng Zhang and Norbert Perrimon, unpublished data). Since an activation of the JNK pathway has been reported to increase the aggregation of mutant polyQ protein, especially in the cell nucleus (Cowan et al., 2003), these genes were tested for their modulatory effects on EGFP-Q75 aggregates subcellular localization.

The five targets identified as modifiers of mutant Htt aggregation in the JNK pathway were *jra, raw, Tao-1, Cka* and *lic* (Sheng Zhang and Norbert Perrimon, unpublished data). Thus, these genes were knocked down in EGFP-Q75-expressing BG2 cells by specific dsRNAs. Among them, the knockdown of *jra, jun related antigen*, resulted in a significant increase in the percentage of nuclear aggregate-containing cells while the knockdown of the other four genes did not exert any modulatory effect (Falling Fong and Edwin Chan, unpublished data).

### 3.3.1.1 Modulatory Effects of Jra and Fra on the Subcellular Localization of EGFP-Q75 Aggregates

Similar to its mammalian homolog c-jun (Zhang et al., 1990), the *Drosophila* Jun protein, Jra, homodimerizes with another molecule of itself or heterodimerizes with the *Drosophila* Fos protein, Fos Related Antigen (Fra) (Perkins et al., 1990), to form the activator protein-1 (AP1) transactivation complex and regulate gene transcription (Riesgo-Escovar and Hafen, 1997). Thus, the effect of Fra on EGFP-Q75 aggregate localization was also tested. The knockdown efficiency of dsRNAs against *jra* and *fra* was confirmed by RT-PCR (Fig. 3.5A). Similar to *jra*, the knockdown of *fra* expression resulted in a significant increase in the nuclear to cytoplasmic ratio of EGFP-Q75 aggregates (Fig. 3.5B). However, no detectable difference between the modulatory effect of *jra* and *fra* knockdown was observed (Fig. 3.5B). To check if their modulatory effects were specific to protein with an expanded polyQ domain, dsRNAs against *jra* and *fra* were treated against EGFP-Q27-expressing cells. The knockdown of neither *jra* nor *fra* expression altered the distribution of EGFP-Q27 in BG2 cells (Fig. 3.6).

**A.**
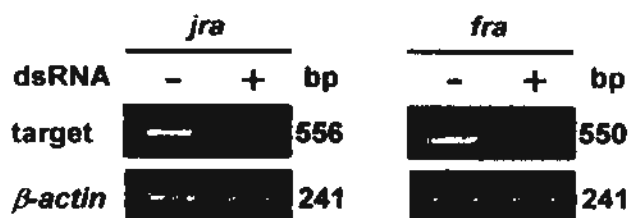


**B.**
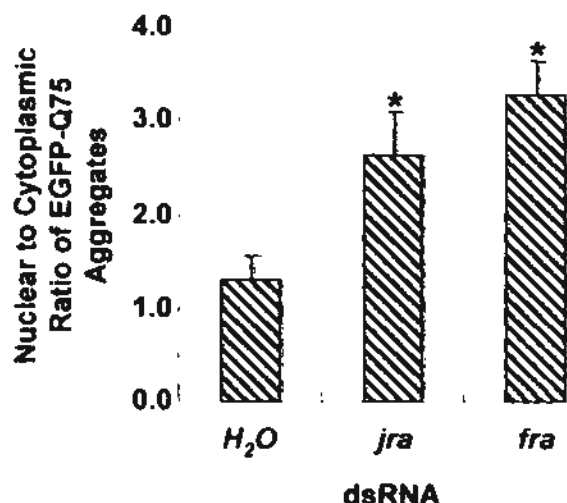


Figure 3.5. Modulatory effect of *jra* and *fra* knockdown on EGFP-Q75 aggregates subcellular localization in stable BG2 cells. (A) RT-PCR analysis of *jra* and *fra* expression in dsRNA-treated cells. Compared to the $H_2O$-treated (-) cells, BG2 cells treated with dsRNAs (+) resulted in a reduction of mRNA level of target genes. *β-actin* was used as loading control. (B) The nuclear to cytoplasmic ratio of EGFP-Q75 aggregates in dsRNA-treated cells. After incubating with dsRNAs for 72 hours, EGFP-Q75 protein expression was induced by 1 mM $CuSO_4$. At 96 hours post-induction, cells were fixed and stained with Hoechst to label cell nuclei, and examined under fluorescence microscope on a single-blind approach. The ratio was calculated by dividing the number of cells with nuclear aggregates by the number of cells with cytoplasmic aggregates. The knockdown of either *jra* or *fra* expression led to nuclear accumulation of EGFP-Q75 aggregates (* $p$ < 0.05, compared to $H_2O$-treated control, by Student's t-test). Error bars represent S.E.M. of three independent experiments.
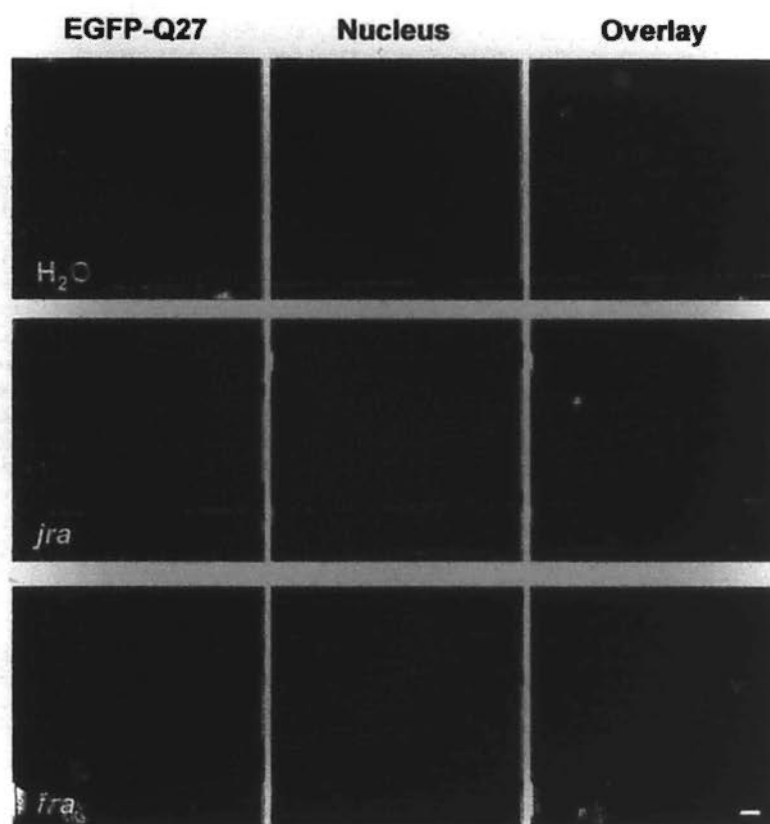
**Figure 3.6. Modulatory effect of *jra* and *fra* knockdown on EGFP-Q27 protein subcellular localization in stable BG2 cells.**
Expression of EGFP-Q27 was induced by 1 mM $CuSO_4$ after 72 hours of incubation with dsRNAs. At 96 hours post-induction, cells were fixed and stained with Hoechst (in blue) to label cell nuclei. When treated with $H_2O$, the EGFP-Q27 protein localized homogeneously in both cytoplasm and nucleus in BG2 cells. Upon the knockdown of *jra* or *fra* expression by dsRNAs, no alteration of the diffuse localization of EGFP-Q27 in BG2 cells was observed. Scale bar represents 5 μm.

### 3.3.1.2 Effects of Upstream Effectors of Jra and Fra on Mutant Polyglutamine

### Protein Subcellular Localization

The effect of Jra and Fra upstream effector, JNK, was also investigated. Consistent with previous findings (Cowan et al., 2003), the blockage of JNK pathway by its specific inhibitor SP600125 (Bennett et al., 2001), resulted in a significant decrease in aggregation of EGFP-Q75 protein in BG2 cells (Fig. 3.7A). However, SP600125 did not exert any significant modulatory effect on the subcellular localization of EGFP-Q75 aggregates (Fig. 3.7B).

Apart from the JNK pathway, the Jun activation domain-binding protein 1, Jab1, has also been reported to regulate AP-1 transcriptional activity in a JNK-independent fashion (Claret et al., 1996; Lu et al., 2002). Thus, the possible effect of Jab1 on mutant polyQ protein subcellular localization was also examined. In contrast to SP600125, the knockdown of *Jab1* expression in BG2 cells led to a nuclear accumulation of EGFP-Q75 aggregates (Fig. 3.7C). The underlying mechanisms of jra, fra and Jab1 on mutant polyQ protein nucleocytoplasmic localization awaits further investigation.

**A.**



**B.**



**C.**
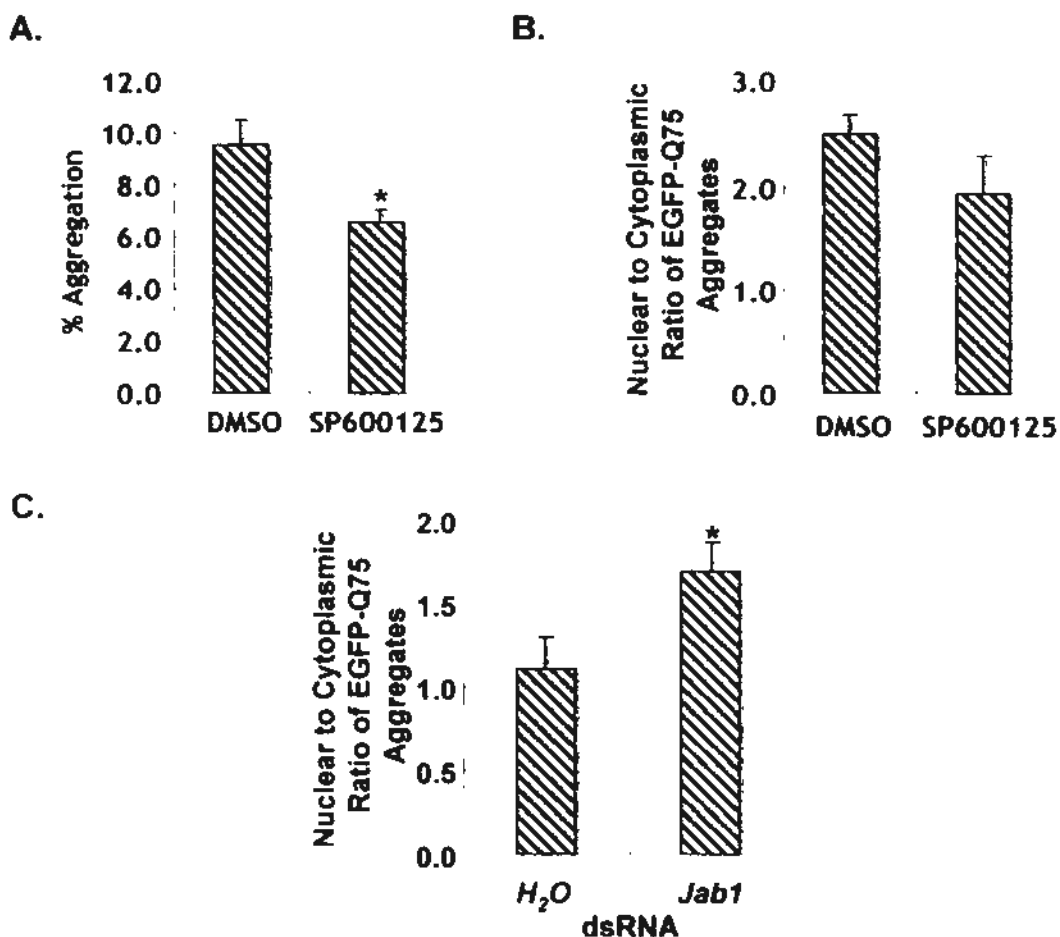


**Figure 3.7. Modulatory effect of upstream regulators of Jra and Fra on EGFP-Q75 aggregation and subcellular localization in stable BG2 cells. (A)** Treatment of stable BG2 cells with SP600125 (10 $\mu$M for 96 h in 1 mM $CuSO_4$-containing medium) suppressed EGFP-Q75 aggregate formation (* $p < 0.05$, compared to DMSO-treated control, by Student's t-test). **(B)** Blockage of the JNK pathway by SP600125 did not affect the nuclear to cytoplasmic distribution of EGFP-Q75 aggregates. **(C)** Knockdown of *Jab1* expression, a JNK-independent activator of AP-1, resulted in a significant increase in the nuclear to cytoplasmic ratio of EGFP-Q75 aggregates (* $p < 0.05$, compared to $H_2O$-treated control, by Student's t-test). Error bars represent S.E.M. of three independent experiments.

### 3.3.2 Members of the Karyopherins Family

Apart from the JNK pathway mentioned above, the effects of karyopherins, nuclear transport receptor/adaptors, in the *Drosophila* genome on EGFP-Q75 protein subcellular localization were also tested.

Among the nineteen karyopherins tested, six of them modulated the subcellular localization of EGFP-Q75 aggregates and they were *cadmus (cdm), karyopherin-α3 (Kap-α3), CSE1 segregation protein (Cas), karyopherin-α1 (Kap-α1), karyopherin-β3 (Kary-β3)* and *embargoed (emb)* (Appendix 1, in collaboration with Frankie Tsoi). These six selected karyopherins were further tested for their modulatory effects on mutant polyQ-induced toxicity *in vivo*. It was found that the knockdown of *kap-α3* or *emb* expression enhanced MJDtrQ78-induced toxicity (Appendix 2, in collaboration with Frankie Tsoi). In this project, the modulatory mechanism of *emb*, the *Drosophila* ortholog of human exportin-1, was studied in detail (Chapters 4-6).

## 3.4 Discussion

### 3.4.1 A Stable Inducible *Drosophila* Cell Model

An inducible cell model was developed in the present study to elucidate the nuclear transport pathways responsive to an expanded polyQ domain, which would reflect a general situation applicable to all polyQ disorders. The *Drosophila* BG2 cells were chosen because of its neuronal characteristics (Ui et al., 1994) and its established use in polyQ studies (Kanuka et al., 2003; Nelson et al., 2005). Constitutive expression of a toxic gene product, i.e. the mutant polyQ protein, in cell culture system would possibly impose growth problem on the stably transfected cells. Thus, an inducible system was employed in this study (Fig. 3.2).

By taking advantage of the *MT* promoter, a higher degree of flexibility in controlling the expression level of recombinant proteins was achieved by adjusting the concentration of $CuSO_4$ supplemented to the cell culture medium (Otto et al., 1987). Although the addition of $CuSO_4$ to untransfected BG2 cells elicited a slight growth-inhibitory effect (Fig. 3.1A), the cell number was maintained at a steady level and no additional cell death was observed at 1 mM of $CuSO_4$, the concentration of which was therefore used throughout the course of experiments (Fig. 3.1A). Since neurons, which remain quiescent in adulthood, are the major affected cell population in polyQ diseases (Zoghbi and Orr, 2000), the lack of

cell division in BG2 cells upon CuSO$_4$ treatment would in fact better model the cellular environment of polyQ-induced neurodegeneration in patients. In line with other EGFP-polyQ models (Kazantsev et al., 1999; Moulder et al., 1999; Takahashi et al., 2007), the present BG2 cell model recapitulated the characteristic features of polyQ diseases, including the formation of SDS-insoluble protein species and microscopically visible aggregates (Fig. 3.2).

### 3.4.2 RNA Interference Experiments performed in BG2 Cells

RNA interference has been widely employed to dissect genetic pathways for various cellular processes (Bai et al., 2008; Boutros et al., 2004). One of the advantages of performing RNAi experiments in cultured *Drosophila* cells is attributed to the use of dsRNAs, which is long enough to avoid positional effects as observed with siRNAs in mammalian systems (Holen et al., 2002). In addition, the simple experimental procedures, simply by soaking the dsRNAs with cells in culture medium without the use of potentially toxic transfection reagents; and the convenient validation of gene knockdown data *in vivo* in *Drosophila* justified the use of RNAi in cultured BG2 cells be the initial step in this study. In fact, RNAi has previously been demonstrated to be useful in the investigation of polyQ pathogenesis in cultured *Drosophila* cells (Kanuka et al., 2003). In a Htt BG2 cell model, the knockdown of *Dsec61α* expression by dsRNA results in a reduction of cell

death induced by mutant Htt (Kanuka et al., 2003). In the present study, the EGFP-polyQ

protein expression was only induced after the target genes have been knocked down. This

ensures the target mRNAs have been depleted prior to the synthesis of EGFP-polyQ

proteins.

Owing to the failure of using genome-wide RNAi screen to identify genetic factors

that are involved in mutant polyQ protein nuclear translocation (Section 3.2), a candidate

gene approach has then been employed. In this regard, several cellular factors, including

components in the JNK pathway as well as members of the karyopherin family, were found

to be potential mediators of mutant polyQ protein subcellular localization.

## 3.4.3 Possible Involvement of Jra and Fra in the Regulation of Mutant Polyglutamine

### Protein Nucleocytoplasmic Localization

The knockdown of *jra* or *fra* expression resulted in an expanded polyQ specific

alteration of EGFP-Q75 protein subcellular localization (Figs. 3.5 and 3.6). One of the

most well-defined functions of Jra and Fra is on gene transcription regulation, via the

formation of AP-1 transcription factor (Riesgo-Escovar and Hafen, 1997). Activator

protein 1 is composed of either homodimers of Jra or heterodimers of Jra and Fra

(Riesgo-Escovar and Hafen, 1997). From the RNAi experiments in BG2 cells, the

modulatory effect on EGFP-Q75 aggregate localization was similar upon the knockdown of either *jra* or *fra* expression (Fig. 3.5B). Homodimers of Jra and Jra-Fra heterodimers display different transcriptional specificities due to their distinct orientation and conformation upon binding to gene promoters (Ramirez-Carrozzi and Kerppola, 2003). If Jra-Jra homodimers play a dominant role, the knockdown of *fra* expression would not give similar extend of modulation as *jra* knockdown (Fig. 3.5B). Thus, it is speculated that AP-1 composed of Jra-Fra heterodimers specifically regulate the expression of certain genes that play roles in regulating the subcellular localization of mutant polyQ proteins. This explains why the depletion of either gene product exerted similar modulatory effect on EGFP-Q75 aggregate subcellular localization (Fig. 3.5B).

One of the well-established functions of JNK is to activate Jra through protein phosphorylation (Weston and Davis, 2007). The JNK specific inhibitor, SP600125, abolishes the kinase activity of JNK which results in hypophosphorylation of Jra (Bennett et al., 2001). However, the hypophosphorylated Jra protein, though being transcriptionally inactive, still retains its function as a repressor of transcription (Herdegen and Waetzig, 2001). For example, the hypophosphorylated AP-1 can achieve transcriptional repression by binding to regulatory DNA promoter sequences without activating RNA-polymerase II complex (Herdegen and Waetzig, 2001). Since an inhibition of JNK by SP600125 did not

exert any modulatory effect on the subcellular localization of EGFP-Q75 aggregates (Fig. 3.7B), this would support a transcription-independent function of Jra in regulating mutant polyQ protein subcellular localization.

Nevertheless, the existence of JNK-independent activation of Jra, such as through Jab1 (Claret et al., 1996; Lu et al., 2002), preserves the possible involvement of AP-1 transactivation property in regulating the nucleocytoplasmic localization of mutant polyQ proteins. Interestingly, the knockdown of *Jab1* expression in BG2 cells led to a nuclear accumulation of EGFP-Q75 aggregates (Fig. 3.7C). Thus, the interplay between Jab1, Jra and Fra warrants further investigation.

# *Chapter 4. Modulatory Effects of the Drosophila Ortholog of Exportin-1, embargoed, on Mutant Polyglutamine Protein Subcellular Localization and Toxicity*

From the RNAi experiments in BG2 cells which tested the effects of all *karyopherins* in the *Drosophila* genome on EGFP-Q75 subcellular localization, *emb* was the only *karyopherin* whose knockdown led to a nuclear accumulation of EGFP-Q75 aggregates (Appendix 1, in collaboration with Frankie Tsoi). Embargoed, the *Drosophila* ortholog of exportin-1, is the most well-studied karyopherin participating in protein nuclear export (Fornerod et al., 1997). In order to accomplish its role as an export receptor, emb first forms a protein complex with its export substrate, RanGTP as well as RanBP3 in the nucleus, and then translocate through the NPCs to the cytoplasm (Englmeier et al., 2001; Lindsay et al., 2001).

In this chapter, the possible influence of *emb* gene knockdown and over-expression on mutant polyQ-induced toxicity was examined in *Drosophila*, and its effect on the subcellular localization of mutant polyQ protein was further investigated *in vivo*.

112

## 4.1 Opposing Effects of Knockdown and Over-expression of *embargoed* on Full-length Mutant MJD-induced Toxicity *in vivo*

Since the knockdown of *emb* expression enhanced MJDtrQ78-induced toxicity (Appendix 2, in collaboration with Frankie Tsoi), it was hypothesized that its over-expression could rescue the degenerative phenotype. To test this hypothesis, flies expressing the full length disease protein of SCA3 carrying 84 glutamine repeats, MJDQ84 (Warrick et al., 2005), were crossed with those bearing an EP insertion in the 5' upstream region of the *emb* locus (Bilen and Bonini, 2007). Crosses between flies carrying the *MJDQ84* transgene and that bear *emb* dsRNA were also set up in parallel to confirm the enhancement effect due to *emb* gene knockdown. The full length MJD model allows the investigation of *emb* knockdown and over-expression in a single model. Experiments with flies carrying the *MJDQ27* transgene, encoding the full-length MJD protein carrying 27 glutamine repeats, were conducted in parallel to ensure there was not any dominant phenotype due to *emb* gene knockdown or over-expression. Expression of transgenes was directed to the fly eyes with the *gmr*-gal4 line, which drives transgene expression in the pigment cells and photoreceptor neurons (Ellis et al., 1993).

Before proceeding to the determination of its modulatory effect, an alteration of *emb* expression level in the flies used in this study was first confirmed by RT-PCR. The

endogenous *emb* gene was either knocked down by dsRNA or over-expressed through an EP insertion (Fig. 4.1A). In addition, expression of the *MJDQ27* transgene was also examined by RT-PCR and immunoblotting. The result showed that expression level of transgene driven by the gal4/UAS system (Brand and Perrimon, 1993), exemplified by *MJDQ27* (Fig. 3.8B and C), was not significantly altered upon the co-expression of other transgenes (*UAS-emb-dsRNA* or *EP-emb* in this study). Thus, any modification on degenerative phenotype observed in flies with altered *emb* expression level was not simply a consequence of an alteration of *MJD* transgene expression.

Deep pseudopupil assay (Jackson et al., 1998; Wong et al., 2008) was performed to measure the modulatory effect of *emb* on MJDQ84-induced neurodegenerative phenotype. The internal unit of *Drosophila* adult eye is made up of ommatidia, each of which contains eight rhabdomeres, organelles found in photoreceptor neurons. Normally, seven of the rhabdomeres are visible as a regular trapezoidal arrangement in a single plane. Since retinal degeneration results in the appearance of fewer rhabdomeres (Fig. 4.2) (Jackson et al., 1998; Wong et al., 2008), the number of rhabdomeres per ommatidium between different genetic backgrounds were compared so as to check if an alteration of *emb* expression level would exert any modulatory effect on MJDQ84-induced neurodegeneration.

**A.**



**B.**



**C.**
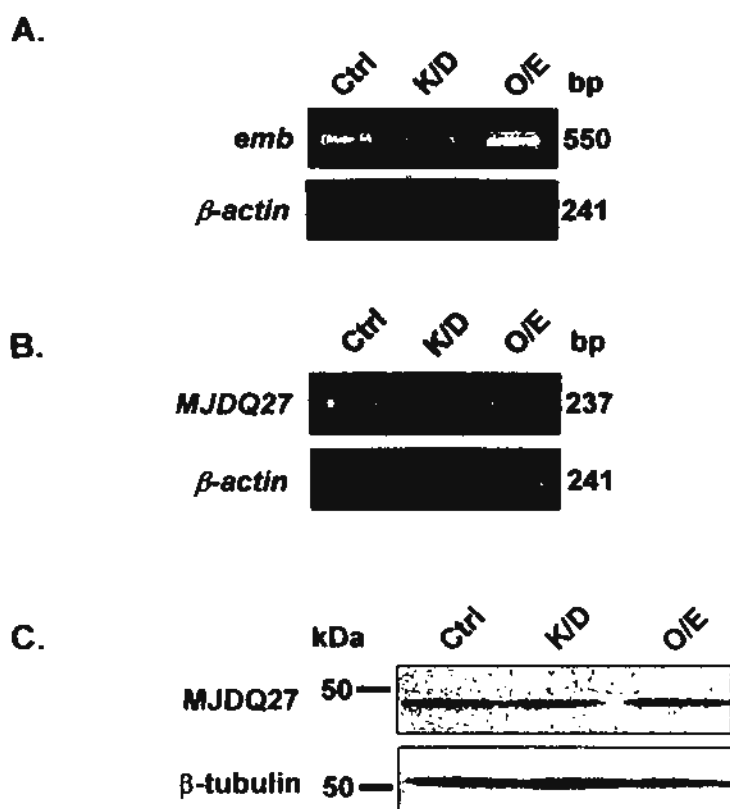


**Figure 4.1. Expression levels of *emb* and *MJDQ27* in *emb* knockdown or over-expressed transgenic flies. (A)** RT-PCR was performed to confirm the knockdown (K/D) and over-expression (O/E) of *emb* in transgenic flies as compared to control (ctrl) flies. *β-actin* was used as loading control. **(B and C)** Upon an alteration of *emb* expression level, transgenic expression of full length MJDQ27 remained unaffected, at both **(B)** mRNA and **(C)** protein levels. Immunoblot analysis was performed with anti-myc antibody (9B11). *β-actin* and β-tubulin were used as loading controls for RT-PCR and immunoblotting respectively. The flies were of genotypes *w; gmr-gal4 UAS-myc-MJDQ27/+, w; gmr-gal4 UAS-myc-MJDQ27/UAS-emb dsRNA, and w; gmr-gal4 UAS-myc-MJDQ27/emb[EP-E128-1A]*.

When MJDQ84 was expressed alone, the number of rhabdomeres per ommatidium decreased from 7 to 3.52±0.46 (Fig. 4.2). When the *emb* dsRNA was co-expressed with MJDQ84, the number of rhabdomeres further decreased to 1.45±0.27 (Fig. 4.2). On the contrary, the over-expression of *emb* rescued the degenerative phenotype, as revealed by an increase in the number of rhabdomeres to 6.56±0.15 (Fig. 4.2). The number of rhabdomeres between different crosses involved MJDQ27 showed no significant difference and there was not any dominant phenotype observed (Fig. 4.2). This thus demonstrated a specific modulatory effect of *emb* on MJDQ84-induced toxicity.

**A.**



**B.**
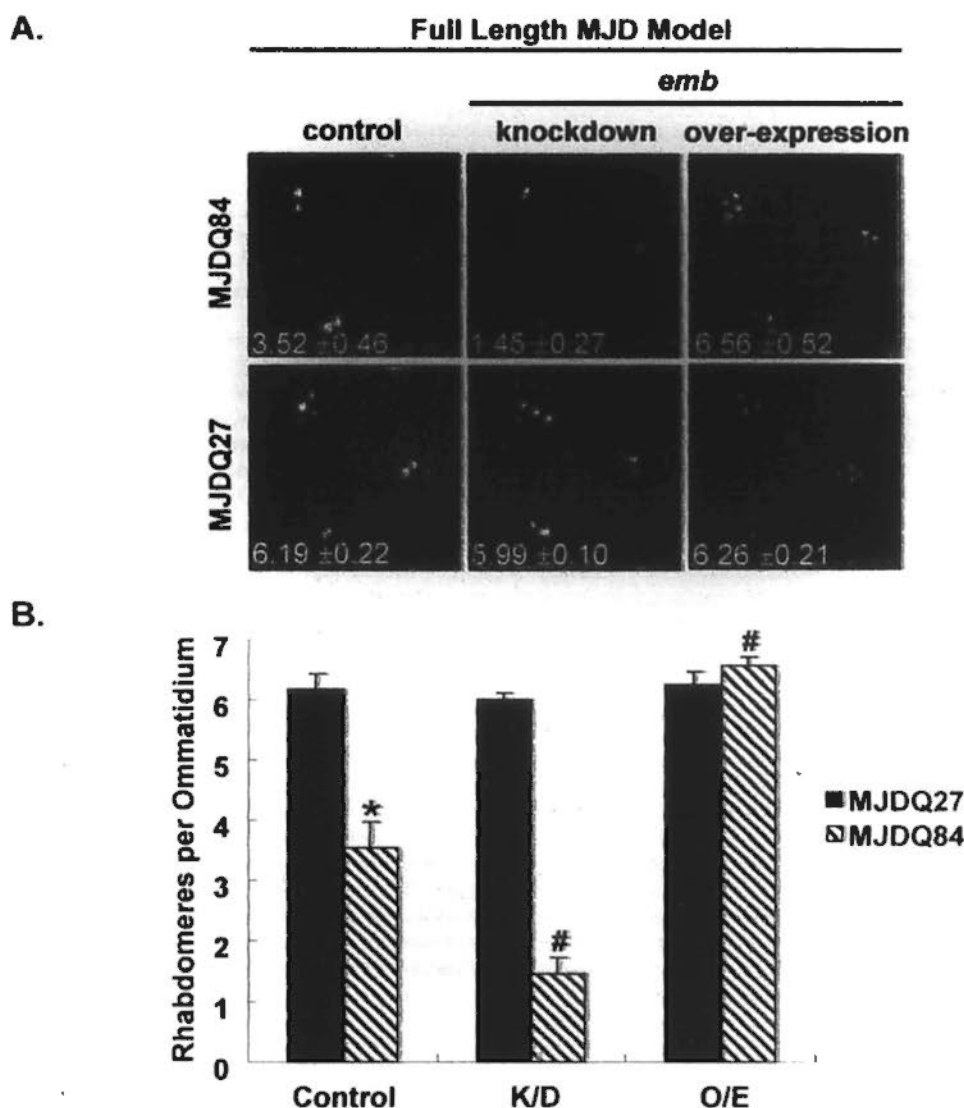


**Figure 4.2. Modulatory effect of *emb* on MJDQ84-induced toxicity.** **(A)** Representative images of rhabdomeres isolated from adult flies (0-2 days post-eclosion) cultured at 22°C. Each panel shows a field of three units of ommatidium. **(B)** Quantification of (A). MJDQ27 flies showed normal numbers of rhabdomeres regardless *emb* expression level. Expression of MJDQ84 alone caused a significant reduction in the number of rhabdomeres (* $p < 0.001$, compared to MJDQ27 alone, by Rank Sum Test). Both the knockdown (K/D) and over-expression (O/E) of *emb* resulted in a significant alteration in the number of rhabdomeres per ommatidium (# $p < 0.001$, compared to MJDQ84 alone, by Rank Sum Test). Error bars represent S.E.M. of three independent experiments. The flies were of genotypes *w; gmr-gal4 UAS-myc-MJDQ27/+, w; gmr-gal4 UAS-myc-MJDQ27/UAS-emb dsRNA, w; gmr-gal4 UAS-myc-MJDQ27/emb^EP-E128-1A, w; gmr-gal4/+; UAS-myc-MJDQ84/+, w; gmr-gal4/UAS-emb dsRNA; UAS-myc-MJDQ84/+, and w; gmr-gal4/emb^EP-E128-1A; UAS-myc-MJDQ84/+.*

**4.2 Modulatory Effects of *embargoed* in Different *Drosophila* Models of Polyglutamine**

    **Diseases**

The modulatory effects of *emb* on mutant polyQ-induced toxicity were further confirmed with different *Drosophila* models of polyQ diseases (Chan et al., 2002; Steffan et al., 2001; Warrick et al., 1998; Wong et al., 2008). Similar to the study with the full-length MJD model, transgene expressions were driven by the *gmr*-gal4 driver in adult fly eyes (Ellis et al., 1993) and the degenerative phenotype was assayed by external eye depigmentation.

When a disease unrelated protein, EGFP, was tagged with 76 glutamines (EGFPQ76), its expression in the adult *Drosophila* eyes resulted in external eye depigmentation (Fig. 4.3A; (Wong et al., 2008)). Upon the knockdown of *emb* expression, the EGFPQ76 degenerative phenotype was enhanced as indicated by the appearance of scars on the eye (Fig. 4.3A). It should be noted that dead pupae, which were absent from flies expressing the *EGFPQ76* transgene alone, were also observed when EGFP-Q76 was expressed in an *emb* knockdown background. On the other hand, the over-expression of *emb* rescued EGFPQ76 degeneration as shown by the restoration of external eye pigmentation (Fig. 4.3B). Similar results were also observed in other disease models, including truncated MJD (Fig. 4.3C and D; (Warrick et al., 1998)), truncated AR (Fig. 4.3E and F; (Chan et al.,

2002)), and exon1 of Htt (Fig. 4.3G; (Steffan et al., 2001)). Noted that since no external

eye modification was observed when the mutant Htt protein was expressed alone, the

suppressive effect due to *emb* over-expression could not be demonstrated in such model.
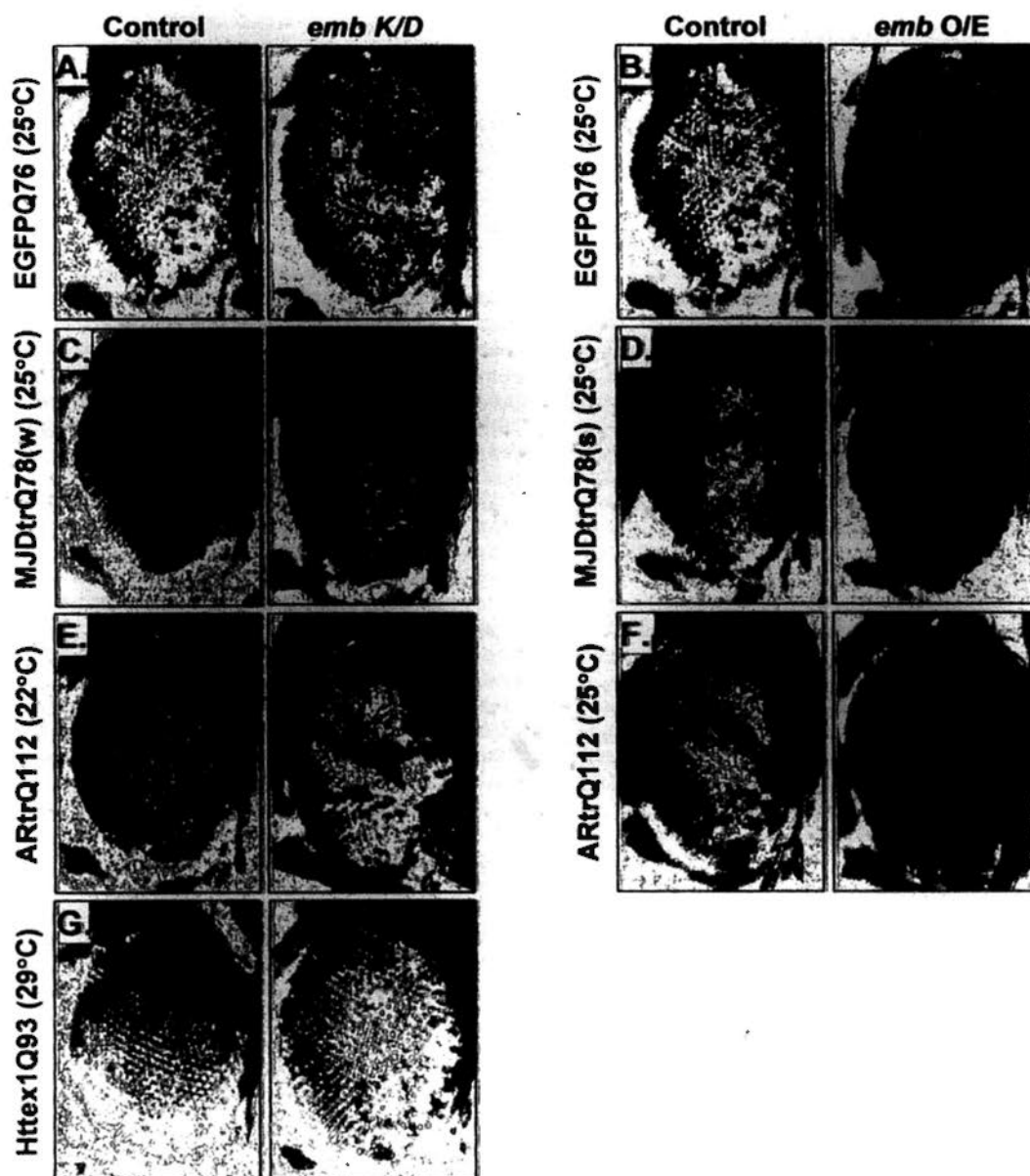
**Figure 4.3. Modulatory effect of *emb* on different polyQ disease models.** Knockdown (K/D) of *emb* expression enhanced the degenerative phenotype caused by the expression of mutant polyQ proteins in flies transgenic for **(A)** EGFPQ76, **(C)** truncated MJDQ78(weak) (MJDtrQ78(w)), **(E)** truncated ARQ112 (ARtrQ112) and **(G)** exon1 of HttQ93 (Httex1Q93). On the contrary, over-expression (O/E) of *emb* rescued degeneration caused by **(B)** EGFPQ76, **(D)** MJDtrQ78(strong) (MJDtrQ78(s)) and **(F)** ARtrQ112. External eye phenotypes were captured from flies of 0-2 dpe. The flies were of genotypes *w; gmr-gal4/+; UAS-EGFPQ76-FLAG/+, w; gmr-gal4/UAS-emb dsRNA; UAS-EGFPQ76-FLAG/+, w; gmr-gal4/emb$^{EP-E128-1A}$; UAS-EGFP-Q76-FLAG/+, w; gmr-gal4/+; UAS-HA-MJDtrQ78(w)/+, w; gmr-gal4/UAS-emb dsRNA; UAS-HA-MJDtrQ78(w)/+, w; gmr-gal4 UAS-HA-MJDtrQ78(s)/+, w; gmr-gal4 UAS-HA-MJDtrQ78(s)/emb$^{EP-E128-1A}$, w; gmr-gal4/+; UAS-HA-ARtrQ112/+, w; gmr-gal4/UAS-emb dsRNA; UAS-HA-ARtrQ112/+, w; gmr-gal4/emb$^{EP-E128-1A}$; UAS-HA-ARtrQ112/+, Httex1Q93/w; gmr-gal4/+, and Httex1Q93/w; gmr-gal4/UAS-emb dsRNA.*

## 4.3 Specific Modulatory Effect of *embargoed* on Mutant Polyglutamine Toxicity

The modulatory effect of *emb* was next tested in another *Drosophila* model of

neurodegenerative disease, Parkinson's Disease (PD). The expression of the disease protein

of PD α-synuclein in the adult fly eyes, as driven by the *gmr*-gal4 driver (Ellis et al., 1993),

caused a reduction in the number of rhabdomeres per ommatidium to 2.38±0.03 (Fig. 4.4)

(Auluck et al., 2002). No significant difference in terms of the number of rhabdomeres in

α-synuclein flies was found when *emb* was either knocked down or over-expressed (Fig.

4.4). The co-expression of human heat shock protein 70, HSPA1L with α-synuclein was a

positive control to show the toxicity induced by α-synuclein could be modified by

suppressor transgene expression (Fig. 4.4) (Auluck et al., 2002). The result obtained from

this PD model highlighted the specific modulatory effect of *emb* on mutant polyQ-induced
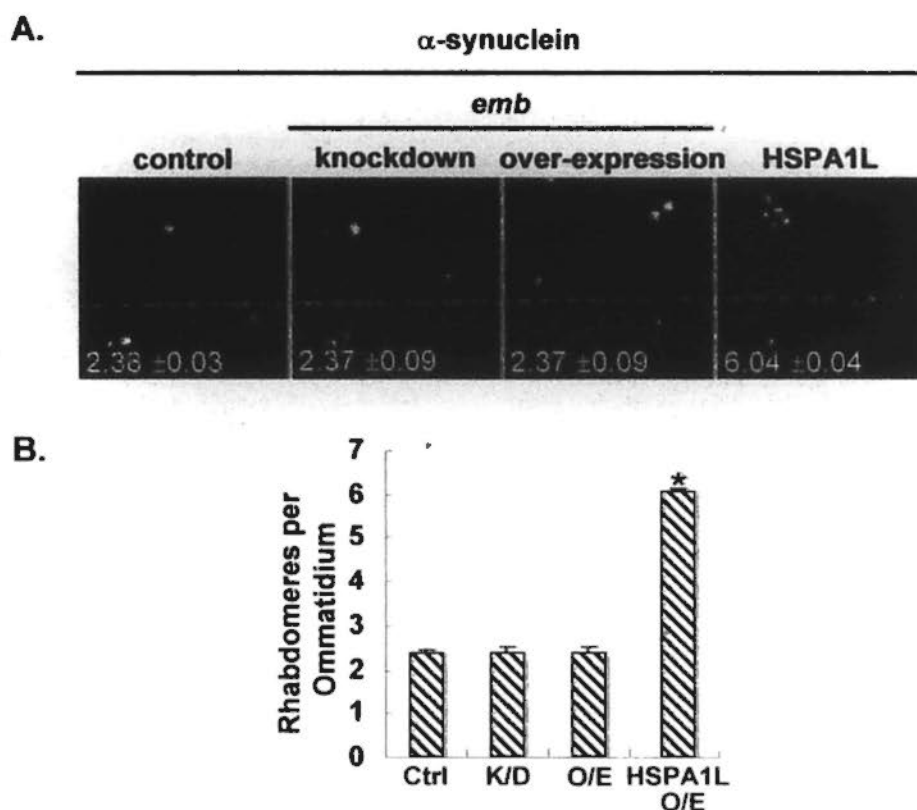
toxicity.

**Figure 4.4. Modulatory effect of *emb* on α-synuclein-induced toxicity. (A)** Representative images of rhabdomeres captured from adult flies cultured at 25°C (< 8 hours post-eclosion). Each panel shows a field of three units of ommatidium. **(B)** Quantification of (A). Expression of α-synuclein alone (control, ctrl) caused a reduction in rhabdomeres number. Neither the knockdown (K/D) nor over-expression (O/E) of *emb* exerted modulatory effect on α-synuclein-induced toxicity. Co-expression of human hsp70 protein, HSPA1L, with α-synuclein rescued the degenerative phenotype as indicated by an increase in the number of rhabdomeres per ommatidium (* $p <$ 0.001, compared to α-synuclein alone, by Rank Sum Test). Error bars represent S.E.M. of three independent experiments. The flies were of genotypes *w; gmr-gal4/+; UAS-α-synuclein/+, w; gmr-gal4/UAS-emb dsRNA; UAS-α-synuclein/+, w; gmr-gal4/emb[EP-E128-1A]; UAS-α-synuclein/+, and w; gmr-gal4/UAS-HSPA1L; UAS-α-synuclein/+.*

**4.4 Correlation between Mutant Polyglutamine Protein Nucleocytoplasmic Localization and Toxicity**

As mentioned, a well-established function of emb is to mediate protein nuclear export (Fornerod et al., 1997). In order to determine if the modulation on toxicity by *emb* (Fig. 4.2) would associate with an altered subcellular localization of mutant polyQ protein, the nucleocytoplasmic distribution of mutant MJD protein was investigated in different *emb* expression backgrounds.

Since mutant polyQ proteins might exist in different conformations (Ross and Poirier, 2005), formic acid was employed to solubilize the SDS-insoluble conformers (Hazeki et al., 2000) so that the majority of, if not all, mutant polyQ proteins appeared as monomer when resolved by SDS-PAGE. Formic acid treatment therefore allows the determination of the subcellular localization of polyQ proteins of all forms at a glance. The mutant MJDQ84 protein distributed evenly between the cytoplasmic and nuclear compartments, as indicated by a nuclear to cytoplasmic ratio of MJDQ84 protein of ~1 (Fig. 4.5). Upon depletion of *emb* mRNA by dsRNA, the MJDQ84 protein predominantly accumulated in the nucleus (Fig. 4.5). On the contrary, the over-expression of *emb* due to an EP insertion resulted in a cytoplasmic accumulation of MJDQ84 protein (Fig. 4.5). The modulatory effect of *emb* was demonstrated to be specific for mutant polyQ protein because the unexpanded

MJDQ27 protein localized predominantly to the cytoplasm regardless the expression level

of *emb* (Fig. 4.5).

A.



B.
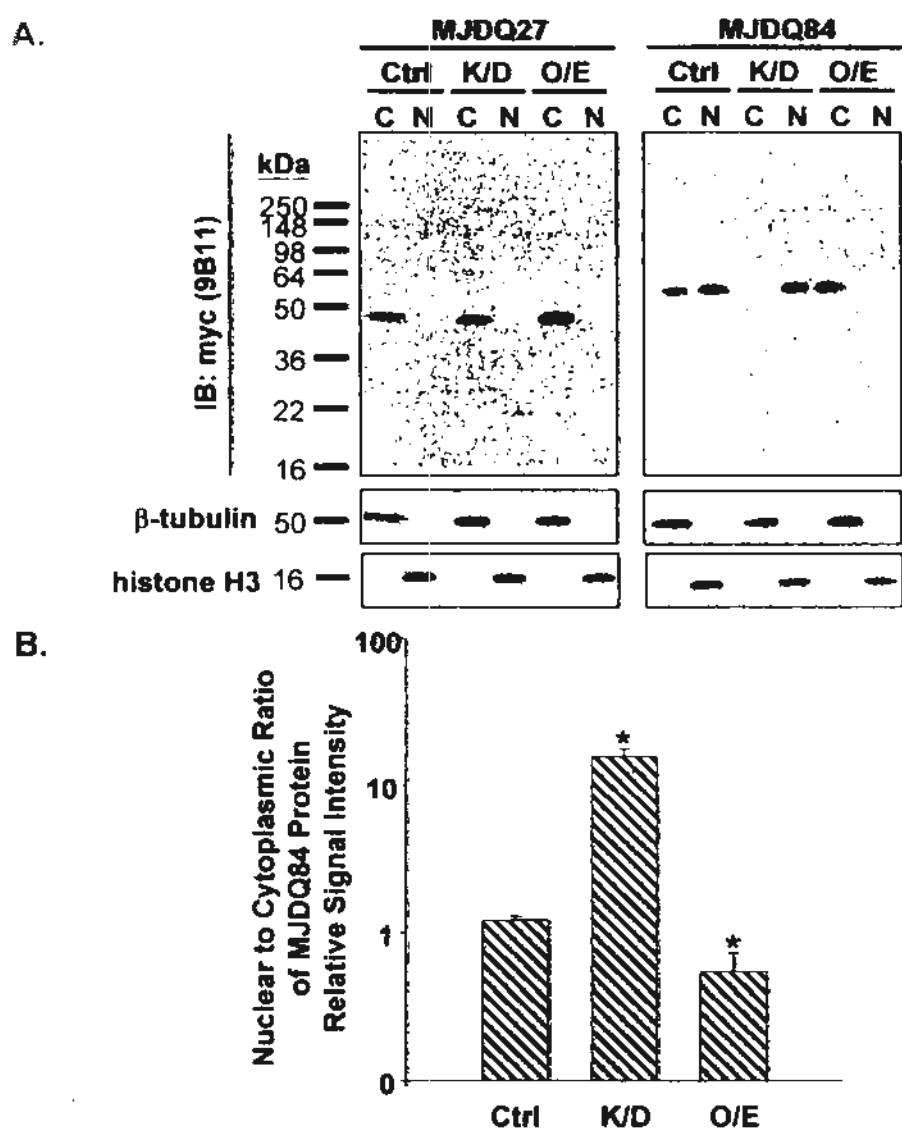


**Figure 4.5. Nucleocytoplasmic fractionation of MJDQ27 and MJDQ84 proteins from adult flies. (A)** Immunoblot (IB) analysis of cytoplasmic (C) and nuclear (N) MJD proteins isolated from transgenic flies of 0-2 days post-eclosion cultured at 25°C. Protein samples (4 fly heads) were treated with formic acid before SDS-PAGE. β-tubulin and histone H3 were used to reveal the quality of fractionation and as loading controls. Vertical bar indicates the position of stacking gel. **(B)** Quantification of (A). The knockdown (K/D) of *emb* expression increased the N/C ratio while *emb* over-expression (O/E) decreased the ratio (* $p < 0.05$, compared to MJDQ84 alone (ctrl), by Rank Sum Test). Error bars represent S.E.M. of three independent experiments. The flies were of genotypes *w; gmr-gal4 UAS-myc-MJDQ27/+, w; gmr-gal4 UAS-myc-MJDQ27/UAS-emb dsRNA, w; gmr-gal4 UAS-myc-MJDQ27/emb[EP-E128-1A], w; gmr-gal4/+; UAS-myc-MJDQ84/+, w; gmr-gal4/UAS-emb dsRNA; UAS-myc-MJDQ84/+, and w; gmr-gal4/emb[EP-E128-1A]; UAS-myc-MJDQ84/+.*

## 4.5 Modulatory Effect of *embargoed* on the Enhancement of Polyglutamine Toxicity

### caused by *karyopherin-α3* Gene Knockdown

Apart from *emb*, *kap-α3* was another modifier identified to modulate the subcellular

localization of mutant polyQ protein and its toxicity (Appendixes 1 and 2, in collaboration

with Frankie Tsoi). The enhancement of toxicity due to the knockdown of *kap-α3*

expression was further confirmed in the full-length MJDQ84 model (Fig. 4.6B). However,

unlike *emb*, the modulation by *kap-α3* of mutant polyQ-induced toxicity was not

accompanied by a significant alteration of the nucleocytoplasmic distribution of mutant

polyQ protein (Fig. 4.6C), suggesting that *emb* and *kap-α3* modulated mutant polyQ

toxicity through different mechanisms. It was thus of interest to determine whether the

suppression by *emb* over-expression of polyQ toxicity was still effective in a *kap-α3*

knockdown background. To do this, a transgenic line carrying both the *kap-α3* dsRNA and

*emb* EP-inserts was first generated, and the over-expression and knockdown of *emb* and

*kap-α3* respectively in the double transgenic flies (DT) were confirmed by RT-PCR (Fig.

4.6A). The over-expression of *emb* in a *kap-α3* knockdown background was still able to

rescue MJDQ84 toxicity (Fig. 4.6B), and a cytoplasmic accumulation of mutant polyQ

protein was also noted (Fig. 4.6C). Such data suggests that the *emb*-mediated suppression,

through an alteration of the nucleocytoplasmic localization of mutant polyQ protein, plays

a dominant role over *kap-α3*.
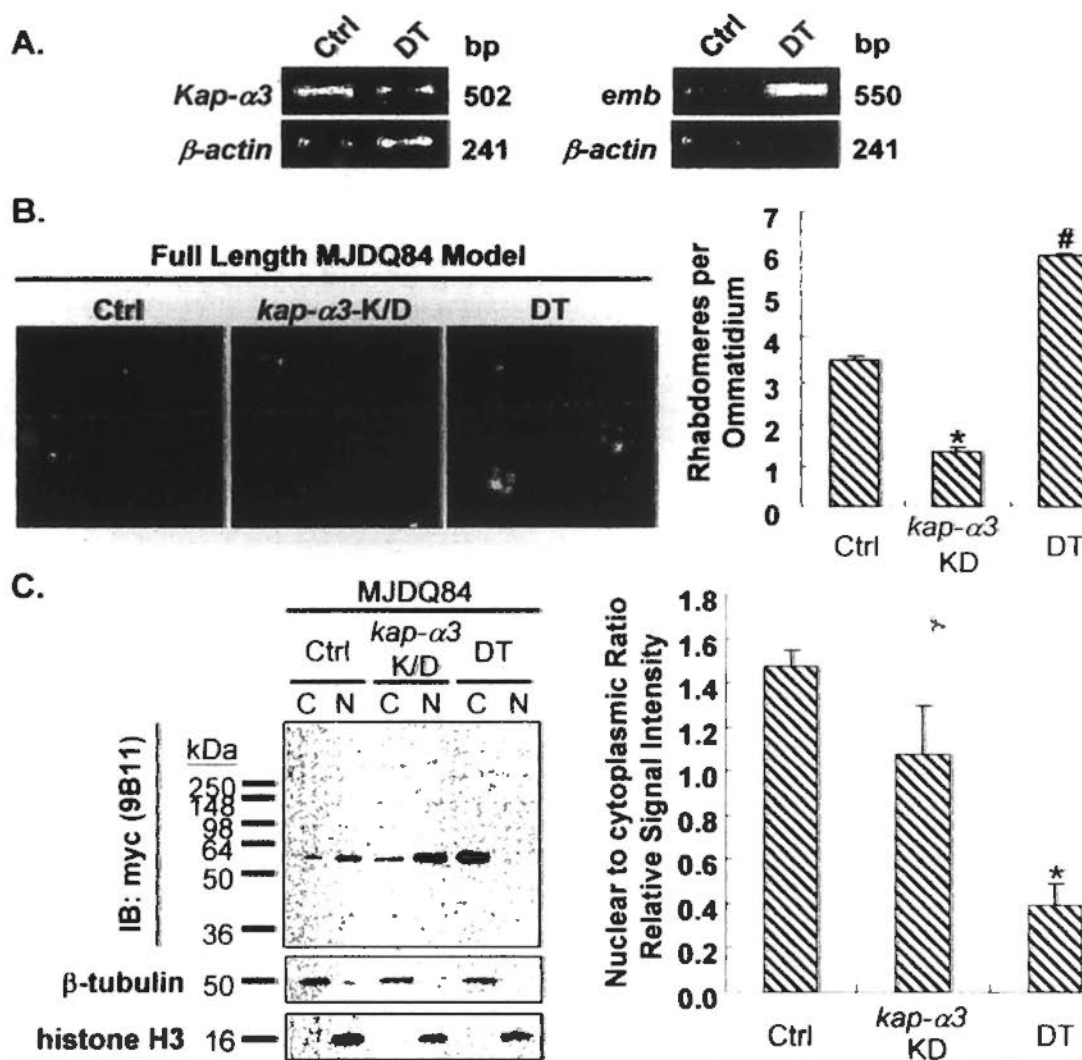
**Figure 4.6. Epistatic analysis of *emb* and *kap-α3* on MJDQ84-induced toxicity. (A)** RT-PCR analysis of *kap-α3* and *emb* expression in the double transgenic flies (DT). **(B)** Pseudopupil assay of transgenic flies cultured at 22°C (0-2 dpe). Knockdown (K/D) of *kap-α3* expression enhanced MJDQ84-induced degenerative phenotype (* $p < 0.001$, compared to MJDQ84 alone (Ctrl), by Rank Sum Test). However, enhancement was rescued by the simultaneous over-expression of *emb* (# $p < 0.001$, compared to Ctrl or kap-α3 K/D, by one way ANOVA on ranks followed by Dunn post-test). Error bars represent S.E.M. of three independent experiments. **(C)** Immunoblot (IB) analysis of cytoplasmic (C) and nuclear (N) MJDQ84 proteins from transgenic flies cultured at 25°C (0-2 dpe). knockdown of *kap-α3* expression alone did not alter the nucleocytoplasmic distribution of MJDQ84 protein. However, MJDQ84 was predominantly localized to the cytoplasm in DT (* $p < 0.05$, compared to MJDQ84 flies with *kap-α3* K/D alone, by Rank Sum Test). Error bars represent S.E.M. of three independent experiments. The flies were of genotypes *w; gmr-gal4/+; UAS-myc-MJDQ84/+, w; gmr-gal4/UAS-kap-α3 dsRNA; UAS-myc-MJDQ84/+,* and *w; gmr-gal4/UAS-kap-α3 dsRNA emb^{EP-E128-1A}; UAS-myc-MJDQ84/+.*

## 4.6 Discussion

Flanking sequences of the polyQ domain on different disease proteins have been reported to play roles in polyQ pathogenesis (Chai et al., 2001; Steffan et al., 2004). In this study, no sequence homology apart from the expanded polyQ domain can be found among the different polyQ disease models employed (Fig. 4.3). Nonetheless, they all showed the same modification upon an alteration of *emb* expression levels (Fig. 4.3). This implies that the polyQ domain, rather than the flanking sequences on disease proteins, is responsive to the *emb*-mediated pathway in polyQ toxicity. This argument was further consolidated by the result obtained from the EGFPQ76 model (Fig. 4.3A and B). The EGFP protein is well-known for its inertness and has been widely adopted in studies focused solely on the expanded polyQ domain itself (Kazantsev et al., 1999; Moulder et al., 1999; Takahashi et al., 2007).

## 4.6.1 Possible Nuclear Transport Activities conferred by Expanded Polyglutamine Domain

Similar to the truncated MJDQ27 protein (Warrick et al., 1999), full-length MJDQ27 protein remained cytoplasmic (Fig. 4.5). However, an expansion of polyQ domain in MJDQ84 caused a redistribution of the MJD protein to the nucleus (Fig. 4.5). This data implies that the presence of an expanded polyQ domain initiates nuclear import of the host

protein, which is consistent with that reported earlier in a transgenic mouse model (Ordway et al., 1997).

Apart from the involvement of protein nuclear import machinery, the nucleocytoplasmic distribution of the MJDQ84 protein was also shown to be dependent on the nuclear export receptor, emb. Consistent with its well established role in protein nuclear export, the knockdown of *emb* expression was accompanied by a nuclear accumulation of mutant MJDQ84 whereas its over-expression resulted in a cytoplasmic build-up of the mutant protein (Fig. 4.5). Although it is not known which form(s) of the expanded, misfolded mutant protein represents the most toxic species, this result raises a possible function of expanded polyQ domain as an NES, and its activity is mediated through the emb-dependent protein nuclear export pathway.

Altogether, the nucleocytoplasmic fractionation data from MJDQ27 and MJDQ84 transgenic flies (Fig. 4.5) suggests that an expansion of polyQ domain confers both nuclear import and export activities to the mutant host protein. Therefore, apart from classical nuclear transport signals (Table 1.2) present on disease proteins (Bessert et al., 1995; Chen et al., 2004; Jenster et al., 1993; Kaytor et al., 1999; Klement et al., 1998; Kordasiewicz et al., 2006; Nucifora et al., 2003; Saporita et al., 2003; Taylor et al., 2006; Xia et al., 2003),

expanded polyQ domain itself also plays role(s) in regulating the nucleocytoplasmic localization of mutant proteins. In particular for MJD, although both classical NLS and NES have been predicted on the normal protein (Albrecht et al., 2004), their transport activities have not been confirmed experimentally. However, no matter these transport signals are functional or not, the nucleocytoplasmic fractionation data from MJDQ27 and MJDQ84 transgenic flies (Fig. 4.5) demonstrates a dominant role of the expanded polyQ domain on governing the localization of mutant MJD protein.

### 4.6.2 Nuclear Toxicity of Mutant Polyglutamine Protein

Nuclear toxicity of mutant polyQ proteins has been reported in numerous disease models (Benn et al., 2005; Jackson et al., 2003; Klement et al., 1998; Kordasiewicz et al., 2006; Nucifora et al., 2003; Peters et al., 1999; Saudou et al., 1998; Schilling et al., 2004; Schilling et al., 1999). The accumulation of MJDQ84 protein in the nucleus was associated with an enhanced toxicity (Figs. 4.2 and 4.5), suggesting that nuclear mutant protein confers more toxicity than its cytoplasmic counterpart. This result is in good agreement with previous report on transgenic mice (Bichelmeier et al., 2007). By taking advantage of exogenous NLS and NES, the localization of mutant MJD protein in transgenic mice was altered and degenerative phenotypes were monitored (Bichelmeier et al., 2007). Targeting the MJDQ148 protein in the cytoplasm by an NES alleviates the pathologic effects while

restricting the mutant protein in the nucleus by an NLS aggravates the toxic effects of an

expanded polyQ domain (Bichelmeier et al., 2007).

Results obtained from this study further consolidate the toxicity attributed by nuclear

mutant protein, and confirm the modulatory effect of *emb* on mutant polyQ-induced

toxicity reported earlier (Bilen and Bonini, 2007). It is also demonstrated here for the first

time that endogenous karyopherins, particularly emb, play roles in modulating mutant

polyQ-induced toxicity though modifying the subcellular localization of mutant polyQ

proteins.

### 4.6.3 Specific Modulatory Effect of *embargoed* on Polyglutamine Toxicity

The specificity of *emb* modification for mutant polyQ-induced toxicity was addressed

with the use of a *Drosophila* model of PD (Auluck et al., 2002). The expression of

α-synuclein in the adult fly eyes caused toxicity (Auluck et al., 2002); nonetheless, neither

the knockdown nor over-expression of *emb* modulated such toxic effect (Fig. 4.4). Unlike

Hsp70, a molecular chaperone that is able to suppress both polyQ- and

α-synuclein-induced toxicity (Auluck et al., 2002; Warrick et al., 1999), *emb* specifically

modulates polyQ toxicity. Molecular chaperones rescue neurodegenerative disorders by

assisting the refolding of misfolded proteins in general (Barral et al., 2004; Liberek et al.,

2008). In contrast, *emb* is proposed to suppress polyQ toxicity in a more specific manner by promoting nuclear export of mutant polyQ protein; a phenomenon which depends on the recognition of expanded polyQ domain by emb. Although toxicity of nuclear α-synuclein has also been reported (Kontopoulos et al., 2006), it is speculated that the inability of *emb* to suppress α-synuclein-induced toxicity is attributed to a lack of receptor-substrate interaction between them, and thus α-synuclein is not exported out from the nucleus by emb.

## 4.6.4 Dominant Effect of *embargoed* Over *karyopherin-α3* on Mutant Polyglutamine-induced Toxicity

*embargoed* and *karyopherin-α3* were the two *karyopherins* identified in the *Drosophila* genome that modulate mutant polyQ-induced toxicity (Appendix 2, in collaboration with Frankie Tsoi). However, they were found to modulate toxicity through different mechanisms. The enhancement on MJDQ84-induced toxicity due to *emb* knockdown was accompanied by nuclear accumulation of the MJDQ84 protein (Figs. 4.2 and 4.5). Yet, the nucleocytoplasmic distribution of mutant protein remained unchanged when MJDQ84-induced toxicity was enhanced by *kap-α3* gene knockdown (Fig. 4.6). This implies the existence of mechanism that modulates polyQ toxicity without any effect on the subcellular localization of mutant proteins. The modulation by *kap-α3* might be an

indirect effect from the altered nucleocytoplasmic distribution of other cellular proteins.

Since *emb* over-expression was able to rescue mutant polyQ-induced toxicity in a *kap-α3*

knockdown background (Fig. 4.6), it is believed that *emb* can suppress polyQ toxicity in

the absence of *kap-α3*, and the *emb*-mediated pathway plays a dominant role over *kap-α3*

in modulating polyQ toxicity.

In summary, it was demonstrated in this chapter that depletion of *emb* expression led to an enhancement of MJDQ84-induced degeneration, which was accompanied by a nuclear accumulation of the mutant protein (Figs. 4.2 and 4.5). On the contrary, increased *emb* expression resulted in suppression of the degenerative phenotype and a concomitant cytoplasmic buildup of the mutant polyQ protein (Figs. 4.2 and 4.5). This supports the notion that nucleus is the primary major toxic site for polyQ toxicity observed in MJDQ84 model.

# *Chapter 5. Nucleocytoplasmic Shuttling Properties of Mutant*

# *Polyglutamine Protein*

Subcellular localization of mutant polyQ protein is crucial for mutant polyQ-induced toxicity (detailed in Section 1.5). From the *in vivo* data described in Chapter 4, an expanded polyQ domain was shown to possess both nuclear import and export activities. Since the mechanism of nucleocytoplasmic localization of expanded polyQ domain remained largely undefined, cultured cell models were developed to investigate this localization in detail.

## 5.1 Expanded Polyglutamine-mediated Protein Nuclear Import

An EGFP-based reporter for protein nuclear import study in cultured *Drosophila* cells

has been established based on a chimeric reporter protein composed of 2 copies of EGFP

and 1 copy of GST (Appendix 3) (Chan et al., 2007). A unique advantage of the

EGFP2GST reporter is attributed to its size, which is over the diffusion limit across the

NPCs (Pemberton and Paschal, 2005). Although the trimeric EGFP reporter (EGFP3) has

been adopted in nuclear transport study to eliminate passive diffusion in mammalian cell

culture system, low levels of GFP signal were still detected in the nuclei of transfected

cells (Fig. 5.1A) as reported (Nakahara et al., 2006). Thus, the EGFP2GST reporter was

tested in mammalian cell culture system. Similar to *Drosophila* cells, human embryonic

kidney 293 cells transfected with the *EGFP2GST* construct showed a restrictive diffuse

cytoplasmic GFP signal (Fig. 5.1B). As expected, the addition of the SV40 large T antigen

NLS sequence (Kalderon et al., 1984) to EGFP2GST was able to target the reporter

exclusively to the nucleus (Fig. 5.1C). Thus, the EGFP2GST reporter was employed to

study the nuclear import property of the expanded polyQ domain.
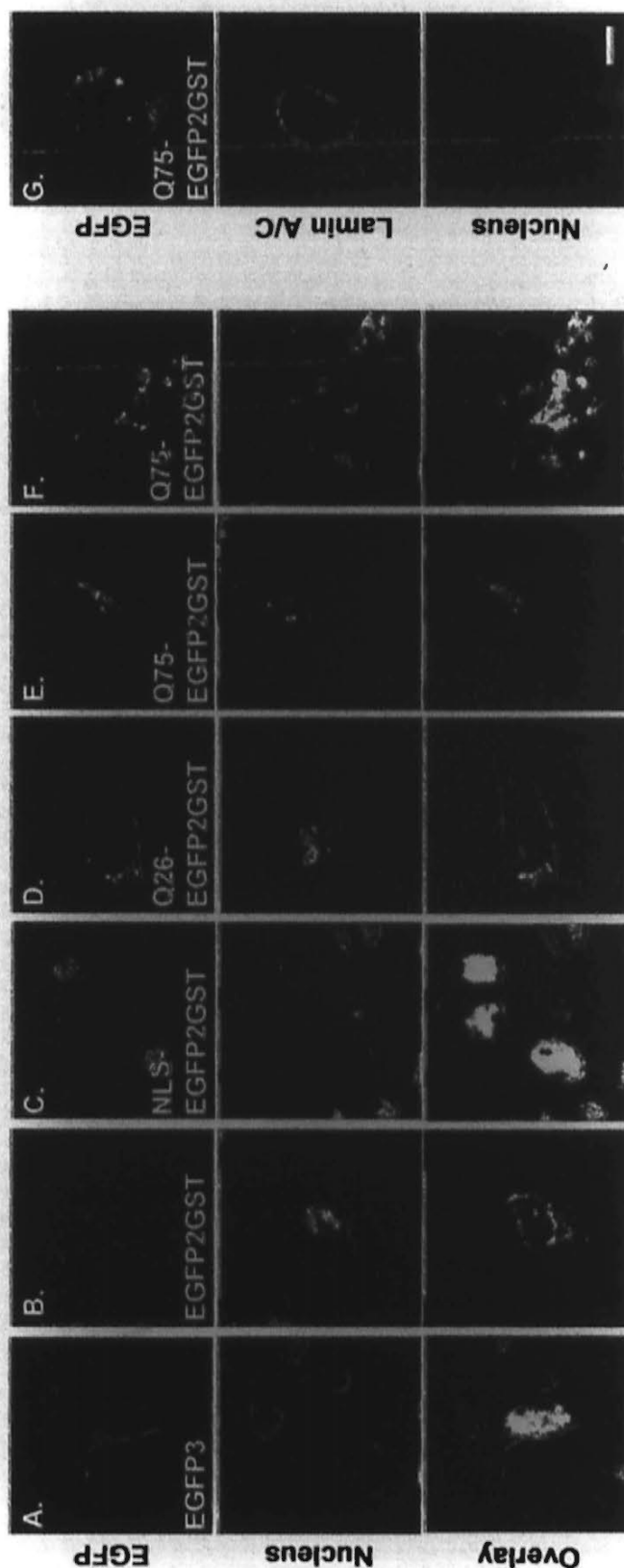
**Figure 5.1. Confocal images of HEK 293 cells expressing different EGFP-based reporters.** At 48h post-transfection, HEK 293 cells were fixed and stained with propidium iodide (in red) to label the cell nuclei. **(A)** Low level of GFP signal was detected in the nucleus of cell expressing the trimeric EGFP reporter, EGFP3. **(B)** The EGFP2GST reporter localized exclusively to the cytoplasm, **(C)** and the addition of SV40 NLS sequence targeted the reporter to the nucleus. **(D)** The presence of an unexpanded polyQ domain (Q26) did not alter the cytoplasmic localization of EGFP2GST. However, the addition of an expanded polyQ domain (Q75) redistributed part of the EGFP2GST protein to the nucleus, either **(E)** in diffuse form or **(F)** as aggregates. **(G)** Cells transfected with Q75-EGFP2GST reporter were stained for Lamin A/C (in red) to show the integrity of the nuclear envelope. The cell nucleus was labeled with Hoechst (in blue). Scale bar represents 10 μm.

137

### 5.1.1 Subcellular Localization of Q26/Q75-EGFP2GST Proteins in HEK 293 and BG2 Cells

To focus on the protein nuclear import mediated by a naked polyQ domain, EGFP2GST reporters carrying either an unexpanded (Q26) or expanded (Q75) polyQ domain were constructed. Subcellular localization of the Q26- and Q75-EGFP2GST proteins in HEK 293 cells was examined by confocal microscopy (Fig. 5.1D-F). Similar to the EGFP2GST reporter (Fig. 5.1B), the Q26-EGFP2GST protein displayed an exclusive cytoplasmic localization (Fig. 5.1D). On the contrary, the addition of an expanded polyQ domain to the EGFP2GST reporter resulted in partial nuclear localization of the reporter; the Q75-EGFP2GST protein appeared in the nucleus either in a diffuse form (Fig. 5.1E) or as microscopically visible aggregates (Fig. 5.1F).

To investigate the integrity of the nuclear envelope, lamin A/C immunostaining of Q75-EGFP2GST-expressing HEK 293 cells was performed. Lamin A/C localizes specifically on the nuclear envelope (Gerace and Blobel, 1980). It was found that the nuclear envelope remained intact despite the presence of nuclear aggregates in HEK 293 cells expressing Q75-EGFP2GST (Fig. 5.1G). This ruled out the possibility that the presence of the Q75-EGFP2GST protein in the nucleus was merely due to the collapse of nuclear envelope upon mutant polyQ protein expression.

A complementary nucleocytoplasmic fractionation experiment was also performed to consolidate the confocal microscopy data (Fig. 5.2). Formic acid treatment was first performed to solubilize any SDS-insoluble polyQ protein species in the HEK 293 cell lysates (Hazeki et al., 2000). Consistent with the confocal microscopy findings, the Q26-EGFP2GST protein was only detected in the cytoplasmic fractions at all time points examined (Fig. 5.2), while the Q75-EGFP2GST protein was initially detected in the cytoplasmic fractions but gradually appeared in the nuclear fractions at later time points (Fig. 5.2). Since the molecular weight of the Q75-EGFP2GST protein was over the passive diffusion limit (~60 kDa) across the NPC (Pemberton and Paschal, 2005), the detection of Q75-EGFP2GST by immunoblotting in the nuclear fractions implied an active transport mechanism was involved.

Consistently, nuclear localization of the Q75-EGFP2GST protein was also observed in the *Drosophila* BG2 neuronal cells. Both SDS-soluble and formic acid-soluble Q75-EGFP2GST protein accumulated in the nuclear fractions of BG2 cell lysates in a time-dependent manner (Fig. 5.3A). Complementary confocal images also revealed the presence of nuclear aggregates in transfected BG2 cells (Fig. 5.3B). Taken together, the translocation of Q75-EGFP2GST from cytoplasm to nucleus is mediated by an active process, and such phenomenon is specific to expanded polyQ domain-containing protein.
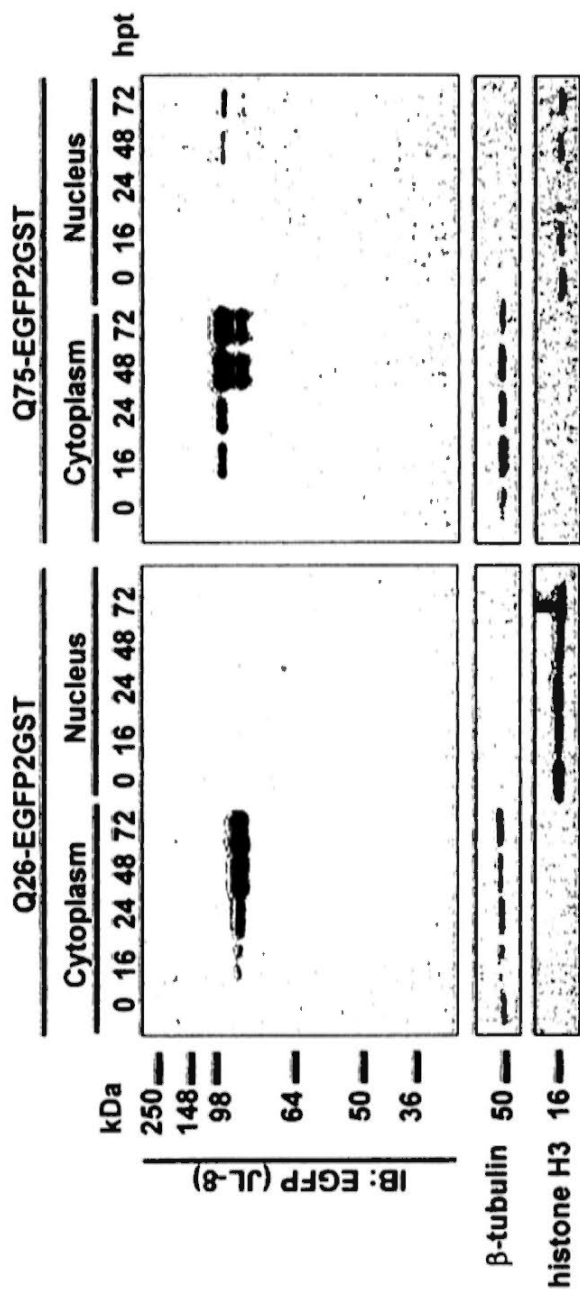
**Figure 5.2. Nucleocytoplasmic fractionation of Q26- and Q75-EGFPGST proteins from transiently transfected HEK 293 cells.** At different hours post-transfection (hpt), lysates of HEK 293 cells transfected with Q26-or Q75-*EGFP2GST* construct were fractionated into cytoplasmic and nuclear extracts, followed by formic acid treatment. Five microgram of proteins were loaded into each lane. The Q26 protein was only detected in the cytoplasm. The Q75 protein was initially detected in the cytoplasm, and appeared in the nucleus starting from 48 hpt. β-tubulin and histone H3 were used to reveal the quality of fractionation and as loading controls.

A.



B.
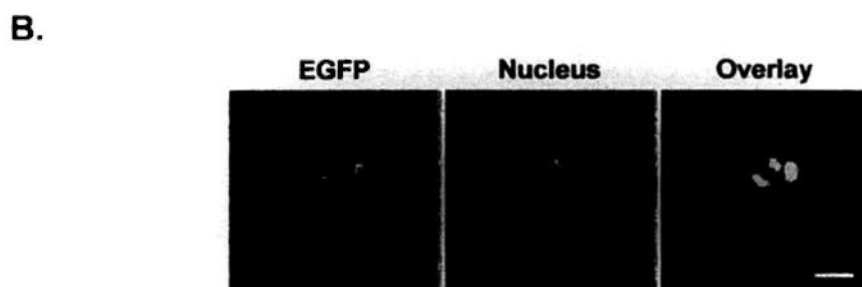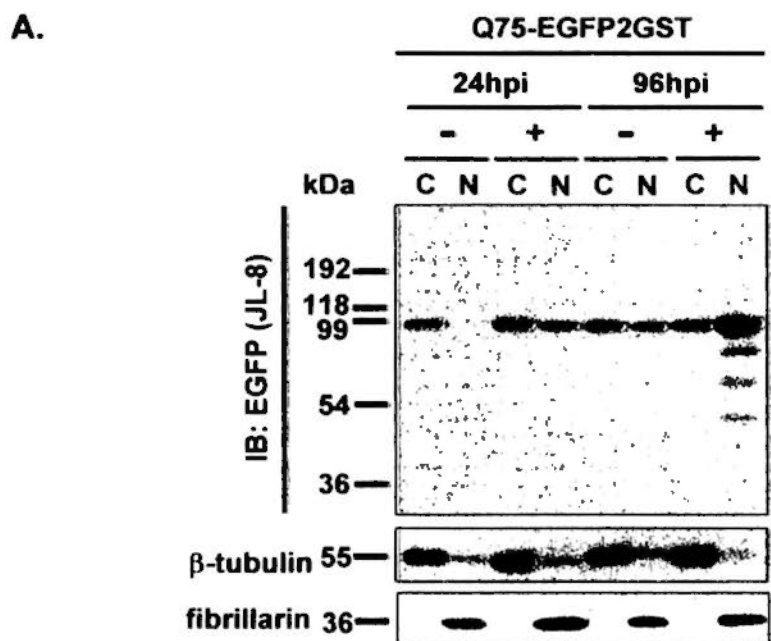


**Figure 5.3. Subcellular localization of Q75-EGFP2GST protein in transiently transfected BG2 cells. (A)** Immunoblot (IB) analysis of cytoplasmic (C) and nuclear (N) Q75-EGFP2GST proteins from BG2 cells at 24 and 96 hours post-induction, hpi. Compared to the untreated control (-), formic acid treatment (+) specifically solubilized Q75-EGFP2GST in the nuclear extracts. The amount of Q75-EGFP2GST protein accumulated in the nucleus in a time-dependent manner. β-tubulin and fibrillarin were used to reveal the quality of fractionation and as loading controls. Vertical bar represents stacking gel. **(B)** Confocal image of a representative BG2 cell expressing Q75-EGFP2GST protein. At 96 hpi, cells were fixed and stained with propidium iodide (in red) to label the cell nuclei. Nuclear aggregates were detected in Q75-EGFP2GST-expressing BG2 cells. Scale bar represents 5 μm.

**5.1.2 Time-lapse Microscopy of Q26/Q75-EGFP2GST Proteins in HEK 293 Cells**

Since both diffuse and aggregated mutant polyQ proteins were detected in the nucleus, time-lapse experiment was next performed to determine in which form(s) did the mutant polyQ protein translocate from the cytoplasm to the nucleus. Since the Q75-EGFP2GST protein started to appear in the nuclear fraction at 48 h post-transfection (hpt; Fig. 5.2), its movement in HEK 293 cells was monitored in a real time manner from 24 – 48 hpt. The Q75-EGFP2GST protein localized predominantly to the cytoplasm at 24 hpt, but its abundance in the nucleus increased gradually with time and eventually aggregates were detected inside the nucleus (Appendix 4A, performed by Dr. Eric Wong). Cells expressing the Q26-EGFP2GST protein were monitored in parallel as control, and the GFP signal remained cytoplasmic throughout the course of the experiment (Appendix 4A, performed by Dr. Eric Wong). From the time-lapse microscopy observation, no aggregated mutant polyQ protein was found to translocate from the cytoplasm to the nucleus. Rather, the imported Q75-EGFP2GST protein subsequently formed microscopically visible aggregates *de novo* inside the nucleus. Thus, the diffuse Q75-EGFP2GST protein was responsible for entering the nucleus from the cytoplasm.

### 5.1.3 Time-lapse Microscopy of Q75-EGFP2GST Proteins in a RanGEF-depleted Cell

####    Line tsBN2

To determine whether the nuclear entry of mutant polyQ protein occurred via a Ran-dependent mechanism, a temperature sensitive mutant of baby hamster kidney cell line tsBN2 was used (Nishimoto et al., 1978). The tsBN2 cells carry a temperature-sensitive *RanGEF* allele (Tachibana et al., 1994). At permissive temperature (33.5°C), an intact Ran gradient across the nuclear envelope is maintained. However, growth of tsBN2 cells at the non-permissive temperature (39.5°C) depletes RanGEF, which results in a collapse of the Ran gradient and hence inhibits Ran-dependent protein nuclear transport (Tachibana et al., 1994). As shown in Appendix 4B (performed by Dr. Eric Wong), incubation of tsBN2 cells transfected with the *Q75-EGFP2GST* construct at 39.5°C did not affect the nuclear appearance of Q75-EGFP2GST protein. This indicates that nuclear import of mutant polyQ protein was independent of Ran.

## 5.2 Expanded Polyglutamine-mediated Protein Nuclear Export

After studying the protein nuclear import mediated by an expanded polyQ domain, its possible nuclear export properties were examined.

## 5.2.1 Effect of Leptomycin B on the Subcellular Localization of Q81-EGFP Protein in SH-SY5Y Cells

The nuclear export mediated by expanded polyQ domain was examined in a human neuroblastoma cell line, SH-SY5Y. Cells transiently transfected with either *Q19-* or *Q81-EGFP-myc* construct were induced by retinoic acid to undergo neuronal differentiation (Encinas et al., 2000). After differentiation, the Q19-EGFP protein was found to localize homogeneously in both cytoplasm and nucleus (Fig. 5.4A), whereas the Q81-EGFP protein displayed three distinct localization patterns: 1) predominantly in the cytoplasm (Fig. 5.4B), 2) uniformly in both cytoplasm and nucleus (Fig. 5.4C) and 3) predominantly in the nucleus (Fig. 5.4D). Since it has been demonstrated that the expression level of emb is tightly correlated with the nucleocytoplasmic localization of mutant polyQ protein *in vivo* (Chapter 3), similar effect of its human ortholog, exportin-1 (Xpo1), was also examined. Differentiated SH-SY5Y cells expressing the Q81-EGFP protein were treated with Leptomycin B (LMB), a specific inhibitor of Xpo1-mediated protein nuclear export (Kudo et al., 1999). The Q81-EGFP protein in the majority of cells

treated with the ethanol solvent control showed either a predominant cytoplasmic localization or a uniform distribution between the cytoplasmic and nuclear compartments (Fig. 5.4E). On the contrary, LMB treatment caused the Q81-EGFP protein to localize predominantly to the nucleus (Fig. 5.4E). This suggests that the expanded polyQ domain was able to initiate nuclear export via the Xpo1-dependent pathway.
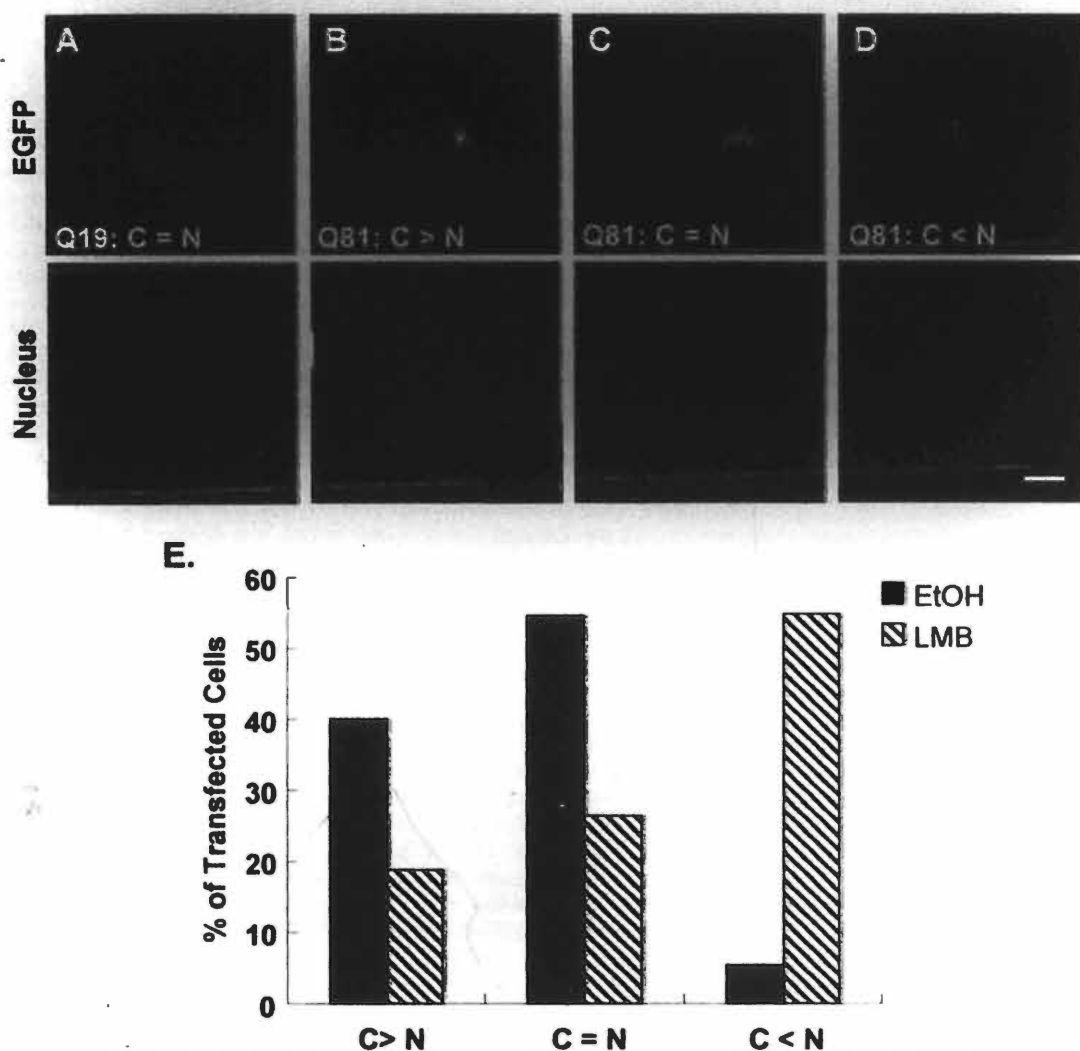
**Figure 5.4. Subcellular localization of Q81-EGFP protein in transiently transfected SH-SY5Y cells.** Neuronal differentiation of SH-SY5Y cells expressing Q19- or Q81-EGFP was induced by 10 μM retionic acid. At 96 h post-induction, cells were either treated with ethanol (EtOH) or 20 ng/ml Leptomycin B (LMB) for 18h. **(A-D)** The subcellular localization of Q19- or Q81-EGFP (in green) was examined under a fluorescence microscope after the cell nuclei were labeled with Hoechst (in blue). **(A)** The Q19-EGFP protein localized homogeneously in both cytoplasm and nucleus while the Q81-EGFP protein displayed three major types of localization patterns, including **(B)** predominantly cytoplasmic (C > N), **(C)** uniform distribution between cytoplasm and nucleus (C = N), and **(D)** predominantly nuclear (C < N). Scale bar represents 10 μm. **(E)** Quantification of Q81-EGFP localization upon treatment of LMB. Treatment of LMB caused a redistribution of Q81-EGFP predominantly to the nucleus.

**5.2.2 Interaction Studies between Mutant Polyglutamine Protein and Exportin-1**

To be a transport substrate of Xpo1, mutant polyQ protein is expected to physically interact with Xpo1 (Fornerod et al., 1997). To test this hypothesis, HEK 293 cells transfected with various *polyQ* constructs were subjected to co-immunoprecipitation.

**5.2.2.1 Polyglutamine Length-dependent Interaction between Polyglutamine Protein and Exportin-1**

Leptomycin B inhibits nuclear export by preventing the formation of protein complex between Xpo1 and its substrates (Kudo et al., 1999). Treatment of LMB resulted in nuclear accumulation of Q81-EGFP (Fig. 5.4E), suggesting that nuclear export of the Q81-EGFP protein involved the formation of protein complex with Xpo1. Thus, the possible interaction between polyQ protein and Xpo1 was first determined. Lysates from cells transfected with either *Q19-* or *Q81-EGFP-myc* construct were immunoprecipitated (IP) with anti-myc antibody, followed by immunoblotting (IB) with anti-Xpo1 antibody. Reciprocal co-IP experiment was also performed using anti-Xpo1 antibody for IP, and anti-myc antibody for IB. It was found that the Q81-EGFP protein interacted specifically with Xpo1 and such protein-protein interaction was absent from Q19-EGFP samples (Fig. 5.5). From the polyQ-EGFP co-IP experiment, it was shown that the presence of an expanded polyQ domain was crucial for EGFP to interact with Xpo1. In particular,

although the high molecular weight SDS-insoluble Q81-EGFP protein was detected in the

cell lysates, it was not found in the IP samples (Fig. 5.5B). This indicates that only the

SDS-soluble Q81-EGFP protein was responsible for the interaction with Xpo1. Taken

together the SH-SY5Y subcellular localization data (Fig. 5.4A-D), only protein carrying an

expanded polyQ domain possessed nuclear export activity and formed protein complex

with Xpo1.
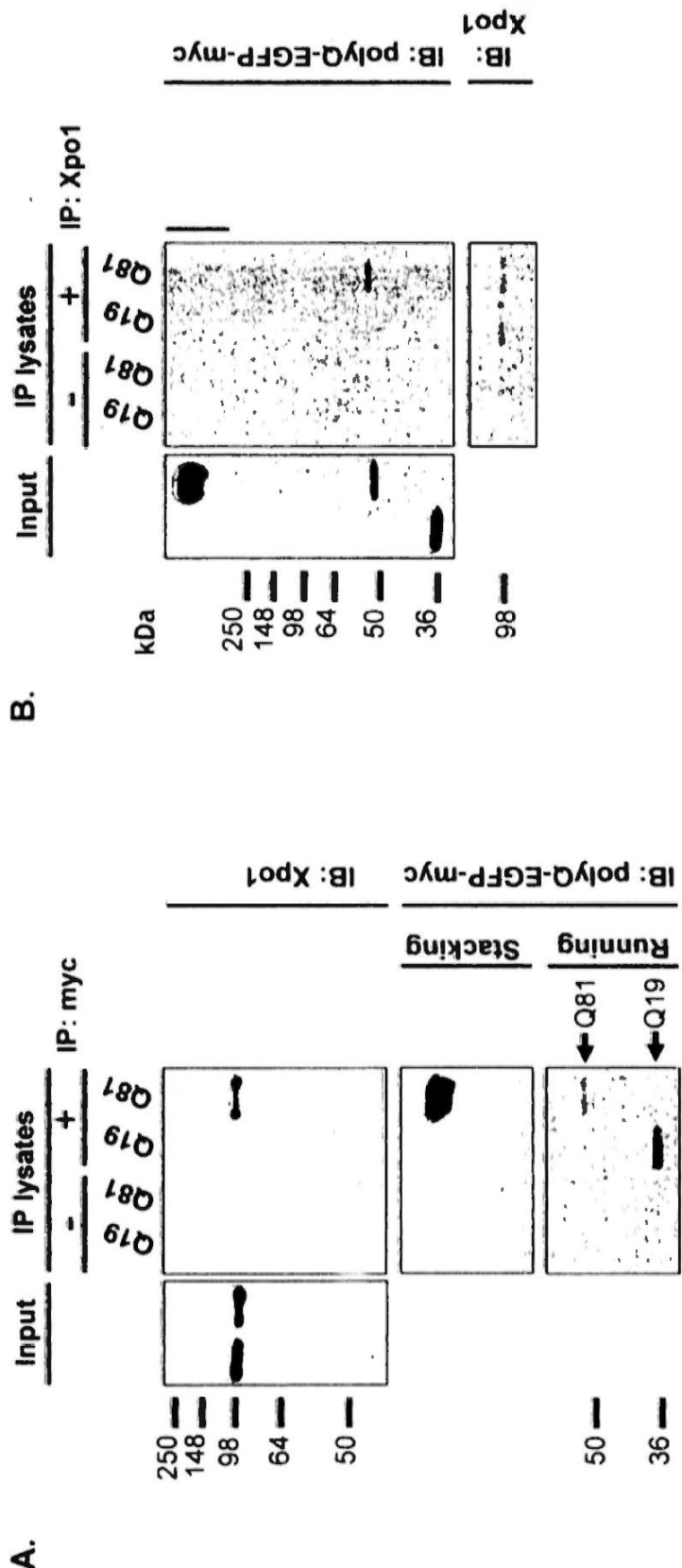
**Figure 5.5. Co-Immunoprecipitation experiments between Q19/Q81-EGFP proteins and exportin-1 in transiently transfected HEK 293 cells. (A)** Lysates isolated from polyQ-EGFP-myc-transfected cells were immunoprecipitated (IP) with anti-myc 9B11 antibody (+), followed by immunoblotting (IB) with anti-exportin-1 (Xpo1) antibody. Immunoprecipitates without anti-myc antibody (–) were negative controls. Only the Q81-EGFP protein interacted with Xpo1. The membrane was stripped and re-probed with anti-myc 71D10 antibody to confirm the expression of both Q19- and Q81-EGFP proteins. SDS-insoluble Q81-EGFP protein was detected in the stacking gel. **(B)** Reciprocal co-IP of (A). Lysates were IP with anti-Xpo1 antibody (+), followed by IB with anti-myc 9B11 antibody. Despite the detection of both Q19- and Q81-EGFP protein in the input, only SDS-soluble Q81-EGFP was immunoprecipitated out. The membrane was stripped and re-probed with anti-Xpo1 antibody to demonstrate the presence of Xpo1 protein in the samples. Vertical bar indicates the location of stacking gel.

149

### 5.2.2.2 Interaction between Individual Polyglutamine Disease Proteins and Exportin-1

Further, the interaction between expanded polyQ domain and Xpo1 was examined in particular polyQ disease proteins. Constructs encoding FLAG-tagged truncated disease proteins for MJD and HD were used to transfect HEK 293 cells and similar co-IP experiments were performed using anti-FLAG antibody as described above. Similarly, both mutant disease proteins, FLAG-MJDtrQ76 and FLAG-Htt$_{1-550}$Q83, physically interacted with Xpo1 (Fig. 5.6).
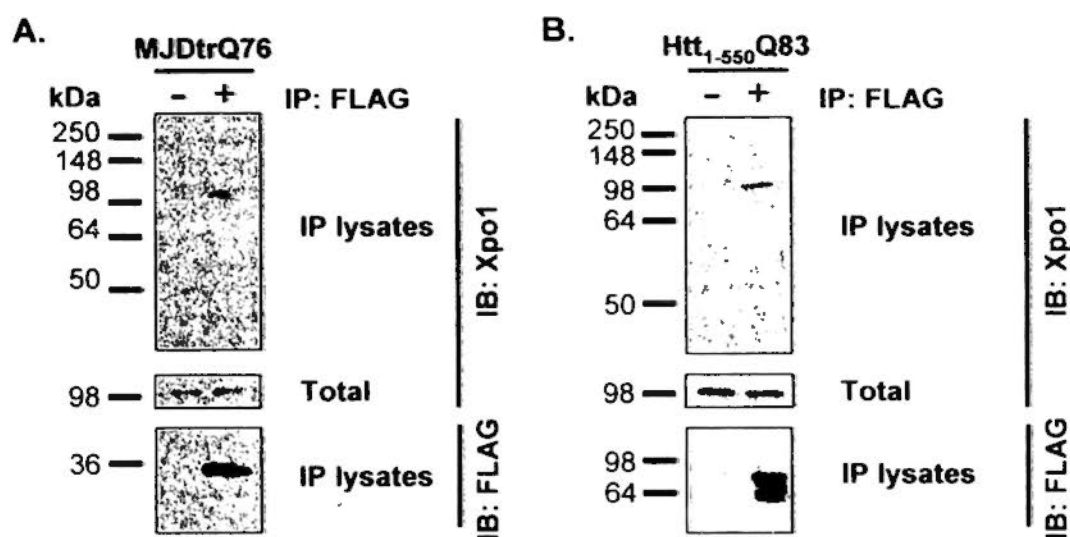
**Figure 5.6. Interaction between polyQ disease proteins and exportin-1 in transiently transfected HEK 293 cells.** Lysates from HEK 293 cells expressing **(A)** FLAG-MJDtrQ76 or **(B)** FLAG-Htt$_{1-550}$Q83 proteins were immunoprecipitated (IP) with anti-FLAG M2 antibody (+), followed by immunoblotting (IB) with anti-exportin-1 (Xpo1) antibody. Immunoprecipitates without anti-FLAG antibody (-) were negative controls. Both mutant disease proteins interacted with Xpo1. The membranes were stripped and re-probed with anti-FLAG antibody to confirm the expression of both mutant proteins.

### 5.2.2.3 Specific Interaction between Mutant Polyglutamine Protein with Exportin-1

The specificity of interaction between mutant polyQ protein and Xpo1 was demonstrated using exportin-t, another member of the same karyopherin family responsible for nuclear export of tRNA (Mosammaparast and Pemberton, 2004). Similar to the co-IP experiment for Xpo1, cell lysates were IP with anti-myc antibody and then IB with anti-exportin-t antibody. Despite its detection in total cell lysates, exportin-t was co-immunoprecipitated neither with Q19-EGFP nor Q81-EGFP (Fig. 5.7). The result indicates that mutant polyQ protein did not interact with all members from the exportin karyopherin family.
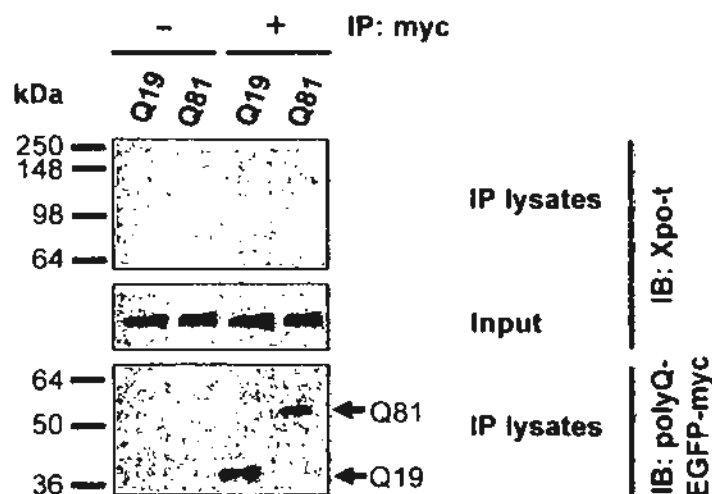
**Figure 5.7. Co-Immunoprecipitation experiments between Q19-/Q81-EGFP proteins and exportin-t.** Lysates isolated from polyQ-EGFP-myc-transfected HEK 293 cells were immunoprecipitated (IP) with anti-myc 9B11 antibody (+), followed by immunoblotting (IB) with anti-exportin-t (Xpo-t) antibody. Immunoprecipitates without anti-myc antibody (-) were negative controls. No observable interaction between Q19/Q81-EGFP proteins and Xpo-t was detected. The membrane was stripped and re-probed with anti-myc 71D10 antibody to confirm the expression of both Q19- and Q81-

（）

### 5.2.2.4 Interaction between an Interrupted Expanded Polyglutamine Domain and

### Exportin-1

Since an expanded polyQ domain preferentially interacted with Xpo1 (Fig. 5.5), it was of interest to determine if the continuity of an expanded polyQ domain would be important for such interaction. The continuous 81 glutamine repeats in the *Q81-EGFP-myc* construct were interrupted by various proline residues (Takahashi et al., 2007). Lysates from HEK 293 cells expressing polyQ-EGFP proteins with different numbers of proline insertion, Q75P2 and Q73P7, were used in the co-IP experiment. Cells transfected with *Q81-EGFP-myc* construct were used as the positive control. It was found that Q75P2-EGFP, which carried two proline insertions in the polyQ domain separating 25 successive glutamine residues, showed a reduced interaction with Xpo1 when compared to Q81-EGFP (Fig. 5.8). The Q73P7-EGFP protein, which has seven proline insertions separating 9-10 successive glutamines, exhibited a more drastic reduction in the interaction with Xpo1 when compared to Q81-EGFP (Fig. 5.8). This result clearly shows that splitting a long expanded continuous polyQ domain into multiple shorter ones weakened its interaction with Xpo1.
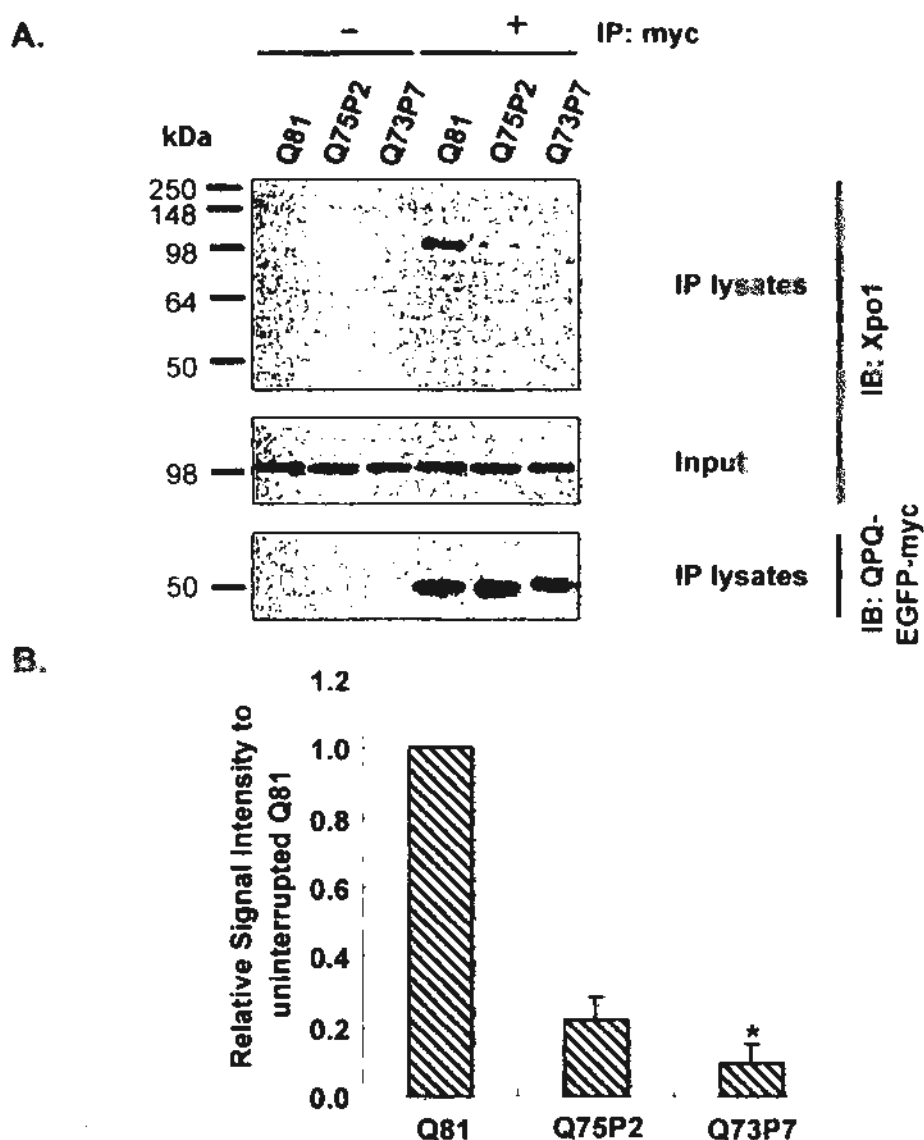
**Figure 5.8. Importance of the continuity of an expanded polyQ domain on its interaction with exportin-1. (A)** Lysates isolated from QPQ-EGFP-myc-transfected HEK 293 cells were immunoprecipitated (IP) with anti-myc 9B11 antibody (+), followed by immunoblotting (IB) with anti-exportin-1 (Xpo1) antibody. Immunoprecipitates without anti-myc antibody (-) were negative controls. Interruption of a continuous expanded polyQ domain by proline residues reduced its interaction with Xpo1. The membrane was stripped and re-probed with anti-myc 71D10 antibody to confirm the expression of Q81- and QPQ-EGFP proteins. **(B)** Quantification of (A). The reduced interaction between mutant polyQ protein and Xpo1 was in correlation with the number of inserted prolines. Error bars represent S.E.M. of three independent experiments (* $p < 0.05$, compared to Q81, by one way ANOVA on ranks followed by Dunn post-test).

## 5.3 Discussion

### 5.3.1 Mutant Polyglutamine Protein as a Nucleocytoplasmic Shuttling Protein

In this section, protein carrying an expanded polyQ domain was shown to carry both nuclear import and export activities, implying its capability to shuttle between the cytoplasm and nucleus. The M9 domain of the heterogeneous nuclear ribonucleoproteins A1 is another sequence that shows nucleocytoplasmic shuttling properties (Michael et al., 1995; Siomi and Dreyfuss, 1995). Similar to the M9 domain, whose nuclear import is transportin-mediated (Pollard et al., 1996) while nuclear export is mediated by an uncharacterized export receptor (Bogerd et al., 1999), the expanded polyQ domain adopted different transport pathways for nuclear import and export.

### 5.3.1.1 Nuclear Import of Mutant Polyglutamine Protein

The nuclear import activity of an expanded polyQ domain was first reported by Ordway and colleagues (1997). Transgenic mice expressing $HPRT^{Q146}$, which otherwise localizes to the cytoplasm in the absence of the 146 glutamine repeats, develop nuclear aggregates in affected neurons and show a progressive degenerative phenotype (Ordway et al., 1997). Here, by taking advantage of the artificial *EGFP* constructs, *Q26-* and *Q75-EGFP2GST*, it was further demonstrated that only expanded polyQ domain confers nuclear import properties (Fig. 5.1). In contrast to transport substrates in the classical

156

protein nuclear import pathways (Pemberton and Paschal, 2005), nuclear import of mutant polyQ protein was further found to be Ran-independent (Appendix 4. performed by Dr. Eric Wong). Yet, the precise mechanistic details of mutant polyQ protein nuclear import await further investigation.

In addition, mutant polyQ protein exists in different conformations (Ross and Poirier, 2005). Although both diffuse and aggregated Q75-EGFPGST proteins were detected in the nuclei of transfected cells, the majority of GFP signal was still present in the cytoplasm (Fig. 5.1). And from the time-lapse microscopy experiment (Appendix 4A, performed by Dr. Eric Wong), the Q75-EGFP2GST protein did not translocate through the NPCs into the nucleus in an aggregated form. Rather, nuclear aggregates formed *de novo* inside the nucleus from the imported diffuse Q75-EGFP2GST protein (Appendix 4A, performed by Dr. Eric Wong). Thus, it is believed that only certain form(s) of mutant polyQ conformers is/are responsible for such import property.

## 5.3.1.2 Nuclear Export of Mutant Polyglutamine Protein

A pre-requisite for the study of nuclear export is the ability of transport substrate to first enter into the nucleus. In view of this, a polyQ-EGFP, instead of the polyQ-EGFP2GST, model was employed. It has been demonstrated that the

Q26-EGFP2GST protein did not show nuclear import activity and remained in the cytoplasm (Figs. 5.1 and 5.2; Appendix 4A, performed by Dr. Eric Wong). Thus, the EGFP2GST-based reporters would not be ideal for nuclear export investigations. Since both the Q19- and Q81-EGFP proteins are small enough to enter into the nucleus by passive diffusion, the use of Q19- and Q81-EGFP proteins would allow a direct comparison of the nuclear export property between expanded and unexpanded polyQ domains.

Here, it was reported for the first time that an expanded polyQ domain served as a nuclear export signal and mediated protein export through Xpo1 (Fig. 5.4). Despite a redistribution of the Q81-EGFP protein to the nuclei of the majority of cells treated with LMB (> 50%), the Q81-EGFP protein remained cytoplasmic in some of the transfected cells (~ 20%) (Fig. 5.4). Similar to nuclear import, it is believed that only certain form(s) of mutant polyQ proteins could act as the transport substrate for Xpo1. Such speculation is further supported by the preferential interaction between SDS-soluble Q81-EGFP protein with Xpo1 (Fig. 5.5B), indicating that not all forms of Q81-EGFP protein could interact with Xpo1.

**5.3.2 Mutant Polyglutamine Protein as a Novel Substrate for Exportin-1**

There are seven karyopherins reported to participate in protein nuclear export thus far, namely Cas, exportin-t, exportin-4, exportin-5, exportin-6, importin-13 and Xpo1 (Mosammaparast and Pemberton, 2004). Most of these export receptors only have a limited number of transport substrates: importin-α for CAS (Kutay et al., 1997); mature tRNA for exportin-t (Arts et al., 1998; Kutay et al., 1998); eIF5A for exportin-4 (Lipowsky et al., 2000); double-stranded RNA binding protein for exportin-5 (Brownawell and Macara, 2002); profiling-actin complex for exportin-6 (Stuven et al., 2003) and eIF1A for importin-13 (Mingot et al., 2001). However, Xpo1 is responsible for the nuclear export of a broad range of substrates carrying the leucine-rich NESs involved in various cellular responses (Fornerod et al., 1997). Here, mutant polyQ protein was demonstrated to be a novel substrate for Xpo1. Unlike conventional substrates, the continuity of the expanded polyQ domain, rather than a short stretches of leucine-rich residues, was found to be essential for Xpo1 recognition. This is supported by the reduced interaction with Xpo1 when a continuous expanded polyQ domain was interrupted (Fig. 5.8). Apart from the classical leucine-rich NESs, this study provides evidence that Xpo1 could mediate protein nuclear export of non-leucine-rich NES-containing proteins.

## *Chapter 6. Exportin-1-mediated Modification of Polyglutamine Toxicity*

An expanded polyQ domain was demonstrated to possess nuclear export activity in this study (Section 5.2). The aberrant interaction between mutant polyQ protein and Xpo1 might elicit adverse effect on the transport function of Xpo1. On the other hand, nuclear export of mutant polyQ protein by Xpo1 might ameliorate the toxic effect of mutant polyQ protein on cellular events occur in the nucleus. Thus, the possible influences of the nuclear export property of mutant polyQ protein on toxicity were studied in this section.

## 6.1 Possible Consequences of Interaction between Mutant Polyglutamine Protein and Exportin-1

Consistent with the immunoprecipitation experiment which showed that SDS-soluble, but not SDS-insoluble, mutant polyQ protein was responsible for interacting with Xpo1 (Fig. 5.5B), it was found that Xpo1 was not recruited to mutant polyQ protein-containing SDS-insoluble fraction (Fig. 6.1). Formic acid has been shown to successfully solubilize cellular components recruited to polyQ aggregates (Hazeki et al., 2000). The SDS-insoluble Q81-EGFP protein was solubilized by formic acid and became SDS-soluble. This accounts for the obvious increase in band intensity of Q81-EGFP after formic acid treatment in the running gel (Fig. 6.1A). However, Xpo1 was not detected in the stacking gel, and that no alteration in the SDS-soluble Xpo1 level was observed before and after formic acid treatment in the running gel (Fig. 6.1B). Thus, Xpo1 was not sequestrated to SDS-insoluble mutant polyQ-containing protein species (Fig. 6.1). However, the aberrant interaction between itself and mutant polyQ protein preserves possible deleterious effects on its protein export function.
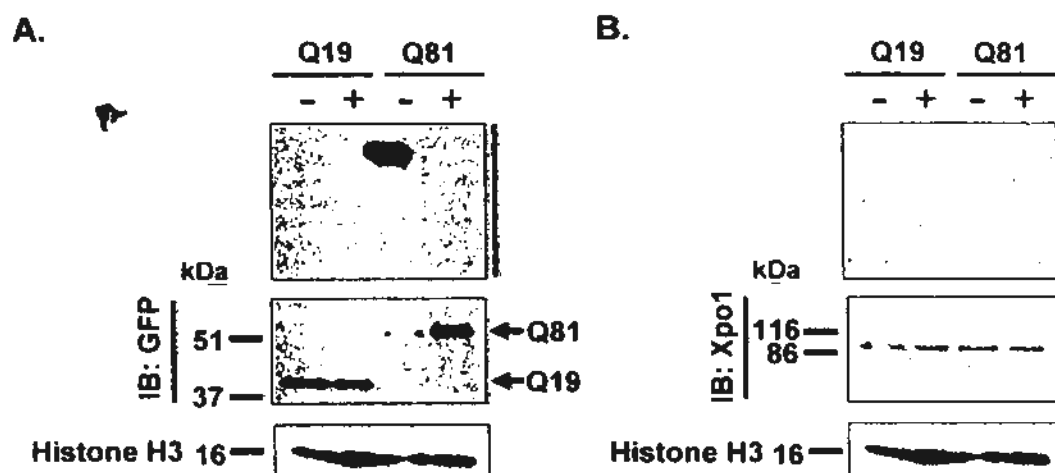
**Figure 6.1. Solubilization of SDS-insoluble polyQ protein by formic acid.** At 48 hours post-transfection, total lysates were prepared from HEK 293 cells transiently transfected with *Q19-* or *Q81-EGFP* construct. Five micrograms of total proteins were treated with formic acid (+) followed by SDS-PAGE and immunoblotting (IB). Equal amount of untreated sample (-) was loaded in parallel. **(A)** SDS-insoluble Q81-EGFP protein was detected in the stacking gel (vertical bars on the right), which was solubilized by formic acid and became SDS-soluble (+). This accounts for the increased band intensity of Q81-EGFP in the running gel. The band intensity for Q19-EGFP remained almost the same in both (-) and (+) lanes. **(B)** Protein band intensities of Xpo1 remained the same in both Q19- and Q81-EGFP samples, regardless of formic acid treatment. Histone H3 was used as loading control.

## 6.1.1 Possible Disruptive Effect of Mutant Polyglutamine Protein on Exportin-1/Endogenous Export Substrate Protein Complex Formation

One of the possible consequences from the interaction between mutant polyQ protein and Xpo1 (Fig. 5.5) would be the perturbation of protein complex formation between Xpo1 and its endogenous export substrates (Section 1.1.3), which would affect Xpo1 cellular function as a nuclear export receptor. To address this issue, size-exclusion chromatography was performed on HEK 293 cell lysates transfected with either *Q19-* or *Q81-EGFP* construct. Due to the preferential interaction between Xpo1 and Q81-EGFP, but not Q19-EGFP (Fig. 5.5), the elution profile of Xpo1 in Q19-EGFP sample served as reference for the high molecular weight Xpo1 protein complex. Exportin-1 was detected in two distinct peaks, one corresponded to the Xpo1-substrate protein complex (Fig. 6.2, fractions 5-10) and the other one corresponded to the Xpo1 monomer (Fig. 6.2, fractions 31-37). However, no observable difference between the elution profiles of Q19- and Q81-EGFP samples was noted (Fig. 6.2). This indicates that Xpo1-substrate complex formation was not affected by mutant polyQ protein.

Since the interaction between mutant polyQ protein and Xpo1 exerted no modulatory effect on protein complex formation involving Xpo1 and its endogenous export substrates, it is speculated that the modulatory effect of Xpo1 on toxicity was

attributed to its influence on mutant polyQ protein subcellular localization.
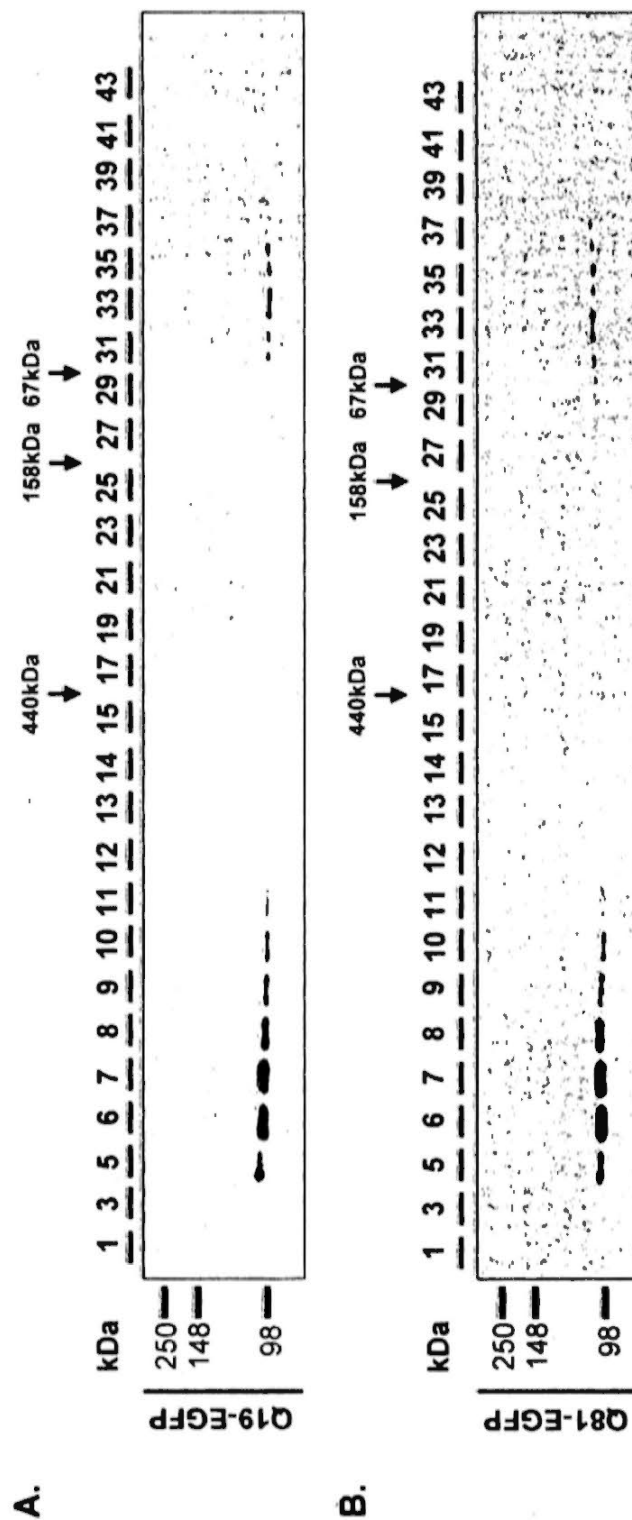
**Figure 6.2. The elution profile of exportin-1 in HEK 293 cells transiently expressing Q19- or Q81-EGFP protein.** At 48 hours post-transfection, lysates of HEK 293 cells transfected with either *Q19-* or *Q81-EGFP-myc* construct were harvested and subjected to gel filtration chromatography. Fractions (25 µl/lane) were separated by SDS-PAGE and membranes were probed against an exportin-1 specific antibody. High molecular weight complexes containing exportin-1 (fractions 5 – 10) were observed in both **(A)** Q19- and **(B)** Q81-EGFP lysates, indicating that the interaction between Q81-EGFP and exportin-1 did not disrupt the complex formation between exportin-1 and its endogenous nuclear export substrates. Immunoblots shown are representative of three independent experiments.

## 6.2 Influences of Exportin-1 on Gene Transcription

Transcriptional dysregulation is one of the major pathologic hallmarks in polyQ diseases (Huen et al., 2007; Truant et al., 2007). Mutant polyQ protein was reported here for the first time as a transport substrate of Xpo1 (Section 5.2). By promoting the nuclear export of mutant polyQ protein, a possible role played by Xpo1 was to restore normal transcription by reducing the level of mutant protein in the nucleus. This would therefore explain the suppression of polyQ toxicity when *emb* was over-expressed (Figs. 4.2 and 4.3).

### 6.2.1 Effects of *embargoed* Knockdown on *Heat Shock Protein* Gene Transcription in Mutant Polyglutamine Flies

The knockdown of *emb* expression in transgenic flies enhanced mutant polyQ-induced toxicity (Figs. 4.2 and 4.3). Since the expression of mutant polyQ protein induces *heat shock protein (hsp)* gene transcription (Huen and Chan, 2005), a cellular protective mechanism against misfolded proteins (Barral et al., 2004; Liberek et al., 2008), it was hypothesized that the nuclear accumulation of mutant polyQ protein in an *emb* knockdown background would lead to an impairment on *hsp* gene transcription. An inability to induce the heat shock response would therefore account for the enhancement of the degenerative phenotype observed (Figs. 4.2 and 4.3).

Compared to the control flies carrying the *gmr*-gal4 driver alone, the expression of normal MJDQ27 protein in flies did not induce the expression of *hsp* genes (Fig. 6.3). However, an induction of *hsp*, including *hsp22*, *hsp40 (hdj1)* and *hsp70* mRNAs, was observed in transgenic flies expressing the mutant MJDQ84 protein (Fig. 6.3). Interesting, such an induction was absent in flies co-expressing the *MJDQ84* transgene and *emb* dsRNA (Fig. 6.3). Hereafter, *hsp70* was used as an example to further illustrate the influence of *emb*-mediated nuclear export pathway on heat shock response in polyQ toxicity.
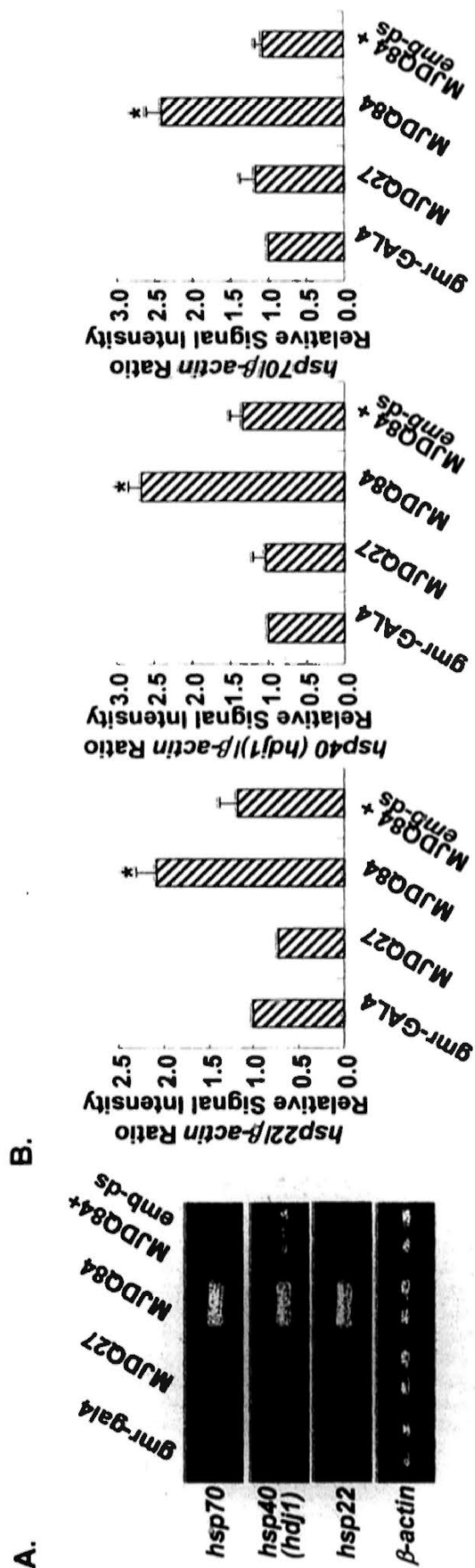
**Figure 6.3. Induction of *hsp* mRNAs in adult flies. (A)** Total RNA was isolated from transgenic flies of 0-2 days post-eclosion cultured at 25°C. Semi-quantitative RT-PCR analysis revealed that the expression of mutant MJDQ84 protein in adult fly eyes induced the expression of various *hsp* genes, including *hsp22*, *hsp40* (*hdj1*) and *hsp70*. This induction was found to be mutant polyQ specific as the expression of normal MJDQ27 protein did not elicit such induction. However, *hsp* induction was compromised in flies co-expressing *MJDQ84* and *emb* dsRNA. *β-actin* was used as the loading control. **(B)** Quantification of (A). The mRNA levels of *hsp* genes were only significantly induced in flies carrying the *MJDQ84* transgene alone (* *p* < 0.05, by one way ANOVA on ranks followed by Dunn post-test). Error bars represent S.E.M. from three independent experiments. The flies were of genotypes *w; gmr-gal4/+*, *w; gmr-gal4 UAS-myc-MJDQ27/+*, *w; gmr-gal4/+; UAS-myc-MJDQ84/+* and *w; gmr-gal4/UAS-emb dsRNA; UAS-myc-MJDQ84/+*.

### 6.2.2 Effects of *embargoed* Knockdown on Non-polyglutamine-induced Heat Shock Response

To check if the knockdown of *emb* expression would impair the heat shock response mechanism in general, heat shock, instead of mutant polyQ protein, was used as an independent stimulus. RNA was extracted from flies that had been subjected to heat shock treatment and the mRNA level of *hsp70* was investigated. Transgenic flies carrying the *gmr*-gal4 driver alone was used as positive control, and *hsp70* induction was observed (Fig. 6.4; lanes 1 and 2). A similar *hsp70* induction was also observed in transgenic flies expressing *emb* dsRNA alone (Fig. 6.4; lane 3) or those co-expressing *emb* dsRNA with the *MJDQ27* transgene (Fig. 6.4; lane 4). In flies expressing *MJDQ84* alone, similar *hsp70* induction was also observed; however no such induction was observed in flies co-expressing *emb* dsRNA with the *MJDQ84* transgene (Fig. 6.4; lanes 5 and 6). Thus, the result clearly demonstrates that general heat shock response, as indicated by the induction of *hsp70* gene transcription, was specifically affected when mutant polyQ protein was expressed in an *emb* knockdown background.
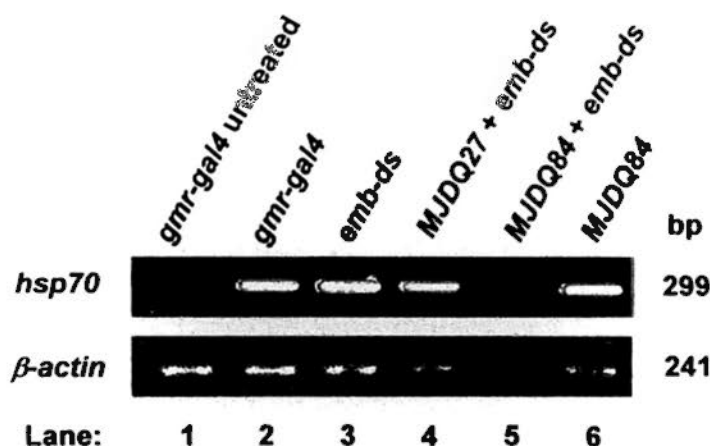
**Figure 6.4. Expression of *hsp70* mRNA upon heat shock treatment of adult flies.** Semi-quantitative RT-PCR analysis revealed that heat shock treatment up-regulated the mRNA level of *hsp70* in control flies (Lanes 1 and 2). Similar increase in *hsp70* mRNA was also observed in flies expressing *emb* dsRNA alone (Lane 3) or co-expressing with *MJDQ27* (Lane 4). Nevertheless, the knockdown of *emb* in MJDQ84 flies impaired the heat shock response, as indicated by the absence of *hsp70* mRNA induction (Lane 5). The effect was found to be specific to *emb* knockdown as flies expressing *MJDQ84* alone were able to induce *hsp70* mRNA (Lane 6). *β-actin* was used as the loading control. Data shown is representative of two independent experiments. The flies were of genotypes *w; gmr-gal4/+, w; gmr-gal4/UAS-emb dsRNA, w; gmr-gal4 UAS-myc-MJDQ27/UAS-emb dsRNA, w; gmr-gal4/UAS-emb dsRNA; UAS-myc-MJDQ84/+ and w; gmr-gal4/+; UAS-myc-MJDQ84/+.*

**6.2.3 Effects of Histone Acetylation on *Heat Shock Protein* Gene Transcription in Mutant Polyglutamine Flies**

Histone acetylation has long been implicated in transcriptional regulation in eukaryotes (Strahl and Allis, 2000). Acetylation of lysine residues on core histone weakens its interaction with DNA, leading to the destabilization of nucleosomal structure and thus facilitates the binding of transcription factors to DNA (Strahl and Allis, 2000). Hence, histone acetylation is considered as a mechanism to promote gene transcription. Since histone acetylation is involved in *hsp70* gene transcription (Chen et al., 2002) and has also been implicated in polyQ pathogenesis (Evert et al., 2006; Sadri-Vakili et al., 2007; Steffan et al., 2001; Taylor et al., 2003), the acetylation status of histone H3 was examined in mutant polyQ-expressing flies. It was hypothesized that an induction of *hsp70* in adult flies expressing *MDJQ84* was accompanied by an up-regulation of acetylated histone H3, while histone acetylation was compromised in flies co-expressing *MJDQ84* and *emb* dsRNA. However, flies expressing *MJDQ84* alone or together with *emb* dsRNA showed comparable levels of histone H3 acetylation (Fig. 6.5). This result indicates that the acetylation status of histone H3 was unrelated to the *hsp70* gene transcription induction failure observed in *MJDQ84/emb* dsRNA flies.

**A.**



**B.**
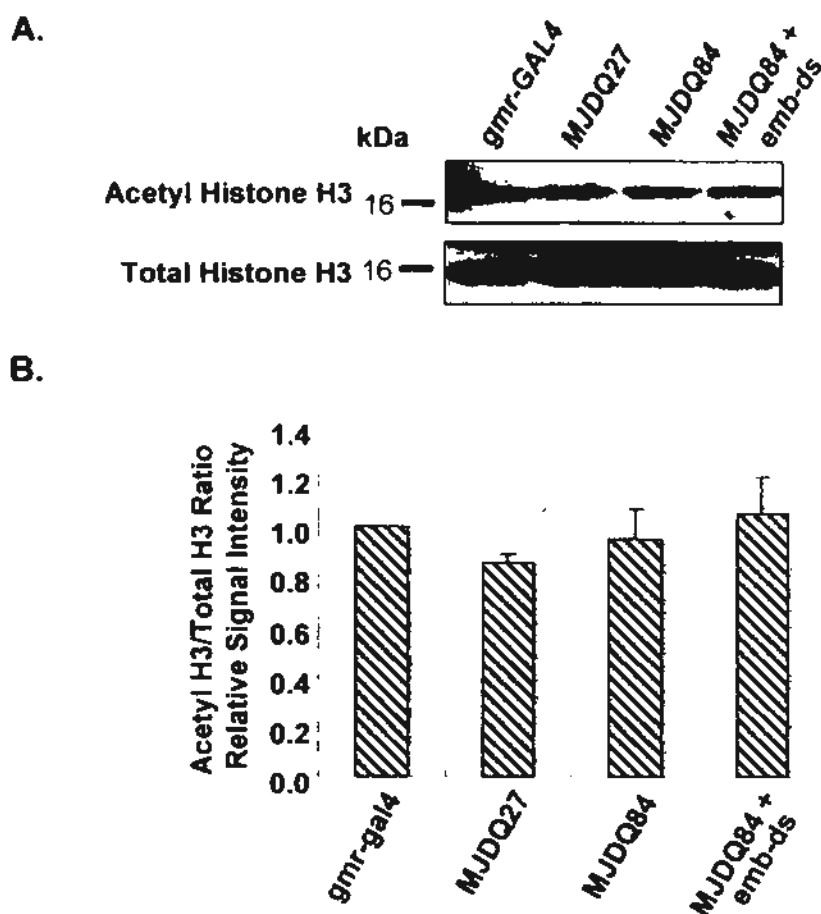


**Figure 6.5. Acetylation of histone H3 in adult flies. (A)**
Immunoblot analysis of nuclear MJDQ84 proteins (4 heads) isolated from transgenic flies of 0-2 days post-eclosion cultured at 25°C. Acetylation of histone H3 was determined using a specific antibody against acetylated histone H3. Membrane was stripped and re-probed with antibody against total histone H3 protein. Neither the expression of polyQ proteins nor the knockdown of *emb* altered the acetylation of histone H3. **(B)** Quantification of (A). No significant difference was observed between different groups. Error bars represent S.E.M. of three independent experiments. The flies were of genotypes *w; gmr-gal4/+, w; gmr-gal4 UAS-myc-MJDQ27/+, w; gmr-gal4/+; UAS-myc-MJDQ84/+ and w; gmr-gal4/UAS-emb dsRNA; UAS-myc-MJDQ84/+*.

### 6.2.4 Effects of *embargoed* Over-expression on the Biphasic Expression Profile of *Heat Shock Protein* Gene in Mutant Polyglutamine Flies

It was reported that the induction of *hsp70* expression in mutant polyQ transgenic flies was followed by a rapid reduction, suggesting that mutant polyQ protein exerts an inhibitory effect on *hsp70* transcription (Huen and Chan, 2005). Because of the recruitment of transcription factors, such as NF-Y, to nuclear polyQ aggregates (Suhr et al., 2001; Yamanaka et al., 2008), it was hypothesized that the inhibition of *hsp70* gene transcription was imposed by the accumulation of mutant polyQ protein in the nucleus. Thus, the temporal expression profile of *hsp70* induction was examined in transgenic flies carrying the *MJDQ84* transgene alone or together with an *emb* EP over-expression insert. As previously reported (Huen and Chan, 2005), the biphasic expression pattern of *hsp70* mRNA was observed in flies expressing *MJDQ84* alone (Fig. 6.6; lanes 1-4). With a concomitant over-expression of *emb*, *hsp70* mRNA induction was maintained for a longer period of time (Fig. 6.6; lanes 5-8). Indeed, *emb* over-expression also strengthened the induction intensity of *hsp70*. At 16-18 dpe, flies co-expressing *MJDQ84/emb* EP insertion showed a significantly higher induction of *hsp70*, whose level has dropped to that of 0-2 dpe in flies expressing *MJDQ84* alone (Fig. 6.6). Thus, the result indicates that *emb* over-expression helped in sustaining the heat shock response induced by mutant MJDQ84 protein.

**A.**



**B.**
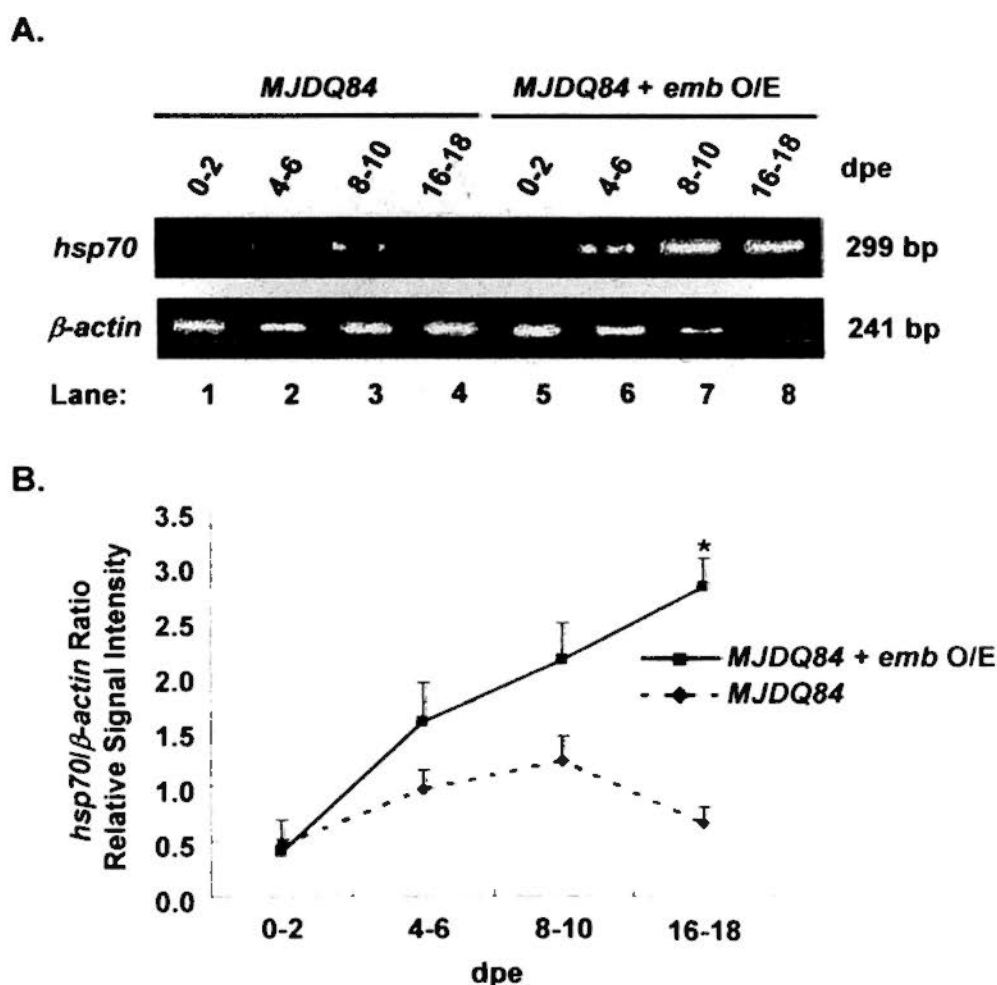


**Figure 6.6. Temporal analysis of *hsp70* mRNA expression profile in adult flies. (A)** Semi-quantitative RT-PCR analysis revealed that *emb* over-expression (O/E) further induced and prolonged *hsp70* expression. The previously reported biphasic expression pattern of *hsp70* (Huen and Chan, 2005) was observed in control flies expressing *MJDQ84* transgene alone (Lanes 1 – 4). Upon *emb* O/E, a more intense *hsp70* induction was observed and a relatively higher level of *hsp70* was maintained at later time points (Lanes 5 – 8). **(B)** Quantification of (A). The over-expression of *emb* sustained the induction of hsp70 in mutant MJDQ84 flies. Error bars represent S.E.M. of three independent experiments. *β-actin* was used as the loading control. (* $p < 0.05$, compared to 0-2 dpe, by one way ANOVA on ranks followed by Dunn post-test). The flies were of genotypes *w; gmr-gal4/+; UAS-myc-MJDQ84/+* and *w; gmr-gal4/emb^{EP-E128-1A}; UAS-myc-MJDQ84/+*.

## 6.3 Expression Level of Exportin-1 and Ageing

The enhancing effect of *emb* knockdown on mutant polyQ-induced degenerative phenotype (Figs. 4.2 and 4.3) was accompanied by a reduction of *hsp* gene transcription (Fig. 6.3). This suggests Xpo1 plays role in the maintenance of heat shock response in polyQ toxicity. The progressive nature of polyQ diseases provoked the idea of checking the expression level of Xpo1 in the normal ageing process. It was hypothesized that the expression level of Xpo1 would decline upon ageing, which would then result in an accumulation of mutant polyQ protein in the nucleus and thus exaggerate mutant polyQ toxicity. Immunoblot analysis of whole brain lysates from wild type mice indicated that the protein level of Xpo1 decreased from 2 weeks to 12 weeks by approximately three fold, and remained at such low level until 22 weeks (Fig. 6.7). The expression profile of Xpo1 protein in normal ageing correlated well with the progressive degenerative phenotype of polyQ diseases.

**A.**



**B.**
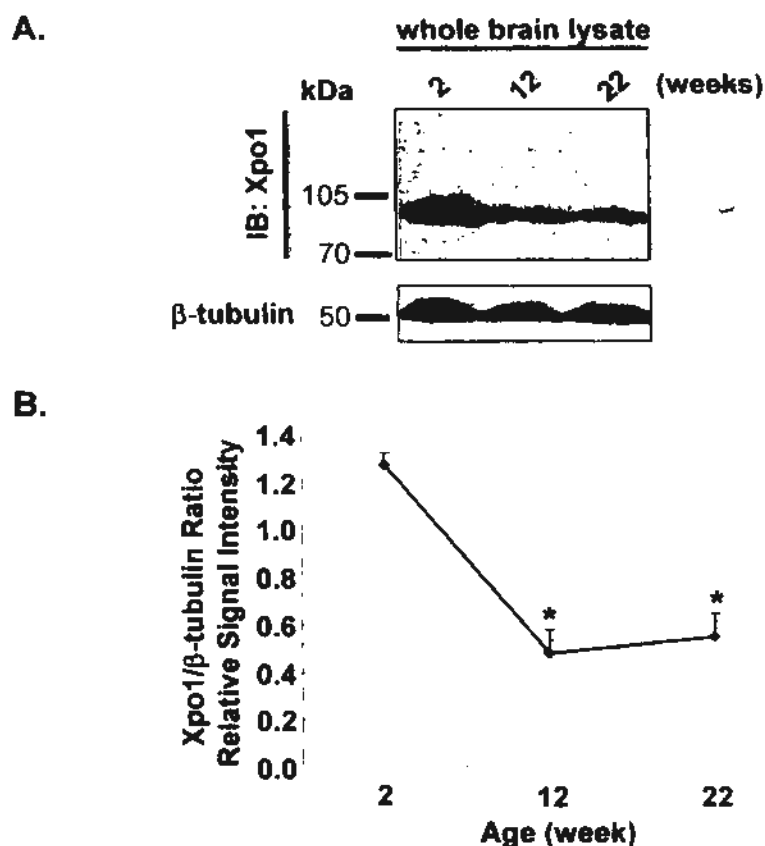


**Figure 6.7. Temporal analysis of exportin-1 protein level in wild-type mice. (A)** Immunoblot (IB) analysis of whole brain lysates from wild-type mice at 2, 12 and 22 weeks of age. Exportin-1 (Xpo1) level decreased from 2 weeks to 12 weeks, and remained at the same level until 22 weeks. β-tubulin was used as loading control. **(B)** Quantification of (A). Each data point arises from a comparison of three wild-type mice (* $p < 0.05$, compared to 2 weeks, by one way ANOVA on ranks followed by Dunn post-test). Error bars represent

## 6.4 Discussion

### 6.4.1 Transport Function of embargoed in Mutant Polyglutamine Flies

Consistent with the observation that SDS-soluble, but not SDS-insoluble Q81-EGFP protein interacted with Xpo1 (Fig. 5.5B), Xpo1 was not recovered from SDS-insoluble Q81-EGFP protein complex after formic acid treatment (Fig. 6.1B). Thus, it is believed that the normal function of Xpo1 was not influenced by the SDS-insoluble polyQ-containing protein aggregates. Nevertheless, there would still be a possibility that the aberrant interaction between the soluble mutant polyQ protein and Xpo1 (Fig. 5.5) would affect the nuclear export of other Xpo1 transport substrates which then contribute to polyQ toxicity. According to the gel filtration chromatography result, no observable difference was noted between the Q19- and Q81-EGFP samples (Fig. 6.2). Due to the preferential interaction between Xpo1 and Q81-EGFP, but not Q19-EGFP (Fig. 5.5), the elution profile of Xpo1 in Q19-EGFP sample would reflect the normal situation. Thus, the presence of Q81-EGFP protein did not exert any adverse effect on protein complex formation involving Xpo1 and its substrates (Fig. 6.2), and hence the interaction between mutant polyQ protein and Xpo1 is believed not to be affecting the endogenous protein export function of Xpo1. Therefore, the modification of polyQ toxicity as a result of *emb* knockdown or over-expression (Figs. 4.2 and 4.3) was attributed to an alteration of nucleocytoplasmic localization of the mutant polyQ proteins, but not other transport

substrates of Xpo1.

### 6.4.2 *Heat Shock Protein* Gene Transcription upon *embargoed* Knockdown

Compared to the unexpanded proteins, the expression of mutant MJD proteins in both cell culture and transgenic mouse models results in aberrant gene expression (Chou et al., 2008; Evert et al., 2003). In this study, a *Drosophila* model of MJD (Warrick et al., 2005) was employed to study whether gene transcription was affected upon an alteration of *emb* expression level in polyQ toxicity.

Heat shock proteins are molecular chaperones which help in protecting cells from the disturbance by misfolded proteins, such as mutant polyQ protein (Barral et al., 2004; Liberek et al., 2008). It is well documented that over-expression of *hsp70* is able to rescue mutant polyQ toxicity in *Drosophila* (Warrick et al., 1998), and the expression of different classes of *hsp* has also been shown to be induced by mutant polyQ proteins (Huen and Chan, 2005; Huen et al., 2007). Since the induction of *hsp* genes is an intrinsic cellular defense mechanism to combat polyQ toxicity, it is of importance to determine if the expression of *hsp* genes was affected and associated with the enhancing phenotype observed due to the knockdown of *emb* expression.

It is demonstrated that in an *emb* knockdown background, the expression of MJDQ84

protein was unable to induce *hsp* gene transcription (Fig. 6.3). And such inhibitory effect

was also found to be applicable to different classes of *hsp* genes (Fig. 6.3). Although

histone acetylation is involved in the regulation of different *hsp* genes transcription (Chen

et al., 2002; Zhao et al., 2007; Zhao et al., 2005) and has been implicated in polyQ

pathogenesis (Evert et al., 2006; Sadri-Vakili et al., 2007; Steffan et al., 2001; Taylor et al.,

2003), no difference in terms of the acetylation status of histone H3 could be observed

between *MJDQ84* and *MJDQ84/emb* dsRNA flies (Fig. 6.5). This indicates that histone

acetylation level could not explain the observed reduction of *hsp* genes expression (Figs.

6.3 and 6.5). Nevertheless, there are two other possible reasons accounting for the

reduction of *hsp* genes transcription in *MJDQ84/emb* dsRNA flies.

Direct DNA binding property has recently been demonstrated for polyQ disease

proteins (Benn et al., 2008). The mutant Htt localized in the nucleus is able to bind directly

to the DNA promoter regions of various genes, including that of *dopamine D2 receptor* and

*brain derived neurotrophic factor*, with a higher affinity when compared to normal Htt

(Benn et al., 2008). This in turn leads to altered DNA conformation and aberrant

transcription factors binding, which ultimately results in transcriptional dysregulation

(Benn et al., 2008). Thus, one of the possible explanations for the absence of *hsp* gene

induction in *MJDQ84/emb* dsRNA flies (Fig. 6.3) would be that the knockdown of *emb* expression resulted in a nuclear accumulation of MJDQ84 (Fig. 4.5), which would facilitate the binding of mutant polyQ protein to the *hsp* gene promoters and thus interfere *hsp* gene transcription.

Another possible explanation for the absence of *hsp* gene induction in *MJDQ84/emb* dsRNA flies (Fig. 6.3) is attributed to the sequestration of transcription factors to polyQ nuclear aggregates. Multiple transcription factors, including HSF1 (Tonkiss and Calderwood, 2005), NF-Y (Li et al., 1998), STAT (Stephanou and Latchman, 1999) have been shown to be involved in *hsp* gene transcription. The recruitment of transcription factors to mutant polyQ protein aggregates, such as NF-Y (Yamanaka et al., 2008), would reduce the level of soluble functional ones to induce *hsp* gene transcription.

### 6.4.3 Correlation between the Age-dependent Decline of Exportin-1 and Heat Shock Response in Polyglutamine Pathogenesis

Immunoblot analysis of whole brain lysates from wild type mice indicated that the protein level of Xpo1 decreased in the normal ageing process (Fig. 6.7). This is in good agreement with the progressive decrease in hsp70 protein level reported in transgenic mouse models of polyQ diseases (Hay et al., 2004; Merienne et al., 2003; Yamanaka et al.,

2008). A decline in Xpo1 level would result in nuclear accumulation of mutant polyQ protein which would then disrupt *hsp70* transcription through mechanism(s) discussed above, and hence leading to a reduction in its protein level.

Taken together the Xpo1 immunoblot data (Fig. 6.7) and those published findings from transgenic polyQ mouse models (Hay et al., 2004; Merienne et al., 2003; Yamanaka et al., 2008), the result obtained from the *Drosophila* MJDQ84/emb dsRNA model (Fig. 3.24) is coherent with the results obtained from mouse models that all highlight the importance of Xpo1 on *hsp* induction in polyQ pathogenesis. The mouse data (Fig. 6.7) is also in line with the temporal expression of *hsp70* upon *emb* over-expression (Fig. 6.6). The over-expression of endogenous *emb* by an EP-insertion (Bilen and Bonini, 2007) not only strengthened the induction intensity of *hsp70*, but also maintained the induced *hsp70* expression. Thus, these result indicate that the intrinsic defense mechanism of *hsp* induction is tightly correlated to the expression level of Xpo1, implying the importance of Xpo1 in combating against polyQ toxicity.

In summary, it was demonstrated in this section that the modification on mutant polyQ toxicity by Xpo1 was a consequence of an alteration of the subcellular localization of mutant polyQ protein, but not other export substrates of Xpo1. Exportin-1 modulated polyQ toxicity by exporting mutant protein out of the nucleus, and hence reduced the interference of nuclear mutant polyQ protein on *hsp* gene transcription. The protein level of Xpo1 was found to diminish with time during the normal ageing process, as a result transcriptional dysregulation caused by nuclear mutant polyQ protein would become more prominent. This finding correlates well with the progressive degeneration observed in polyQ patients.

## *Chapter 7. Concluding Remarks*

The nucleocytoplasmic localization of mutant polyQ disease proteins plays a pivotal role in polyQ pathogenesis (Section 1.5). To study the correlation between polyQ subcellular localization and toxicity, it has been a widely-adopted strategy, in the past decade, to alter the subcellular localization of mutant polyQ protein by the addition of exogenous NLS or/and NES to disease proteins (Benn et al., 2005; Bichelmeier et al., 2007; Jackson et al., 2003; Peters et al., 1999; Saudou et al., 1998; Schilling et al., 2004). On the other hand, it was demonstrated that the presence of an expanded polyQ domain causes the re-localization of a cytoplasmic protein, HPRT, to the nucleus and premature death of the transgenic mice (Ordway et al., 1997). Thus, it is believed that certain uncharacterized nuclear transport signal(s) are encoded by the expanded polyQ domain which is/are contribute to the regulation of subcellular localization of mutant polyQ disease proteins. The primary objective of this project was to elucidate the nuclear transport pathway(s) that was/were responsive to the naked expanded polyQ domain. The effects of endogenous karyopherins on mutant polyQ protein subcellular localization and the associated toxicity were studied in detail by a gene-knockdown approach in the absence of any exogenous nuclear transport signal (Chapter 3).

This study found that the expression level of exportin-1 was tightly correlated to the

subcellular localization of mutant polyQ protein and toxicity (Section Chapter 4). Mutant polyQ protein was further demonstrated to be a novel transport substrate of exportin-1 (Chapter 5), and nuclear export of mutant polyQ protein was found to play a role in relieving polyQ toxicity by sustaining the heat shock response (Chapter 6).

**7.1 Proposed Model for Exportin-1-mediated Modification of Polyglutamine Toxicity**

Figure 7.1 summarizes the major findings of this project. The aberrant conformation due to an expansion of polyQ domain confers both nuclear import (Section 5.1) and export (Section 5.2) activities to the disease protein it resides. Nevertheless, the regulatory mechanism of expanded polyQ domain-mediated nuclear import and export is apparently different. Mutant polyQ protein is imported into the nucleus via a Ran-independent pathway (Section 5.1); whereas mutant polyQ protein is exported out from the nucleus via the classical exportin-1-mediated pathway (Section 5.2). Owing to the suppression of mutant polyQ-induced toxicity observed when the *Drosophila* ortholog of exportin-1, *embargoed* is over-expressed (Sections 4.1 and 4.2), exportin-1 is believed to play role in polyQ toxicity. Results obtained from the fly polyQ models show that by promoting nuclear export of mutant polyQ protein, exportin-1 helps in combating against polyQ toxicity by reducing its adverse effect on gene transcription. In this study, *heat shock protein* genes were used as examples to illustrate such effect (Section 6.2). Accumulation of mutant polyQ protein in the nucleus may sequester transcription factors to nuclear aggregates or interact directly with gene promoters, and hence interfere with gene transcription. Owing to the age-dependent decline of exportin-1 protein level observed (Section 6.3), the nuclear export of mutant polyQ protein would be diminished and hence transcriptional dysregulation caused by nuclear mutant protein become more prominent

with age. This thus contributes to the progressive degenerative phenotype observed in

polyQ patients.
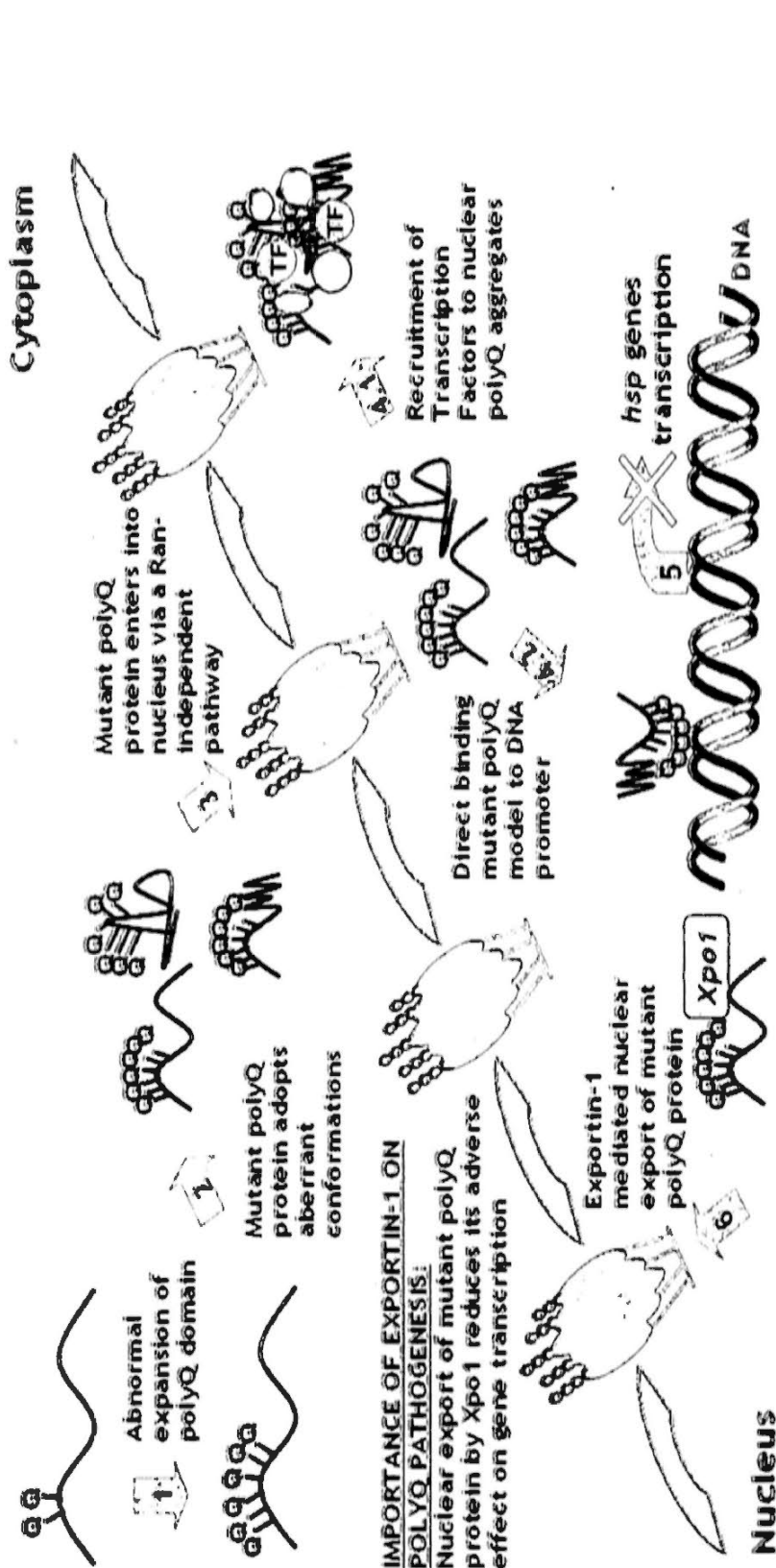
**Figure 7.1. A schematic diagram summarizes the major findings of this project. (1)** The abnormal expansion of polyQ domain results in **(2)** aberrant conformation of disease proteins, **(3)** which confers nuclear import activity to the mutant proteins. The imported mutant polyQ protein can either **(4.1)** sequester cellular proteins, including transcription factors (TFs) to form nuclear aggregates or **(4.2)** bind directly to the promoter regions of genes, e.g. *heat shock protein (hsp)* genes, and **(5)** hinder gene transcription. **(6)** The aberrant conformation of expanded polyQ domain renders the mutant protein an ability to interact with exportin-1 (Xpo1), and thus acts as a transport substrate for Xpo1-mediated nuclear export. Nevertheless, toxicity contributed by nuclear mutant protein becomes more prominent due to the age-dependent decline of Xpo1 protein level, accounting for the progressive degeneration observed in polyQ patients.

## 7.2 Conclusion

This project aims to elucidate the genetic pathways which the expanded polyQ domain adopt to modulate the nucleocytoplasmic localization of mutant polyQ protein and mutant polyQ-induced toxicity. Through a series of genetic and biochemical analyses in *Drosophila*, complemented with data generated from cell culture and mouse models, exportin-1 is found to reduce polyQ toxicity by promoting the nuclear export of mutant protein and thus ameliorate its adverse effect on gene transcription. The fact that exportin-1 expression level diminishes in an age-dependent manner, at least in part, accounts for the progressive degeneration of neurons observed in polyQ patients.

# *References*

Adachi, H., Katsuno, M., Minamiyama, M., Waza, M., Sang, C., Nakagomi, Y., Kobayashi, Y., Tanaka, F., Doyu, M., Inukai, A., Yoshida, M., Hashizume, Y. and Sobue, G. (2005) Widespread nuclear and cytoplasmic accumulation of mutant androgen receptor in SBMA patients. *Brain*, **128**, 659-670.

Al-Ramahi, I., Perez, A.M., Lim, J., Zhang, M., Sorensen, R., de Haro, M., Branco, J., Pulst, S.M., Zoghbi, H.Y. and Botas, J. (2007) dAtaxin-2 mediates expanded Ataxin-1-induced neurodegeneration in a Drosophila model of SCA1. *PLoS Genet*, **3**, e234.

Alba, M.M. and Guigo, R. (2004) Comparative analysis of amino acid repeats in rodents and humans. *Genome Res*, **14**, 549-554.

Albrecht, M., Golatta, M., Wullner, U. and Lengauer, T. (2004) Structural and functional analysis of ataxin-2 and ataxin-3. *Eur J Biochem*, **271**, 3155-3170.

Arts, G.J., Kuersten, S., Romby, P., Ehresmann, B. and Mattaj, I.W. (1998) The role of exportin-t in selective nuclear export of mature tRNAs. *Embo J*, **17**, 7430-7441.

Atwal, R.S., Xia, J., Pinchev, D., Taylor, J., Epand, R.M. and Truant, R. (2007) Huntingtin has a membrane association signal that can modulate huntingtin aggregation, nuclear entry and toxicity. *Hum Mol Genet*, **16**, 2600-2615.

Auluck, P.K., Chan, H.Y., Trojanowski, J.Q., Lee, V.M. and Bonini, N.M. (2002) Chaperone suppression of alpha-synuclein toxicity in a Drosophila model for Parkinson's disease. *Science*, **295**, 865-868.

Bai, J., Binari, R., Ni, J.Q., Vijayakanthan, M., Li, H.S. and Perrimon, N. (2008) RNA interference screening in Drosophila primary cells for genes involved in muscle assembly and maintenance. *Development*, **135**, 1439-1449.

Barral, J.M., Broadley, S.A., Schaffar, G. and Hartl, F.U. (2004) Roles of molecular chaperones in protein misfolding diseases. *Semin Cell Dev Biol*, **15**, 17-29.

Benn, C.L., Landles, C., Li, H., Strand, A.D., Woodman, B., Sathasivam, K., Li, S.H., Ghazi-Noori, S., Hockly, E., Faruque, S.M., Cha, J.H., Sharpe, P.T., Olson, J.M., Li, X.J. and Bates, G.P. (2005) Contribution of nuclear and extranuclear polyQ to neurological phenotypes in mouse models of Huntington's disease. *Hum Mol Genet*, **14**, 3065-3078.

Benn, C.L., Sun, T., Sadri-Vakili, G., McFarland, K.N., DiRocco, D.P., Yohrling, G.J., Clark, T.W., Bouzou, B. and Cha, J.H. (2008) Huntingtin modulates transcription, occupies gene promoters in vivo, and binds directly to DNA in a polyglutamine-dependent manner. *J Neurosci*, **28**, 10720-10733.

Bennett, B.L., Sasaki, D.T., Murray, B.W., O'Leary, E.C., Sakata, S.T., Xu, W., Leisten, J.C., Motiwala, A., Pierce, S., Satoh, Y., Bhagwat, S.S., Manning, A.M. and Anderson, D.W. (2001) SP600125, an anthrapyrazolone inhibitor of Jun N-terminal

kinase. *Proc Natl Acad Sci U S A*, **98**, 13681-13686.

Bernad, R., van der Velde, H., Fornerod, M. and Pickersgill, H. (2004) Nup358/RanBP2 attaches to the nuclear pore complex via association with Nup88 and Nup214/CAN and plays a supporting role in CRM1-mediated nuclear protein export. *Mol Cell Biol*, **24**, 2373-2384.

Bessert, D.A., Gutridge, K.L., Dunbar, J.C. and Carlock, L.R. (1995) The identification of a functional nuclear localization signal in the Huntington disease protein. *Brain Res Mol Brain Res*, **33**, 165-173.

Bichelmeier, U., Schmidt, T., Hubener, J., Boy, J., Ruttiger, L., Habig, K., Poths, S., Bonin, M., Knipper, M., Schmidt, W.J., Wilbertz, J., Wolburg, H., Laccone, F. and Riess, O. (2007) Nuclear localization of ataxin-3 is required for the manifestation of symptoms in SCA3: in vivo evidence. *J Neurosci*, **27**, 7418-7428.

Bier, E. (2005) Drosophila, the golden bug, emerges as a tool for human genetics. *Nat Rev Genet*, **6**, 9-23.

Bilen, J. and Bonini, N.M. (2005) Drosophila as a model for human neurodegenerative disease. *Annu Rev Genet*, **39**, 153-171.

Bilen, J. and Bonini, N.M. (2007) Genome-wide screen for modifiers of ataxin-3 neurodegeneration in Drosophila. *PLoS Genet*, **3**, 1950-1964.

Bogerd, H.P., Benson, R.E., Truant, R., Herold, A., Phingbodhipakkiya, M. and Cullen, B.R. (1999) Definition of a consensus transportin-specific nucleocytoplasmic transport signal. *J Biol Chem*, **274**, 9771-9777.

Boutros, M., Kiger, A.A., Armknecht, S., Kerr, K., Hild, M., Koch, B., Haas, S.A., Paro, R. and Perrimon, N. (2004) Genome-wide RNAi analysis of growth and viability in Drosophila cells. *Science*, **303**, 832-835.

Brand, A.H. and Perrimon, N. (1993) Targeted gene expression as a means of altering cell fates and generating dominant phenotypes. *Development*, **118**, 401-415.

Brignull, H.R., Morley, J.F. and Morimoto, R.I. (2007) The stress of misfolded proteins: C. elegans models for neurodegenerative disease and aging. *Adv Exp Med Biol*, **594**, 167-189.

Brownawell, A.M. and Macara, I.G. (2002) Exportin-5, a novel karyopherin, mediates nuclear export of double-stranded RNA binding proteins. *J Cell Biol*, **156**, 53-64.

Burke, J.R., Enghild, J.J., Martin, M.E., Jou, Y.S., Myers, R.M., Roses, A.D., Vance, J.M. and Strittmatter, W.J. (1996) Huntingtin and DRPLA proteins selectively interact with the enzyme GAPDH. *Nat Med*, **2**, 347-350.

Busch, A., Engemann, S., Lurz, R., Okazawa, H., Lehrach, H. and Wanker, E.E. (2003) Mutant huntingtin promotes the fibrillogenesis of wild-type huntingtin: a potential mechanism for loss of huntingtin function in Huntington's disease. *J Biol Chem*, **278**, 41452-41461.

Carpenter, A.E. and Sabatini, D.M. (2004) Systematic genome-wide screens of gene

function. *Nat Rev Genet*, **5**, 11-22.

Chai, Y., Wu, L., Griffin, J.D. and Paulson, H.L. (2001) The role of protein composition in specifying nuclear inclusion formation in polyglutamine disease. *J Biol Chem*, **276**, 44889-44897.

Chan, H.Y., Warrick, J.M., Andriola, I., Merry, D. and Bonini, N.M. (2002) Genetic modulation of polyglutamine toxicity by protein conjugation pathways in Drosophila. *Hum Mol Genet*, **11**, 2895-2904.

Chan, W.M., Shaw, P.C. and Chan, H.Y. (2007) A green fluorescent protein-based reporter for protein nuclear import studies in Drosophila cells. *Fly (Austin)*, **1**, 340-342.

Chen, S., Peng, G.H., Wang, X., Smith, A.C., Grote, S.K., Sopher, B.L. and La Spada, A.R. (2004) Interference of Crx-dependent transcription by ataxin-7 involves interaction between the glutamine regions and requires the ataxin-7 carboxy-terminal region for nuclear localization. *Hum Mol Genet*, **13**, 53-67.

Chen, T., Sun, H., Lu, J., Zhao, Y., Tao, D., Li, X. and Huang, B. (2002) Histone acetylation is involved in hsp70 gene transcription regulation in Drosophila melanogaster. *Arch Biochem Biophys*, **408**, 171-176.

Chou, A.H., Yeh, T.H., Ouyang, P., Chen, Y.L., Chen, S.Y. and Wang, H.L. (2008) Polyglutamine-expanded ataxin-3 causes cerebellar dysfunction of SCA3 transgenic mice by inducing transcriptional dysregulation. *Neurobiol Dis*, **31**, 89-101.

Claret, F.X., Hibi, M., Dhut, S., Toda, T. and Karin, M. (1996) A new group of conserved coactivators that increase the specificity of AP-1 transcription factors. *Nature*, **383**, 453-457.

Cornett, J., Cao, F., Wang, C.E., Ross, C.A., Bates, G.P., Li, S.H. and Li, X.J. (2005) Polyglutamine expansion of huntingtin impairs its nuclear export. *Nat Genet*, **37**, 198-204.

Cowan, K.J., Diamond, M.I. and Welch, W.J. (2003) Polyglutamine protein aggregation and toxicity are linked to the cellular stress response. *Hum Mol Genet*, **12**, 1377-1391.

Davies, J.E., Sarkar, S. and Rubinsztein, D.C. (2007) The ubiquitin proteasome system in Huntington's disease and the spinocerebellar ataxias. *BMC Biochem*, **8 Suppl 1**, S2.

Diamond, M.I., Robinson, M.R. and Yamamoto, K.R. (2000) Regulation of expanded polyglutamine protein aggregation and nuclear localization by the glucocorticoid receptor. *Proc Natl Acad Sci U S A*, **97**, 657-661.

Duenas, A.M., Goold, R. and Giunti, P. (2006) Molecular pathogenesis of spinocerebellar ataxias. *Brain*, **129**, 1357-1370.

Ellis, M.C., O'Neill, E.M. and Rubin, G.M. (1993) Expression of Drosophila glass protein and evidence for negative regulation of its activity in non-neuronal cells by another DNA-binding protein. *Development*, **119**, 855-865.

Encinas, M., Iglesias, M., Liu, Y., Wang, H., Muhaisen, A., Cena, V., Gallego, C. and Comella, J.X. (2000) Sequential treatment of SH-SY5Y cells with retinoic acid and brain-derived neurotrophic factor gives rise to fully differentiated, neurotrophic factor-dependent, human neuron-like cells. *J Neurochem*, 75, 991-1003.

Englmeier, L., Fornerod, M., Bischoff, F.R., Petosa, C., Mattaj, I.W. and Kutay, U. (2001) RanBP3 influences interactions between CRM1 and its nuclear protein export substrates. *EMBO Rep*, 2, 926-932.

Everett, C.M. and Wood, N.W. (2004) Trinucleotide repeats and neurodegenerative disease. *Brain*, 127, 2385-2405.

Evert, B.O., Araujo, J., Vieira-Saecker, A.M., de Vos, R.A., Harendza, S., Klockgether, T. and Wullner, U. (2006) Ataxin-3 represses transcription via chromatin binding, interaction with histone deacetylase 3, and histone deacetylation. *J Neurosci*, 26, 11474-11486.

Evert, B.O., Vogt, I.R., Vieira-Saecker, A.M., Ozimek, L., de Vos, R.A., Brunt, E.R., Klockgether, T. and Wullner, U. (2003) Gene expression profiling in ataxin-3 expressing cell lines reveals distinct effects of normal and mutant ataxin-3. *J Neuropathol Exp Neurol*, 62, 1006-1018.

Fischer, U., Huber, J., Boelens, W.C., Mattaj, I.W. and Luhrmann, R. (1995) The HIV-1 Rev activation domain is a nuclear export signal that accesses an export pathway used by specific cellular RNAs. *Cell*, 82, 475-483.

Fornerod, M., Ohno, M., Yoshida, M. and Mattaj, I.W. (1997) CRM1 is an export receptor for leucine-rich nuclear export signals. *Cell*, 90, 1051-1060.

Friedman, M.J., Shah, A.G., Fang, Z.H., Ward, E.G., Warren, S.T., Li, S. and Li, X.J. (2007) Polyglutamine domain modulates the TBP-TFIIB interaction: implications for its normal function and neurodegeneration. *Nat Neurosci*, 10, 1519-1528.

Frieman, M., Yount, B., Heise, M., Kopecky-Bromberg, S.A., Palese, P. and Baric, R.S. (2007) Severe acute respiratory syndrome coronavirus ORF6 antagonizes STAT1 function by sequestering nuclear import factors on the rough endoplasmic reticulum/Golgi membrane. *J Virol*, 81, 9812-9824.

Galvao, R., Mendes-Soares, L., Camara, J., Jaco, I. and Carmo-Fonseca, M. (2001) Triplet repeats, RNA secondary structure and toxic gain-of-function models for pathogenesis. *Brain Res Bull*, 56, 191-201.

Gatchel, J.R. and Zoghbi, H.Y. (2005) Diseases of unstable repeat expansion: mechanisms and common principles. *Nat Rev Genet*, 6, 743-755.

Gerace, L. and Blobel, G. (1980) The nuclear envelope lamina is reversibly depolymerized during mitosis. *Cell*, 19, 277-287.

Gidalevitz, T., Ben-Zvi, A., Ho, K.H., Brignull, H.R. and Morimoto, R.I. (2006) Progressive disruption of cellular protein folding in models of polyglutamine diseases. *Science*, 311, 1471-1474.

Goti, D., Katzen, S.M., Mez, J., Kurtis, N., Kiluk, J., Ben-Haiem, L., Jenkins, N.A., Copeland, N.G., Kakizuka, A., Sharp, A.H., Ross, C.A., Mouton, P.R. and Colomer, V. (2004) A mutant ataxin-3 putative-cleavage fragment in brains of Machado-Joseph disease patients and transgenic mice is cytotoxic above a critical concentration. *J Neurosci*, **24**, 10266-10279.

Gunawardena, S., Her, L.S., Brusch, R.G., Laymon, R.A., Niesman, I.R., Gordesky-Gold, B., Sintasath, L., Bonini, N.M. and Goldstein, L.S. (2003) Disruption of axonal transport by loss of huntingtin or expression of pathogenic polyQ proteins in Drosophila. *Neuron*, **40**, 25-40.

Haacke, A., Broadley, S.A., Boteva, R., Tzvetkov, N., Hartl, F.U. and Breuer, P. (2006) Proteolytic cleavage of polyglutamine-expanded ataxin-3 is critical for aggregation and sequestration of non-expanded ataxin-3. *Hum Mol Genet*, **15**, 555-568.

Hackam, A.S., Hodgson, J.G., Singaraja, R., Zhang, T., Gan, L., Gutekunst, C.A., Hersch, S.M. and Hayden, M.R. (1999) Evidence for both the nucleus and cytoplasm as subcellular sites of pathogenesis in Huntington's disease in cell culture and in transgenic mice expressing mutant huntingtin. *Philos Trans R Soc Lond B Biol Sci*, **354**, 1047-1055.

Hackam, A.S., Singaraja, R., Wellington, C.L., Metzler, M., McCutcheon, K., Zhang, T., Kalchman, M. and Hayden, M.R. (1998) The influence of huntingtin protein size on nuclear localization and cellular toxicity. *J Cell Biol*, **141**, 1097-1105.

Hakata, Y., Yamada, M., Mabuchi, N. and Shida, H..(2002) The carboxy-terminal region of the human immunodeficiency virus type 1 protein Rev has multiple roles in mediating CRM1-related Rev functions. *J Virol*, **76**, 8079-8089.

Hay, D.G., Sathasivam, K., Tobaben, S., Stahl, B., Marber, M., Mestril, R., Mahal, A., Smith, D.L., Woodman, B. and Bates, G.P. (2004) Progressive decrease in chaperone protein levels in a mouse model of Huntington's disease and induction of stress proteins as a therapeutic approach. *Hum Mol Genet*, **13**, 1389-1405.

Hazeki, N., Tukamoto, T., Goto, J. and Kanazawa, I. (2000) Formic acid dissolves aggregates of an N-terminal huntingtin fragment containing an expanded polyglutamine tract: applying to quantification of protein components of the aggregates. *Biochem Biophys Res Commun*, **277**, 386-393.

Heidenfelder, B.L. and Topal, M.D. (2003) Effects of sequence on repeat expansion during DNA replication. *Nucleic Acids Res*, **31**, 7159-7164.

Helmlinger, D., Hardy, S., Abou-Sleymane, G., Eberlin, A., Bowman, A.B., Gansmuller, A., Picaud, S., Zoghbi, H.Y., Trottier, Y., Tora, L. and Devys, D. (2006a) Glutamine-expanded ataxin-7 alters TFTC/STAGA recruitment and chromatin structure leading to photoreceptor dysfunction. *PLoS Biol*, **4**, e67.

Helmlinger, D., Tora, L. and Devys, D. (2006b) Transcriptional alterations and chromatin remodeling in polyglutamine diseases. *Trends Genet*, **22**, 562-570.

Herbst, M. and Wanker, E.E. (2006) Therapeutic approaches to polyglutamine diseases: combating protein misfolding and aggregation. *Curr Pharm Des*, **12**, 2543-2555.

Herdegen, T. and Waetzig, V. (2001) AP-1 proteins in the adult brain: facts and fiction about effectors of neuroprotection and neurodegeneration. *Oncogene*, **20**, 2424-2437.

Hoffner, G., Island, M.L. and Djian, P. (2005) Purification of neuronal inclusions of patients with Huntington's disease reveals a broad range of N-terminal fragments of expanded huntingtin and insoluble polymers. *J Neurochem*, **95**, 125-136.

Holen, T., Amarzguioui, M., Wiiger, M.T., Babaie, E. and Prydz, H. (2002) Positional effects of short interfering RNAs targeting the human coagulation trigger Tissue Factor. *Nucleic Acids Res*, **30**, 1757-1766.

Huber, J., Dickmanns, A. and Luhrmann, R. (2002) The importin-beta binding domain of snurportin1 is responsible for the Ran- and energy-independent nuclear import of spliceosomal U snRNPs in vitro. *J Cell Biol*, **156**, 467-479.

Huen, N.Y. and Chan, H.Y. (2005) Dynamic regulation of molecular chaperone gene expression in polyglutamine disease. *Biochem Biophys Res Commun*, **334**, 1074-1084.

Huen, N.Y., Wong, S.L. and Chan, H.Y. (2007) Transcriptional malfunctioning of heat shock protein gene expression in spinocerebellar ataxias. *Cerebellum*, **6**, 111-117.

Hutten, S. and Kehlenbach, R.H. (2006) Nup214 is required for CRM1-dependent nuclear protein export in vivo. *Mol Cell Biol*, **26**, 6772-6785.

Iosef, C., Gkourasas, T., Jia, C.Y., Li, S.S. and Han, V.K. (2008) A functional nuclear localization signal in insulin-like growth factor binding protein-6 mediates its nuclear import. *Endocrinology*, **149**, 1214-1226.

Iwata, A., Christianson, J.C., Bucci, M., Ellerby, L.M., Nukina, N., Forno, L.S. and Kopito, R.R. (2005) Increased susceptibility of cytoplasmic over nuclear polyglutamine aggregates to autophagic degradation. *Proc Natl Acad Sci U S A*, **102**, 13135-13140.

Izaurralde, E., Kutay, U., von Kobbe, C., Mattaj, I.W. and Gorlich, D. (1997) The asymmetric distribution of the constituents of the Ran system is essential for transport into and out of the nucleus. *Embo J*, **16**, 6535-6547.

Jackson, G.R., Salecker, I., Dong, X., Yao, X., Arnheim, N., Faber, P.W., MacDonald, M.E. and Zipursky, S.L. (1998) Polyglutamine-expanded human huntingtin transgenes induce degeneration of Drosophila photoreceptor neurons. *Neuron*, **21**, 633-642.

Jackson, W.S., Tallaksen-Greene, S.J., Albin, R.L. and Detloff, P.J. (2003) Nucleocytoplasmic transport signals affect the age at onset of abnormalities in knock-in mice expressing polyglutamine within an ectopic protein context. *Hum Mol Genet*, **12**, 1621-1629.

Jenster, G., Trapman, J. and Brinkmann, A.O. (1993) Nuclear import of the human

androgen receptor. *Biochem J*, **293 ( Pt 3)**, 761-768.

Julien, C., Coulombe, P. and Meloche, S. (2003) Nuclear export of ERK3 by a CRM1-dependent mechanism regulates its inhibitory action on cell cycle progression. *J Biol Chem*, **278**, 42615-42624.

Kalderon, D., Roberts, B.L., Richardson, W.D. and Smith, A.E. (1984) A short amino acid sequence able to specify nuclear location. *Cell*, **39**, 499-509.

Kanuka, H., Kuranaga, E., Hiratou, T., Igaki, T., Nelson, B., Okano, H. and Miura, M. (2003) Cytosol-endoplasmic reticulum interplay by Sec61alpha translocon in polyglutamine-mediated neurotoxicity in Drosophila. *Proc Natl Acad Sci U S A*, **100**, 11723-11728.

Kau, T.R., Way, J.C. and Silver, P.A. (2004) Nuclear transport and cancer: from mechanism to intervention. *Nat Rev Cancer*, **4**, 106-117.

Kavi, H.H., Fernandez, H., Xie, W. and Birchler, J.A. (2008) Genetics and biochemistry of RNAi in Drosophila. *Curr Top Microbiol Immunol*, **320**, 37-75.

Kaytor, M.D., Duvick, L.A., Skinner, P.J., Koob, M.D., Ranum, L.P. and Orr, H.T. (1999) Nuclear localization of the spinocerebellar ataxia type 7 protein, ataxin-7. *Hum Mol Genet*, **8**, 1657-1664.

Kazantsev, A., Preisinger, E., Dranovsky, A., Goldgaber, D. and Housman, D. (1999) Insoluble detergent-resistant aggregates form between pathological and nonpathological lengths of polyglutamine in mammalian cells. *Proc Natl Acad Sci U S A*, **96**, 11404-11409.

Kim, Y.S., Ko, J., Kim, I.S., Jang, S.W., Sung, H.J., Lee, H.J., Lee, S.Y., Kim, Y. and Na, D.S. (2003) PKCdelta-dependent cleavage and nuclear translocation of annexin A1 by phorbol 12-myristate 13-acetate. *Eur J Biochem*, **270**, 4089-4094.

Klement, I.A., Skinner, P.J., Kaytor, M.D., Yi, H., Hersch, S.M., Clark, H.B., Zoghbi, H.Y. and Orr, H.T. (1998) Ataxin-1 nuclear localization and aggregation: role in polyglutamine-induced disease in SCA1 transgenic mice. *Cell*, **95**, 41-53.

Kontopoulos, E., Parvin, J.D. and Feany, M.B. (2006) Alpha-synuclein acts in the nucleus to inhibit histone acetylation and promote neurotoxicity. *Hum Mol Genet*, **15**, 3012-3023.

Kordasiewicz, H.B., Thompson, R.M., Clark, H.B. and Gomez, C.M. (2006) C-termini of P/Q-type Ca2+ channel alpha1A subunits translocate to nuclei and promote polyglutamine-mediated toxicity. *Hum Mol Genet*, **15**, 1587-1599.

Kudo, N., Matsumori, N., Taoka, H., Fujiwara, D., Schreiner, E.P., Wolff, B., Yoshida, M. and Horinouchi, S. (1999) Leptomycin B inactivates CRM1/exportin 1 by covalent modification at a cysteine residue in the central conserved region. *Proc Natl Acad Sci U S A*, **96**, 9112-9117.

Kutay, U., Bischoff, F.R., Kostka, S., Kraft, R. and Gorlich, D. (1997) Export of importin alpha from the nucleus is mediated by a specific nuclear transport factor. *Cell*, **90**,

1061-1071.

Kutay, U. and Guttinger, S. (2005) Leucine-rich nuclear-export signals: born to be weak. *Trends Cell Biol*, **15**, 121-124.

Kutay, U., Lipowsky, G., Izaurralde, E., Bischoff, F.R., Schwarzmaier, P., Hartmann, E. and Gorlich, D. (1998) Identification of a tRNA-specific nuclear export receptor. *Mol Cell*, **1**, 359-369.

Lange, A., Mills, R.E., Lange, C.J., Stewart, M., Devine, S.E. and Corbett, A.H. (2007) Classical nuclear localization signals: definition, function, and interaction with importin alpha. *J Biol Chem*, **282**, 5101-5105.

Lee, K.S., Kwon, O.Y., Lee, J.H., Kwon, K., Min, K.J., Jung, S.A., Kim, A.K., You, K.H., Tatar, M. and Yu, K. (2008) Drosophila short neuropeptide F signalling regulates growth by ERK-mediated insulin signalling. *Nat Cell Biol*, **10**, 468-475.

Li, Q., Herrler, M., Landsberger, N., Kaludov, N., Ogryzko, V.V., Nakatani, Y. and Wolffe, A.P. (1998) Xenopus NF-Y pre-sets chromatin to potentiate p300 and acetylation-responsive transcription from the Xenopus hsp70 promoter in vivo. *Embo J*, **17**, 6300-6315.

Liberek, K., Lewandowska, A. and Zietkiewicz, S. (2008) Chaperones in control of protein disaggregation. *Embo J*, **27**, 328-335.

Lieberman, A.P., Harmison, G., Strand, A.D., Olson, J.M. and Fischbeck, K.H. (2002) Altered transcriptional regulation in cells expressing the expanded polyglutamine androgen receptor. *Hum Mol Genet*, **11**, 1967-1976.

Lindsay, M.E., Holaska, J.M., Welch, K., Paschal, B.M. and Macara, I.G. (2001) Ran-binding protein 3 is a cofactor for Crm1-mediated nuclear protein export. *J Cell Biol*, **153**, 1391-1402.

Lipowsky, G., Bischoff, F.R., Schwarzmaier, P., Kraft, R., Kostka, S., Hartmann, E., Kutay, U. and Gorlich, D. (2000) Exportin 4: a mediator of a novel nuclear export pathway in higher eukaryotes. *Embo J*, **19**, 4362-4371.

Lu, C., Li, Y., Zhao, Y., Xing, G., Tang, F., Wang, Q., Sun, Y., Wei, H., Yang, X., Wu, C., Chen, J., Guan, K.L., Zhang, C., Chen, H. and He, F. (2002) Intracrine hepatopoietin potentiates AP-1 activity through JAB1 independent of MAPK pathway. *Faseb J*, **16**, 90-92.

Marsh, J.L. and Thompson, L.M. (2006) Drosophila in the study of neurodegenerative disease. *Neuron*, **52**, 169-178.

Marsh, J.L., Walker, H., Theisen, H., Zhu, Y.Z., Fielder, T., Purcell, J. and Thompson, L.M. (2000) Expanded polyglutamine peptides alone are intrinsically cytotoxic and cause neurodegeneration in Drosophila. *Hum Mol Genet*, **9**, 13-25.

Martindale, D., Hackam, A., Wieczorek, A., Ellerby, L., Wellington, C., McCutcheon, K., Singaraja, R., Kazemi-Esfarjani, P., Devon, R., Kim, S.U., Bredesen, D.E., Tufaro, F. and Hayden, M.R. (1998) Length of huntingtin and its polyglutamine tract

influences localization and frequency of intracellular aggregates. *Nat Genet*, **18**, 150-154.

Matsuyama, Z., Yanagisawa, N.K., Aoki, Y., Black, J.L., 3rd, Lennon, V.A., Mori, Y., Imoto, K. and Inuzuka, T. (2004) Polyglutamine repeats of spinocerebellar ataxia 6 impair the cell-death-preventing effect of CaV2.1 Ca2+ channel--loss-of-function cellular model of SCA6. *Neurobiol Dis*, **17**, 198-204.

McMahon, S.J., Pray-Grant, M.G., Schieltz, D., Yates, J.R., 3rd and Grant, P.A. (2005) Polyglutamine-expanded spinocerebellar ataxia-7 protein disrupts normal SAGA and SLIK histone acetyltransferase activity. *Proc Natl Acad Sci U S A*, **102**, 8478-8482.

Merienne, K., Helmlinger, D., Perkin, G.R., Devys, D. and Trottier, Y. (2003) Polyglutamine expansion induces a protein-damaging stress connecting heat shock protein 70 to the JNK pathway. *J Biol Chem*, **278**, 16957-16967.

Michael, W.M., Choi, M. and Dreyfuss, G. (1995) A nuclear export signal in hnRNP A1: a signal-mediated, temperature-dependent nuclear protein export pathway. *Cell*, **83**, 415-422.

Mingot, J.M., Kostka, S., Kraft, R., Hartmann, E. and Gorlich, D. (2001) Importin 13: a novel mediator of nuclear import and export. *Embo J*, **20**, 3685-3694.

Mosammaparast, N. and Pemberton, L.F. (2004) Karyopherins: from nuclear-transport mediators to nuclear-function regulators. *Trends Cell Biol*, **14**, 547-556.

Moulder, K.L., Onodera, O., Burke, J.R., Strittmatter, W.J. and Johnson, E.M., Jr. (1999) Generation of neuronal intranuclear inclusions by polyglutamine-GFP: analysis of inclusion clearance and toxicity as a function of polyglutamine length. *J Neurosci*, **19**, 705-715.

Nakahara, S., Oka, N., Wang, Y., Hogan, V., Inohara, H. and Raz, A. (2006) Characterization of the nuclear import pathways of galectin-3. *Cancer Res*, **66**, 9995-10006.

Nelson, B., Nishimura, S., Kanuka, H., Kuranaga, E., Inoue, M., Hori, G., Nakahara, H. and Miura, M. (2005) Isolation of gene sets affected specifically by polyglutamine expression: implication of the TOR signaling pathway in neurodegeneration. *Cell Death Differ*, **12**, 1115-1123.

Nichols, C.D. (2006) Drosophila melanogaster neurobiology, neuropharmacology, and how the fly can inform central nervous system drug discovery. *Pharmacol Ther*, **112**, 677-700.

Nishimoto, T., Eilen, E. and Basilico, C. (1978) Premature of chromosome condensation in a ts DNA- mutant of BHK cells. *Cell*, **15**, 475-483.

Nucifora, F.C., Jr., Ellerby, L.M., Wellington, C.L., Wood, J.D., Herring, W.J., Sawa, A., Hayden, M.R., Dawson, V.L., Dawson, T.M. and Ross, C.A. (2003) Nuclear localization of a non-caspase truncation product of atrophin-1, with an expanded

polyglutamine repeat, increases cellular toxicity. *J Biol Chem*, **278**, 13047-13055.

Nucifora, F.C., Jr., Sasaki, M., Peters, M.F., Huang, H., Cooper, J.K., Yamada, M., Takahashi, H., Tsuji, S., Troncoso, J., Dawson, V.L., Dawson, T.M. and Ross, C.A. (2001) Interference by huntingtin and atrophin-1 with cbp-mediated transcription leading to cellular toxicity. *Science*, **291**, 2423-2428.

Ordway, J.M., Tallaksen-Greene, S., Gutekunst, C.A., Bernstein, E.M., Cearley, J.A., Wiener, H.W., Dure, L.S.t., Lindsey, R., Hersch, S.M., Jope, R.S., Albin, R.L. and Detloff, P.J. (1997) Ectopically expressed CAG repeats cause intranuclear inclusions and a progressive late onset neurological phenotype in the mouse. *Cell*, **91**, 753-763.

Orr, H.T. and Zoghbi, H.Y. (2007) Trinucleotide repeat disorders. *Annu Rev Neurosci*, **30**, 575-621.

Ortega, Z., Diaz-Hernandez, M. and Lucas, J.J. (2007) Is the ubiquitin-proteasome system impaired in Huntington's disease? *Cell Mol Life Sci*, **64**, 2245-2257.

Otto, E., Allen, J.M., Young, J.E., Palmiter, R.D. and Maroni, G. (1987) A DNA segment controlling metal-regulated expression of the Drosophila melanogaster metallothionein gene Mtn. *Mol Cell Biol*, **7**, 1710-1715.

Pemberton, L.F. and Paschal, B.M. (2005) Mechanisms of receptor-mediated nuclear import and nuclear export. *Traffic*, **6**, 187-198.

Perez, M.K., Paulson, H.L., Pendse, S.J., Saionz, S.J., Bonini, N.M. and Pittman, R.N. (1998) Recruitment and the role of nuclear localization in polyglutamine-mediated aggregation. *J Cell Biol*, **143**, 1457-1470.

Perez, M.K., Paulson, H.L. and Pittman, R.N. (1999) Ataxin-3 with an altered conformation that exposes the polyglutamine domain is associated with the nuclear matrix. *Hum Mol Genet*, **8**, 2377-2385.

Perkins, K.K., Admon, A., Patel, N. and Tjian, R. (1990) The Drosophila Fos-related AP-1 protein is a developmentally regulated transcription factor. *Genes Dev*, **4**, 822-834.

Peters, M.F., Nucifora, F.C., Jr., Kushi, J., Seaman, H.C., Cooper, J.K., Herring, W.J., Dawson, V.L., Dawson, T.M. and Ross, C.A. (1999) Nuclear targeting of mutant Huntingtin increases toxicity. *Mol Cell Neurosci*, **14**, 121-128.

Petosa, C., Schoehn, G., Askjaer, P., Bauer, U., Moulin, M., Steuerwald, U., Soler-Lopez, M., Baudin, F., Mattaj, I.W. and Muller, C.W. (2004) Architecture of CRM1/Exportin1 suggests how cooperativity is achieved during formation of a nuclear export complex. *Mol Cell*, **16**, 761-775.

Pollard, V.W., Michael, W.M., Nakielny, S., Siomi, M.C., Wang, F. and Dreyfuss, G. (1996) A novel receptor-mediated nuclear protein import pathway. *Cell*, **86**, 985-994.

Poukka, H., Karvonen, U., Yoshikawa, N., Tanaka, H., Palvimo, J.J. and Janne, O.A. (2000) The RING finger protein SNURF modulates nuclear trafficking of the androgen receptor. *J Cell Sci*, **113 ( Pt 17)**, 2991-3001.

Ramirez-Carrozzi, V. and Kerppola, T. (2003) Asymmetric recognition of nonconsensus AP-1 sites by Fos-Jun and Jun-Jun influences transcriptional cooperativity with NFAT1. *Mol Cell Biol*, **23**, 1737-1749.

Reid, S.P., Leung, L.W., Hartman, A.L., Martinez, O., Shaw, M.L., Carbonnelle, C., Volchkov, V.E., Nichol, S.T. and Basler, C.F. (2006) Ebola virus VP24 binds karyopherin alpha1 and blocks STAT1 nuclear accumulation. *J Virol*, **80**, 5156-5167.

Reiter, L.T., Potocki, L., Chien, S., Gribskov, M. and Bier, E. (2001) A systematic analysis of human disease-associated gene sequences in Drosophila melanogaster. *Genome Res*, **11**, 1114-1125.

Riesgo-Escovar, J.R. and Hafen, E. (1997) Common and distinct roles of DFos and DJun during Drosophila development. *Science*, **278**, 669-672.

Riley, B.E., Zoghbi, H.Y. and Orr, H.T. (2005) SUMOylation of the polyglutamine repeat protein, ataxin-1, is dependent on a functional nuclear localization signal. *J Biol Chem*, **280**, 21942-21948.

Robbins, J., Dilworth, S.M., Laskey, R.A. and Dingwall, C. (1991) Two interdependent basic domains in nucleoplasmin nuclear targeting sequence: identification of a class of bipartite nuclear targeting sequence. *Cell*, **64**, 615-623.

Ross, C.A. and Poirier, M.A. (2005) Opinion: What is the role of protein aggregation in neurodegeneration? *Nat Rev Mol Cell Biol*, **6**, 891-898.

Roth, P., Xylourgidis, N., Sabri, N., Uv, A., Fornerod, M. and Samakovlis, C. (2003) The Drosophila nucleoporin DNup88 localizes DNup214 and CRM1 on the nuclear envelope and attenuates NES-mediated nuclear export. *J Cell Biol*, **163**, 701-706.

Rubinsztein, D.C. (2006) The roles of intracellular protein-degradation pathways in neurodegeneration. *Nature*, **443**, 780-786.

Rudt, F. and Pieler, T. (2001) Cytosolic import factor- and Ran-independent nuclear transport of ribosomal protein L5. *Eur J Cell Biol*, **80**, 661-668.

Sabri, N., Roth, P., Xylourgidis, N., Sadeghifar, F., Adler, J. and Samakovlis, C. (2007) Distinct functions of the Drosophila Nup153 and Nup214 FG domains in nuclear protein transport. *J Cell Biol*, **178**, 557-565.

Sadri-Vakili, G., Bouzou, B., Benn, C.L., Kim, M.O., Chawla, P., Overland, R.P., Glajch, K.E., Xia, E., Qiu, Z., Hersch, S.M., Clark, T.W., Yohrling, G.J. and Cha, J.H. (2007) Histones associated with downregulated genes are hypo-acetylated in Huntington's disease models. *Hum Mol Genet*, **16**, 1293-1306.

Saporita, A.J., Zhang, Q., Navai, N., Dincer, Z., Hahn, J., Cai, X. and Wang, Z. (2003) Identification and characterization of a ligand-regulated nuclear export signal in androgen receptor. *J Biol Chem*, **278**, 41998-42005.

Saudou, F., Finkbeiner, S., Devys, D. and Greenberg, M.E. (1998) Huntingtin acts in the nucleus to induce apoptosis but death does not correlate with the formation of

intranuclear inclusions. *Cell*, Vol. 95, pp. 55-66.

Schaffar, G., Breuer, P., Boteva, R., Behrends, C., Tzvetkov, N., Strippel, N., Sakahira, H., Siegers, K., Hayer-Hartl, M. and Hartl, F.U. (2004) Cellular toxicity of polyglutamine expansion proteins: mechanism of transcription factor deactivation. *Mol Cell*, **15**, 95-105.

Schilling, G., Savonenko, A.V., Klevytska, A., Morton, J.L., Tucker, S.M., Poirier, M., Gale, A., Chan, N., Gonzales, V., Slunt, H.H., Coonfield, M.L., Jenkins, N.A., Copeland, N.G., Ross, C.A. and Borchelt, D.R. (2004) Nuclear-targeting of mutant huntingtin fragments produces Huntington's disease-like phenotypes in transgenic mice. *Hum Mol Genet*, **13**, 1599-1610.

Schilling, G., Wood, J.D., Duan, K., Slunt, H.H., Gonzales, V., Yamada, M., Cooper, J.K., Margolis, R.L., Jenkins, N.A., Copeland, N.G., Takahashi, H., Tsuji, S., Price, D.L., Borchelt, D.R. and Ross, C.A. (1999) Nuclear accumulation of truncated atrophin-1 fragments in a transgenic mouse model of DRPLA. *Neuron*, **24**, 275-286.

Shaw, G., Morse, S., Ararat, M. and Graham, F.L. (2002) Preferential transformation of human neuronal cells by human adenoviruses and the origin of HEK 293 cells. *Faseb J*, **16**, 869-871.

Shimohata, T., Nakajima, T., Yamada, M., Uchida, C., Onodera, O., Naruse, S., Kimura, T., Koide, R., Nozaki, K., Sano, Y., Ishiguro, H., Sakoe, K., Ooshima, T., Sato, A., Ikeuchi, T., Oyake, M., Sato, T., Aoyagi, Y., Hozumi, I., Nagatsu, T., Takiyama, Y., Nishizawa, M., Goto, J., Kanazawa, I., Davidson, I., Tanese, N., Takahashi, H. and Tsuji, S. (2000) Expanded polyglutamine stretches interact with TAFII130, interfering with CREB-dependent transcription. *Nat Genet*, **26**, 29-36.

Siomi, H. and Dreyfuss, G. (1995) A nuclear localization domain in the hnRNP A1 protein. *J Cell Biol*, **129**, 551-560.

Skinner, P.J., Koshy, B.T., Cummings, C.J., Klement, I.A., Helin, K., Servadio, A., Zoghbi, H.Y. and Orr, H.T. (1997) Ataxin-1 with an expanded glutamine tract alters nuclear matrix-associated structures. *Nature*, **389**, 971-974.

Steffan, J.S., Agrawal, N., Pallos, J., Rockabrand, E., Trotman, L.C., Slepko, N., Illes, K., Lukacsovich, T., Zhu, Y.Z., Cattaneo, E., Pandolfi, P.P., Thompson, L.M. and Marsh, J.L. (2004) SUMO modification of Huntingtin and Huntington's disease pathology. *Science*, **304**, 100-104.

Steffan, J.S., Bodai, L., Pallos, J., Poelman, M., McCampbell, A., Apostol, B.L., Kazantsev, A., Schmidt, E., Zhu, Y.Z., Greenwald, M., Kurokawa, R., Housman, D.E., Jackson, G.R., Marsh, J.L. and Thompson, L.M. (2001) Histone deacetylase inhibitors arrest polyglutamine-dependent neurodegeneration in Drosophila. *Nature*, **413**, 739-743.

Stephanou, A. and Latchman, D.S. (1999) Transcriptional regulation of the heat shock protein genes by STAT family transcription factors. *Gene Expr*, **7**, 311-319.

Strahl, B.D. and Allis, C.D. (2000) The language of covalent histone modifications. *Nature*,

**403**, 41-45.

Stuven, T., Hartmann, E. and Gorlich, D. (2003) Exportin 6: a novel nuclear export receptor that is specific for profilin.actin complexes. *Embo J*, **22**, 5928-5940.

Suhr, S.T., Senut, M.C., Whitelegge, J.P., Faull, K.F., Cuizon, D.B. and Gage, F.H. (2001) Identities of sequestered proteins in aggregates from cells with induced polyglutamine expression. *J Cell Biol*, **153**, 283-294.

Tachibana, T., Imamoto, N., Seino, H., Nishimoto, T. and Yoneda, Y. (1994) Loss of RCC1 leads to suppression of nuclear protein import in living cells. *J Biol Chem*, **269**, 24542-24545.

Tait, D., Riccio, M., Sittler, A., Scherzinger, E., Santi, S., Ognibene, A., Maraldi, N.M., Lehrach, H. and Wanker, E.E. (1998) Ataxin-3 is transported into the nucleus and associates with the nuclear matrix. *Hum Mol Genet*, **7**, 991-997.

Takagi, Y., Ui-Tei, K. and Hirohashi, S. (2000) Adhesion-dependent tyrosine phosphorylation of enabled in Drosophila neuronal cell line. *Biochem Biophys Res Commun*, **270**, 482-487.

Takahashi, Y., Okamoto, Y., Popiel, H.A., Fujikake, N., Toda, T., Kinjo, M. and Nagai, Y. (2007) Detection of polyglutamine protein oligomers in cells by fluorescence correlation spectroscopy. *J Biol Chem*, **282**, 24039-24048.

Taylor, J., Grote, S.K., Xia, J., Vandelft, M., Graczyk, J., Ellerby, L.M., La Spada, A.R. and Truant, R. (2006) Ataxin-7 can export from the nucleus via a conserved exportin-dependent signal. *J Biol Chem*, **281**, 2730-2739.

Taylor, J.P., Taye, A.A., Campbell, C., Kazemi-Esfarjani, P., Fischbeck, K.H. and Min, K.T. (2003) Aberrant histone acetylation, altered transcription, and retinal degeneration in a Drosophila model of polyglutamine disease are rescued by CREB-binding protein. *Genes Dev*, **17**, 1463-1468.

Terry, L.J., Shows, E.B. and Wente, S.R. (2007) Crossing the nuclear envelope: hierarchical regulation of nucleocytoplasmic transport. *Science*, **318**, 1412-1416.

Tonkiss, J. and Calderwood, S.K. (2005) Regulation of heat shock gene transcription in neuronal cells. *Int J Hyperthermia*, **21**, 433-444.

Tota, M.R., Xu, L., Sirotina, A., Strader, C.D. and Graziano, M.P. (1995) Interaction of [fluorescein-Trp25]glucagon with the human glucagon receptor expressed in Drosophila Schneider 2 cells. *J Biol Chem*, **270**, 26466-26472.

Tran, E.J. and Wente, S.R. (2006) Dynamic nuclear pore complexes: life on the edge. *Cell*, **125**, 1041-1053.

Truant, R., Atwal, R.S. and Burtnik, A. (2007) Nucleocytoplasmic trafficking and transcription effects of huntingtin in Huntington's disease. *Prog Neurobiol*, **83**, 211-227.

Ui, K., Nishihara, S., Sakuma, M., Togashi, S., Ueda, R., Miyata, Y. and Miyake, T. (1994) Newly established cell lines from Drosophila larval CNS express neural specific

characteristics. *In Vitro Cell Dev Biol Anim*, **30A**, 209-216.

Wang, C.E., Zhou, H., McGuire, J.R., Cerullo, V., Lee, B., Li, S.H. and Li, X.J. (2008) Suppression of neuropil aggregates and neurological symptoms by an intracellular antibody implicates the cytoplasmic toxicity of mutant huntingtin. *J Cell Biol.*

Wanker, E.E., Scherzinger, E., Heiser, V., Sittler, A., Eickhoff, H. and Lehrach, H. (1999) Membrane filter assay for detection of amyloid-like polyglutamine-containing protein aggregates. *Methods Enzymol*, **309**, 375-386.

Warrick, J.M., Chan, H.Y., Gray-Board, G.L., Chai, Y., Paulson, H.L. and Bonini, N.M. (1999) Suppression of polyglutamine-mediated neurodegeneration in Drosophila by the molecular chaperone HSP70. *Nat Genet*, **23**, 425-428.

Warrick, J.M., Morabito, L.M., Bilen, J., Gordesky-Gold, B., Faust, L.Z., Paulson, H.L. and Bonini, N.M. (2005) Ataxin-3 suppresses polyglutamine neurodegeneration in Drosophila by a ubiquitin-associated mechanism. *Mol Cell*, **18**, 37-48.

Warrick, J.M., Paulson, H.L., Gray-Board, G.L., Bui, Q.T., Fischbeck, K.H., Pittman, R.N. and Bonini, N.M. (1998) Expanded polyglutamine protein forms nuclear inclusions and causes neural degeneration in Drosophila. *Cell*, **93**, 939-949.

Weston, C.R. and Davis, R.J. (2007) The JNK signal transduction pathway. *Curr Opin Cell Biol*, **19**, 142-149.

Weydt, P. and La Spada, A.R. (2006) Targeting protein aggregation in neurodegeneration--lessons from polyglutamine disorders. *Expert Opin Ther Targets*, **10**, 505-513.

Williams, A., Jahreiss, L., Sarkar, S., Saiki, S., Menzies, F.M., Ravikumar, B. and Rubinsztein, D.C. (2006) Aggregate-prone proteins are cleared from the cytosol by autophagy: therapeutic implications. *Curr Top Dev Biol*, **76**, 89-101.

Wong, S.L., Chan, W.M. and Chan, H.Y. (2008) Sodium dodecyl sulfate-insoluble oligomers are involved in polyglutamine degeneration. *Faseb J.*

Xia, J., Lee, D.H., Taylor, J., Vandelft, M. and Truant, R. (2003) Huntingtin contains a highly conserved nuclear export signal. *Hum Mol Genet*, **12**, 1393-1403.

Yamanaka, T., Miyazaki, H., Oyama, F., Kurosawa, M., Washizu, C., Doi, H. and Nukina, N. (2008) Mutant Huntingtin reduces HSP70 expression through the sequestration of NF-Y transcription factor. *Embo J*, **27**, 827-839.

Yang, J., Song, H., Walsh, S., Bardes, E.S. and Kornbluth, S. (2001) Combinatorial control of cyclin B1 nuclear trafficking through phosphorylation at multiple sites. *J Biol Chem*, **276**, 3604-3609.

Yasuhara, N., Shibazaki, N., Tanaka, S., Nagai, M., Kamikawa, Y., Oe, S., Asally, M., Kamachi, Y., Kondoh, H. and Yoneda, Y. (2007) Triggering neural differentiation of ES cells by subtype switching of importin-alpha. *Nat Cell Biol*, **9**, 72-79.

Zhang, K., Chaillet, J.R., Perkins, L.A., Halazonetis, T.D. and Perrimon, N. (1990) Drosophila homolog of the mammalian jun oncogene is expressed during

embryonic development and activates transcription in mammalian cells. *Proc Natl Acad Sci U S A*, **87**, 6281-6285.

Zhao, Y., Lu, J., Sun, H., Chen, X. and Huang, B. (2007) Roles of histone acetylation modification in basal and inducible expression of hsp26 gene in D. melanogaster. *Mol Cell Biochem*, **306**, 1-8.

Zhao, Y., Lu, J., Sun, H., Chen, X., Huang, W., Tao, D. and Huang, B. (2005) Histone acetylation regulates both transcription initiation and elongation of hsp22 gene in Drosophila. *Biochem Biophys Res Commun*, **326**, 811-816.

Zoghbi, H.Y. and Orr, H.T. (2000) Glutamine repeats and neurodegeneration. *Annu Rev Neurosci*, **23**, 217-247.
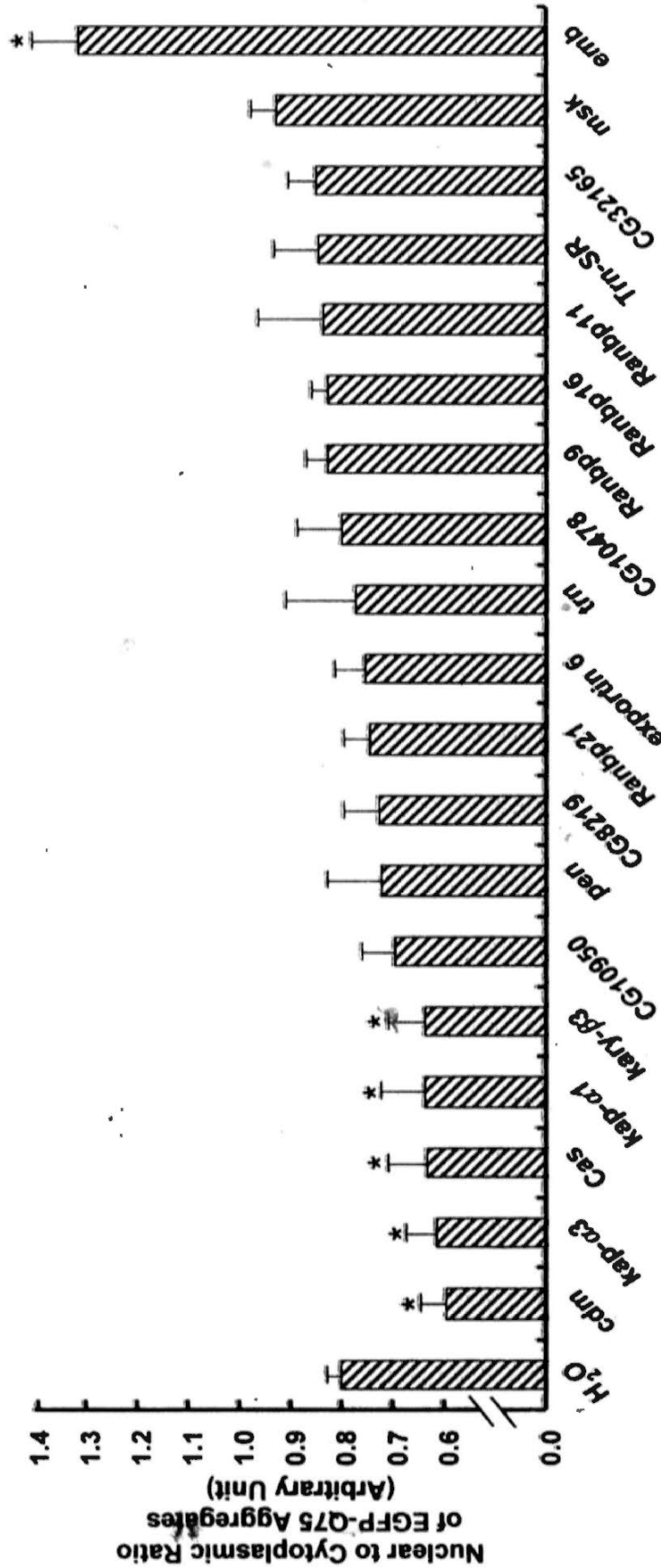
**Appendix 1. Modulatory effects of karyopherins on the subcellular localization of EGFP-Q75 aggregates in stable BG2 cells.** After incubation with dsRNAs for 3 days, EGFP-Q75 expression was induced by 1 mM $CuSO_4$. At 96 hours post-induction, cells were fixed and stained for Hoechst to label the cell nuclei, and the subcellular localization of EGFP-Q75 aggregates was examined on a single-blind approach. The ratio of nuclear (NA) to cytoplasmic (CA) EGFP-Q75 aggregates in dsRNA-treated BG2 cells was arranged in ascending order. The Knockdown of expression of *cdm*, *kap-α3*, *Cas*, *kap-α1*, *kary-β3*, and *emb* resulted in significant changes of the NA to CA ratio when compared to the water-treated control. The subcellular localization of at least 100 aggregates was analyzed in each treatment and data shown represent the average of 3 independent experiments ($*$ $p < 0.05$, by Student's t-test). Error bars represent S.E.M..

(In collaboration with Frankie Tsoi, The Chinese University of Hong Kong, Hong Kong)

204
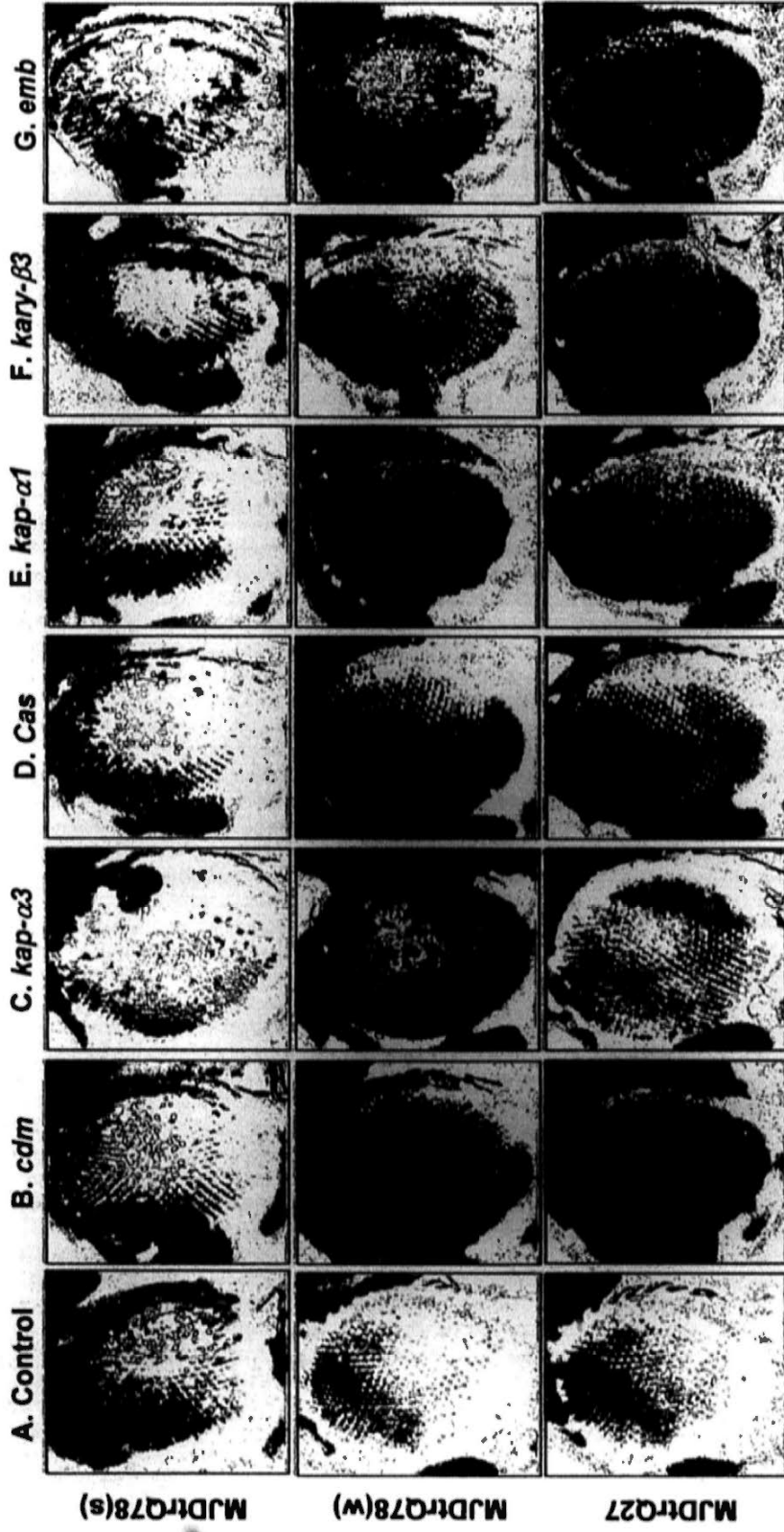
**Appendix 2. Modulatory effects of selected karyopherins on MJDtrQ78-induced toxicity *in vivo*.** The knockdown of expressions of *karyopherins* showed no dominant effect on the external eye morphology in control MJDtrQ27 flies (bottom row). Weak expression of MJDtrQ78 only caused internal retinal degeneration and did not cause any external degenerative phenotype (**A**, middle row) while strong expression of MJDtrQ78 resulted in external eye depigmentation (**A**, upper row). Co-expression of MJDtrQ78 and (**C**) *kap-α3* and (**G**) *emb* dsRNAs caused enhancement of degeneration as indicated by external eye depigmentation in MJDtrQ78(w) flies (middle row) and scar appearance on MJDtrQ78(s) flies (upper row). The knockdown of expression of other *karyopherins* neither enhanced nor suppressed MJDtrQ78-induced toxicity.

(In collaboration with Frankie Tsoi, The Chinese University of Hong Kong, Hong Kong)
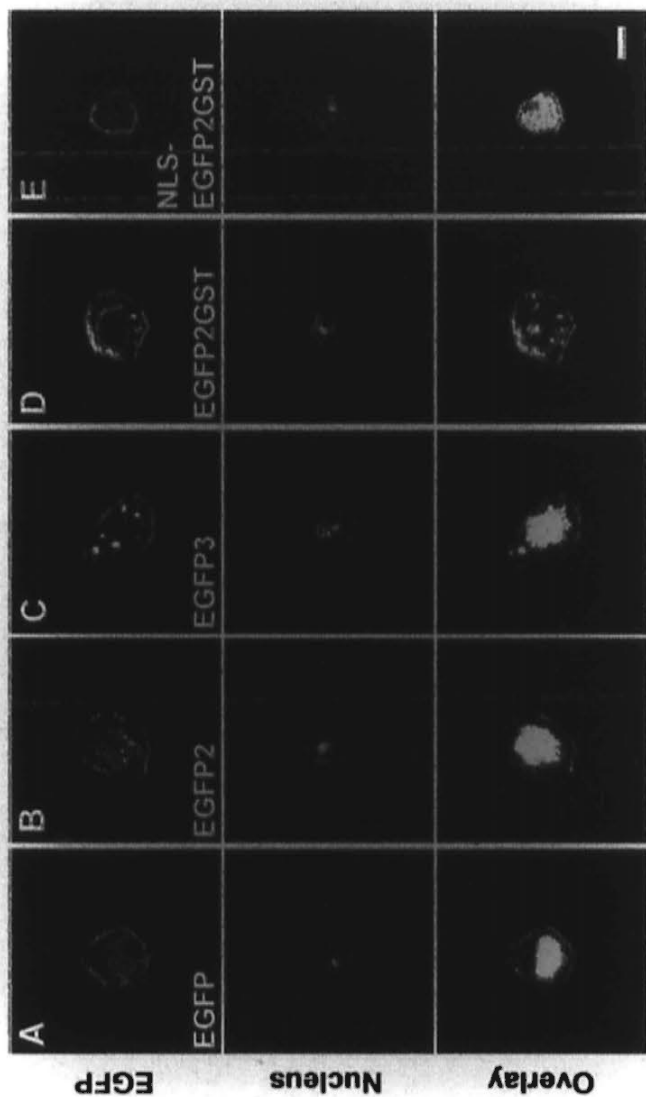
**Appendix 3. Confocal Images of *Drosophila* S2R+ cells expressing different EGFP-based reporters.**

Transiently transfected S2R+ cells with individual EGFP reporters were fixed and stained with 10 µg/ml propidium iodide (in red) to label the cell nuclei. Subcellular localization of the EGFP-based reporters (in green) was examined by confocal microscopy. Both (**A**) monomeric and (**B**) dimeric EGFP reporters localized homogeneously in both cytoplasm and nucleus. (**C**) The trimeric EGFP reporter self-aggregated in S2R+ cells. (**D**) When glutathione-S-transferase (GST) was used to replace 1 EGFP moiety in the EGFP3 reporter, the EGFP2GST reporter localized exclusively to cytoplasm. (**E**) The presence of the SV40 large T antigen NLS sequence directed the EGFP2GST reporter to the nucleus. Scale bar represents 5 µm.
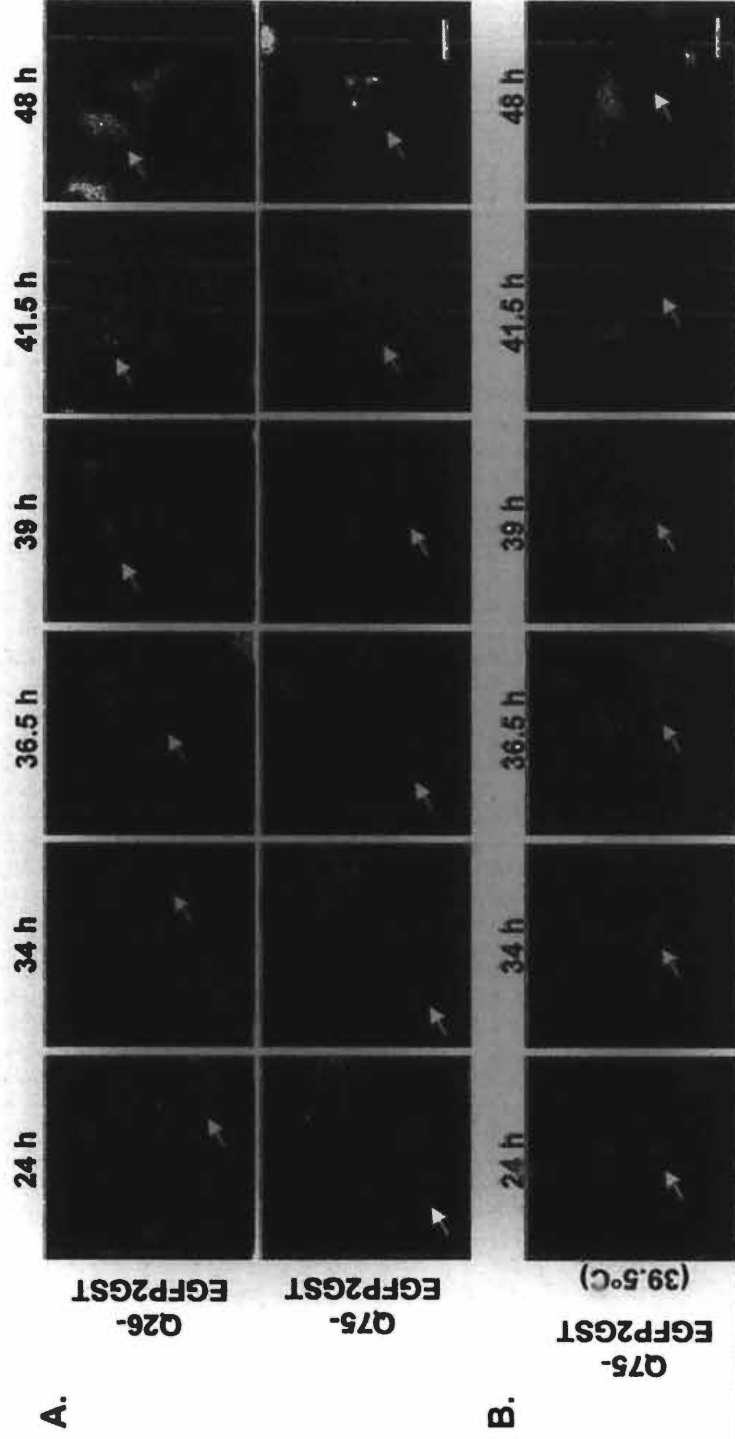
**Appendix 4. Time-lapse microscopy of Q75-EGFP2GST in HEK 293 and tsBN2 cells. (A)** The intracellular movement of Q26/Q75-EGFP2GST was monitored in a real time manner from 24 to 48 h post-transfection in HEK 293 cells. The Q26 protein remained in the cytoplasm throughout the course of the experiment. However, the nuclear GFP signal in Q75-expressing cells accumulated with time. Microscopically visible aggregates started to appear inside the nucleus at 41.5h, and the size increased with time. **(B)** At non-permissive temperature (39.5°C), RanGTP in tsBN2 cells was depleted, which disrupted the RanGDP/GTP gradient across the nuclear envelope and thus inhibited Ran-dependent protein nuclear transport. Under such condition, Q75 was still able to enter the nucleus, suggesting that its nuclear entry is Ran-independent. Arrows indicate the same cell throughout the time-lapse experiment. Scale bars represent 10 μm.

(In collaboration with Eric Wong, Nanyang Technological University, Singapore)